

THE ROLE OF MITOPHAGY IN DAMAGE INCURRED BY MYOCARDIAL ISCHAEMIA/REPERFUSION

by

Sibonginkosi Roselyn Mzezewa

*Thesis presented in fulfilment of the requirements for the degree
of Master of Science in the Faculty of Medical and Health
Sciences at Stellenbosch University*



Supervisor: Professor (Prof) Barbara Huisamen
Co-supervisor: Professor (Prof) Amanda Lochner

March 2017

Declaration

By submitting this thesis electronically, I declare that the entirety of the work contained therein is my own, original work, that I am the sole author thereof (save to the extent explicitly otherwise stated), that reproduction and publication thereof by Stellenbosch University will not infringe any third party rights and that I have not previously in its entirety or in part submitted it for obtaining any qualification.

Sibonginkosi Roselyn Mzezewa

Date: March 2017

Copyright © 2017 Stellenbosch University

All rights reserved

Abstract

Background and aims: Mitophagy is a specialised process of autophagy whereby dysfunctional mitochondria are removed. Mitophagy has been increasingly recognised as an essential process to sustain a healthy pool of mitochondria for cardiomyocytes as mitochondria are critical for cardiac function. Mitophagy has also become of interest as a role player in cardiovascular pathology: previous studies showed that autophagy is activated during ischaemia/reperfusion injury, but whether it is beneficial or detrimental is still unsure. The aims of this study were to evaluate the role of mitophagy in myocardial ischaemia/reperfusion and its association with cardio protection, mitochondrial function and the signalling events of mitophagy. Use was made of 3-methyl adenine (3-MA), an inhibitor of autophagy and FCCP, an uncoupler of mitochondrial oxidative phosphorylation and stimulant of mitophagy, in order to manipulate the process of mitophagy.

Methods: Hearts from male Wistar rats were perfused *ex vivo* and subjected to 25 min global ischaemia or ischaemia followed by 20 min reperfusion with or without pre-or post-ischaemic 3-MA (1 mM) administrations well as pre-ischaemic/20 min reperfusion FCCP administration. Mitochondria were isolated (KCl-EDTA) for measurement of oxidative phosphorylation with glutamate, malate and palmitoyl-L-carnitine as substrates using a Clark electrode. TOM70, PINK1, Parkin and P62/SQSTM1, LC3, BNIP3L/Nix and Beclin1 accumulation were the mitophagy and autophagy markers determined by Western blotting. A separate group of hearts were subjected to 35 min regional ischaemia/60 min reperfusion with drugs administered pre-ischaemia. Infarct size was determined by Triphenyltetrazolium chloride staining. Citrate synthase levels as measurement of intact mitochondria, were determined using an assay kit. ATP levels for certain experiments were measured using HPLC.

Results Mitochondria isolated from hearts treated with 1 mM 3-MA post ischaemia presented with increased QO₂ (S₃) in the carbohydrate substrate and increased RCI levels in fatty acid substrate. 100 nM FCCP also resulted in increased mitochondrial respiration as indicated by increased RCI and increased QO₂(S₃) respiration in the fatty acid substrate, but was associated with increased mitochondrial uncoupling indicated by lower ADP/O, and hence decreased oxidative phosphorylation for both states 3 and 4. 250 nM FCCP led to complete mitochondrial uncoupling. Neither drug affected citrate synthase activity. LC3A/B-II/I ratios were lower in both ischaemic and reperfused hearts in comparison to baseline, while 3-MA had no effect on these levels. BNIP3L/Nix levels were upregulated in reperfusion versus in ischaemia, whereas the opposite effect was observed for Parkin and P62/SQSTM1 levels. 3-MA post-ischaemic treatment resulted in increased PINK1. 100 nM FCCP yielded increased TOM70 in comparison to 250 nM but the opposite was observed with Parkin

levels. 3-MA had no effect on infarct size whereas both 100 nM and 250 nM FCCP reduced infarct size ($p=0.0001$). Both drugs did not affect functional recovery, however, 250 nM FCCP led to complete mechanical heart failure and was associated with significantly higher levels of unconverted ADP.

Conclusion: Manipulation of mitophagy affects the outcome of ischaemia/reperfusion:

Downregulation by 3-MA was (i) of little effect to hindering mitophagy in certain protocols indicated by increased mitochondrial PINK1 levels, however (ii) it yielded increased mitochondrial respiration, but (iii) rendered poor heart functional recovery and (iv) had no effect on the infarct size.

FCCP (100 nM) upregulation of mitophagy, was (i) associated with cardio protection with (ii) decreased infarct size, but (iii) uncoupling effects of FCCP led to decreased oxidative phosphorylation rates and hence (iv) decreased cellular levels of ATP resulting in (v) poor functional recovery observed.

Abstrak

Agtergrond en doelwitte: Mitofagie is 'n gespesialiseerde vorm van outofagie waardeur disfunksionele mitokondrieë verwyder word. Mitofagie word tans beskou as 'n essensiële proses om te verseker dat die poel van beskikbare mitokondrieë in 'n kardiomiosiet goed funksioneer, aangesien hulle krities is vir kardiaale funksie. Mitofagie het ook belangstelling ontlok weens die moontlike rol daarvan in kardiovaskulêre patologie: studies het aangetoon dat outofagie gedurende iskemie/herperfusie besering geaktiveer, die voor- of nadele daarvan is egter onseker. Die doelwitte van hierdie studie was om die rol van mitofagie gedurende miokardiale iskemie/herperfusie te evalueer en die verband daarvan met beskerming, mitokondriale funksie en die seintransduksie geassosieer met mitofagie, te ondersoek. Om hierdie prosesse te manipuleer, is gebruik gemaak van 3-metiel adenien (3-MA) as inhibitor van outofagie en FCCP, 'n ont koppelaar van oksidatiewe fosforilasie en dus stimulant van mitofagie.

Metodes: Harte van manlike Wistar rotte is *ex vivo* perfuseer en onderwerp aan 25 min globale iskemie gevolg deur 20 min herperfusie met of sonder pre- of postiskemiese toediening van 3-MA (1 mM) sowel as pre-iskemiese toediening van FCCP. Mitokondrieë is geïsoleer (KCl-EDTA) vir bepaling van die oksidatiewe fosforileringspotensiaal met glutamaat, malaat en palmitoïel-L-karnitien as onderskeie substrate, deur 'n Clark-tipe elektrode te gebruik. TOM70, PINK1, Parkin en P62/SQSTM1, LC3, BNIP3L/Nix en Beklin1 akkumulering as merkers van mitofagie en outofagie, is deur middel van Westerse kladtegnieke bepaal. 'n Verdere groep harte is onderwerp aan 35 min streeksiskemie/60 min herperfusie met middels voor iskemie toegedien, vir die bepaling van infarkt grootte deur middel van trifenieltetrazolium chloriedkleuring. Sitraatsintasevlakke is deur middel van 'n kommersiële essai bepaal as maatstaf van die intakte, respirerende mitokondrieë per mg proteien. Mitokondriale ATP produksie is in sekere eksperimente deur middel van HPLC analise bepaal.

Resultate: Mitokondrieë berei uit harte wat met 1mM 3-MA na iskemie behandel is, het 'n verhoogde QO₂(3) met glutamaat/malaat en in verhoogde RKI met palmitoïel-L-karnitien/malaat as substrate getoon. 100 nM FCCP het mitokondriale respirasie verhoog soos aangedui deur 'n verhoogde RKI en QO₂(S3) respirasie met palmitoïel-karnitien/malaat as substrate, maar het verhoogde mitokondriale ont koppeling, aangedui deur 'n laer ADP/O verhouding, dus verlaagde oksidatiewe fosforilering snelheid vir beide staat 3 en 4, tot gevolg gehad. 250 nM FCCP het mitokondrieë volledig ont koppel. Nie een van die middels het die sitraatsintase aktiwiteit beïnvloed nie. Die LC3A/B-II/I verhouding was laer in beide iskemie en herperfuseerde harte in vergelyking met die basislyn terwyl 3-MA geen effek hierop getoon het nie. BNIP3L/Nix vlakke was verhoog in

herperfusie vs iskemie terwyl die teenoorgestelde effek met Parkin en P62/SQSTM1 vlakke waargeneem is. Post-iskemiese behandeling met 3-MA het verhoogde PINK1 tot gevolg gehad. 100 nM FCCP het TOM70 uitdrukking verhoog in vergelyking met 250 nM maar die teenoorgestelde is waargeneem vir Parkin vlakke. 3-MA het geen effek op infarkt-grootte gehad nie terwyl beide 100 nM en 250 nM infarkt-grootte verklein het ($p=0.0001$). Beide middels het geen effek op funksionele herstel gehad nie maar 250 nM FCCP het totale meganiese hartversaking veroorsaak en ook gelei tot beduidende hoër vlakke van oorblywende ADP.

Gevolgtrekking: Manipulering van mitofagie het die uitkoms van iskemie/herperfusie beïnvloed: afregulering met 3-MA het (i) baie min effek op mitofagie gedurende sekere protokolle gehad, aangedui deur die verhoogde PINK1 vlakke, alhoewel (ii) dit mitokondriale respirasie verhoog het maar (iii) tot swak funksionele herstel gelei het en (iv) geen effek of infarkt-grootte gehad het nie.

Opregulering van mitofagie met 100 nM FCCP was (i) geassosieer met miokardiale beskerming en (ii) kleiner infarkt-grootte, maar (iii) die ontkoppelingseffekte van FCCP het oksidatiewe fosforileringsnelheid en dus (iv) ATP vorming verlaag met gevolglike (v) swak funksionele herstel.

Acknowledgements

It has been an honour to work closely with two outstanding researchers in their respective fields making this Masters study a very rewarding experience for me. Both have been an inspiration to me.

- To Prof Barbara Huisamen, my supervisor: Thank you for your commitment and always being there to assist. Your input and supporting role has been beyond my expectation and I am truly grateful. This work was completed successfully because of your contribution throughout.
- To Prof Amanda Lochner, my co-supervisor: Thank you also for your support and always being willing and available to help. Your guidance throughout my studies is sincerely appreciated. I would certainly not have achieved this much without your input as well, enthusiasm and confidence in me.

A special thanks to

- the Department of Medical Physiology for affording me the opportunity to further my studies. To all the staff members and my incredible colleagues, you have made my experience pleasant. I am grateful to have crossed paths with you all.
- Dr Ruduwaan Salie and Sonia Genade, for their assistance in my regional ischaemia perfusions. Dr Gassen Naidoo and Dr Erna Marais for their assistance with the HPLC experiments. Dr Karthik Dhanabalan for assisting me in the labs. Your help is deeply appreciated
- The National Research Foundation and Stellenbosch University for funding my studies.
- To my pillars in life, my parents (Salathiel and Verna Mzezewa) and all my loving sisters (Tsongirirai, Nokuthula, Lerato and Ropafadzo), thank you for your support and prayers.

Above all, thank you to the One who makes all good things possible, my Father in heaven and my Lord and Saviour Jesus Christ. Thank you for blessing me with this opportunity and to be able to complete my MSc studies.

Table of Contents

Declaration	i
Abstract	ii
Abstrak	iv
Acknowledgements	vi
Table of Contents	vii
List of Figures	x
List of Tables	xii
Abbreviations	xiv
Chapter 1 Literature Review	1
The Role of Mitophagy in Damage Incurred by Myocardial Ischaemia Reperfusion	1
1.1. The heart and cardiovascular diseases	1
• 1.1.1. Cardiac Metabolism.....	3
• 1.1.2. Mitochondria.....	6
• 1.1.3. Oxidative phosphorylation.....	7
1.2. Mitochondria in cellular mechanisms.....	10
• 1.2.1. Mitochondria and Calcium	10
• 1.2.2. Mitochondria and cell death	12
• 1.2.3. Autophagy.....	14
• 1.2.4. Mitophagy.....	18
• 1.2.5. Mitophagy and the heart	20
1.3. Ischaemia reperfusion.....	21
• 1.3.1. Ischaemia/Reperfusion: Mitochondria and the electron transport chain ...	24
• 1.3.2. Autophagy in the setting of I/R	25
• 1.3.3. Mitophagy in the setting of I/R.....	26
1.4. Pharmacological Tools	28

• 1.4.1. FCCP and Mitophagy	28
• 1.4.2. 3-Methyl-Adenine (3-MA) and Autophagy.....	29
1.5. Concluding Remarks	32
Chapter 2 Methods.....	34
2.1. Perfusion technique of the isolated rat heart.....	34
• 2.1.1. Global ischaemia	35
• 2.1.2. Regional Ischaemia.....	38
2.2. Mitochondrial Isolation	39
• 2.2.1. Mitochondrial Oxidative Phosphorylation	39
• 2.2.2. Lowry Assay	42
• 2.2.3. Citrate Synthase Assay	43
2.3. Western Blotting	45
• 2.3.1. Protein extraction.....	45
• 2.3.2. Protein separation and transfer	47
• 2.3.3. Immunodetection of protein using secondary antibody.....	50
2.4. High Performance Liquid Chromatography	51
2.5. Statistical Analysis.....	52
Chapter 3 Results	53
3.1. Standardisation of Western blotting technique.....	53
3.2. Standardisation of autophagy markers under baseline conditions: effect of 3-methyl-adenine (3-MA) and N, N-dimethylformamide (DMF)	53
• 3.2.1. Effect of 3-MA and DMF on mitochondrial oxidative phosphorylation function of hearts perfused under baseline conditions	61
3.3. Autophagic markers of hearts exposed to ischaemia or reperfusion with or without 3-MA and DMF as a vehicle	61
3.4. Autophagic markers of hearts exposed to ischaemic or reperfusion protocols treated with or without 3-MA and H ₂ O as a vehicle.....	74

• 3.4.1. Mitochondrial Function of hearts from ischaemic or reperfusion protocols treated with or without 3-MA with H ₂ O as a vehicle.....	83
• 3.4.2. Mitophagic markers of hearts exposed to ischaemic or reperfusion protocols treated with or without 3-MA and H ₂ O as a vehicle.	88
• 3.4.3. Citrate synthase activity of hearts treated with or without 3-MA in ischaemic or reperfusion protocols.	91
• 3.4.4. Effects of 3-MA pre-treatment on infarct size and area at risk.	92
3.5. Effect of FCCP pre-treatment on mitochondrial function, heart mechanical function and infarct size.	96
• 3.5.1. Dose response of FCCP concentrations 100nM-1µM.....	97
• 3.5.2. Effects of FCCP pre-treatment after 20 min reperfusion at 100 nM and 250 nM concentrations	101
• 3.5.3. FCCP (100 nM) and Mitochondrial Function	104
• 3.5.4. Infarct size and area at risk of hearts pre-treated with FCCP with DMSO as a vehicle.....	108
• 3.5.5. Mechanical performance and functional recovery of hearts subjected to 35min regional ischaemia: effect of FCCP	110
• 3.5.6. High energy phosphate levels of hearts pre-treated with 250 nM FCCP .	113
3.6. Comparison of the effects of 3-MA and FCCP on infarct size, area at risk and mechanical functional recovery.....	115
Chapter 4 Discussion	116
4.1 Standardisation of Mitophagy Markers	116
• 4.1.1. Effects of 3-MA and DMF on hearts subjected to I/R.....	118
• 4.1.2. Effects of 3-MA dissolved in water on autophagy in hearts subjected to I/R	119
4.2 Effects of 3-MA on mitochondrial mitophagy	120
4.3 Effects of stimulating Mitophagy with FCCP	124
Chapter 5 Conclusion and Future Recommendations	128
5.1. Comparison of the effects of 3-MA and FCCP on infarct size, area at risk and mechanical functional recovery.....	128

5.2. Limitations and Future studies.....	128
References	130

List of Figures

Figure 1:1 Cross-bridge process of sliding filaments (Fox 2009)	3
Figure 1:2 Krebs Cycle with the different intermediates in its metabolism (Kaplan 2014).	5
Figure 1:3 Pathways of cardiac fatty acid oxidation in the mitochondrial matrix and glucose metabolism in the cytosol and mitochondria (Stanley et al. 2005).	6
Figure 1:4 Diagram illustrating the five compartments of the mitochondria (Caprette 2007).	7
Figure 1:5 Aerobic mitochondrial respiration (Schoultz et al. 2011).	8
Figure 1:6 Diagram depicting the overview of the autophagic process (Hamacher-Brady 2012). ..	16
Figure 1:7 Scheme of PINK1/Parkin and receptor mediated mitophagy (Shires & Gustafsson 2015).	20
Figure 1:8 Diagram illustrating the main metabolic changes during ischaemia and reperfusion (Hausenloy & Yellon 2013).	22
Figure 1:9 Diagram illustrating the outcome of mitophagy in normal ,upregulated and downregulated conditions (Shires & Gustafsson 2015).	27
Figure 2:1 Baseline perfusion protocol for preliminary studies	36
Figure 2:2 Outline of baseline, global ischaemia and reperfusion perfusion protocols.....	37
Figure 2:3 Outline of regional ischaemia perfusion protocol.	38
Figure 2:4 Illustration of mitochondrial registration generated by the oxygraph.....	41
Figure 2:5 . Summary flow diagram of citrate synthase assay..	44
Figure 3:1 Mitochondrial levels of PINK1 and p62 of hearts from baseline perfusion and hearts exposed to 20 min of global ischaemia.....	54
Figure 3:2 Perfusion protocol for untreated baseline hearts and hearts treated with 3-MA and DMF as a vehicle.	55
Figure 3:3 LC3 A/B-I level and LC3 A/B-II levels of tissue from un-perfused hearts and hearts perfused with or without 3-MA and DMF as a vehicle.	58
Figure 3:4 LC3A/B-II/I ratio of tissue from un-perfused and perfused hearts treated with or without 3-MA and DMF	59
Figure 3:5 Beclin-1 (D40C5) levels and BNIP3/Nix (D4R4B) levels of tissues from un-perfused and perfused hearts treated with or without 3-MA and DMF.....	60

Figure 3:6 Mitochondrial parameters measured in glutamate plus malate or palmitoyl-L-carnitine plus malate substrate media, isolated from un-perfused hearts and baseline perfused hearts, treated with or without 3-MA with DMF as a vehicle.....	64
Figure 3:7 Perfusion protocols of hearts exposed to untreated 25 min of global ischaemia or pre-treated with 3-MA or DMF before 25 min of global ischaemia.....	65
Figure 3:8 BNIP3L/Nix (D4R4B) levels of heart tissue exposed to ischaemic and reperfusion protocols treated with or without 3-MA and DMF as a vehicle	69
Figure 3:9 Beclin-1 (D40C5) levels of heart tissue exposed to ischaemic and reperfusion protocols treated with or without 3-MA and DMF as a vehicle..	70
Figure 3:10 LC3A/B-I levels of heart tissue exposed to ischaemic and reperfusion protocols treated with or without 3-MA and DMF as a vehicle	71
Figure 3:11 LC3A/B-II levels of heart tissue exposed to ischaemic and reperfusion protocols treated with or without 3-MA and DMF as a vehicle	72
Figure 3:12 LC3 A/B-II/I ratio levels of heart tissue exposed to ischaemic or reperfusion protocols with or without 3-MA and DMF as a vehicle	73
Figure 3:13 Perfusion protocols for hearts exposed to global ischaemia or reperfusion with or without 3-MA administration.....	74
Figure 3:14 Beclin-1 (D40C5) levels of heart tissue from ischaemic or reperfusion protocols treated with or without 3-MA..	78
Figure 3:15 BNIP3L/Nix (D4R4B) levels of heart tissue from ischaemic or reperfusion protocols treated with or without 3-MA.	79
Figure 3:16 LC3A/B- I levels of heart tissue from ischaemic or reperfusion protocols treated with or without 3-MA.	80
Figure 3:17 LC3A/B- II levels of heart tissue from ischaemic or reperfusion protocols treated with or without 3-MA..	81
Figure 3:18 LC3A/B- II/I ratio of hearts from ischaemic or reperfusion protocols treated with or without 3-MA.....	82
Figure 3:19 Mitochondrial parameters measured in glutamate plus malate or palmitoyl-L-carnitine plus malate substrate media, isolated from heart tissue exposed to ischaemic and reperfusion protocols perfused with or without 3-MA.....	87
Figure 3:20 PINK1 levels of mitochondria from hearts perfused with or without 3-MA in ischaemic and reperfusion protocols.....	88
Figure 3:21 Mitochondrial Parkin levels of hearts perfused with or without 3-MA in ischaemic or reperfusion protocols.....	89

Figure 3:22 Mitochondrial p62 levels of hearts perfused with or without 3-MA in ischaemic and reperfusion protocols.	90
Figure 3:23 Citrate synthase activity from mitochondria isolated from hearts from ischaemic and reperfusion protocols treated with or without 3-MA	91
Figure 3:24 Regional ischaemia perfusion protocol for hearts pre-treated with 3-MA.....	92
Figure 3:25 Percentage of infarct size and area at risk for hearts pre-treated with 3-MA before regional ischaemia	93
Figure 3:26 Percentage of cardiac output recovery and total work recovery of hearts pre-treated with 3-MA during regional ischaemia.	95
Figure 3:27 Perfusion protocol used for FCCP dose response and subsequent experiments.	96
Figure 3:28 Mitochondrial PINK1 and Parkin levels of hearts pre-treated with FCCP concentrations ranging from 100 nM to 1000 nM (1 μ M).....	99
Figure 3:29 Mitochondrial p62 levels of hearts pre-treated with FCCP concentrations ranging from 100nM to 1000nM (1 μ M).	100
Figure 3:30 Mitochondrial TOM70 and Parkin levels of hearts pre-treated with 100 nM and 250 nM FCCP concentrations.	102
Figure 3:31 Mitochondrial p62 and PINK1 levels of hearts pre-treated with 100 nM and 250 nM FCCP concentrations.....	103
Figure 3:32 Mitochondrial parameters measured in palmitoyl-L-carnitine plus malate and glutamate plus malate substrates of hearts pre-treated with FCCP (100 nM) during global ischaemia/reperfusion.	106
Figure 3:33 Citrate Synthase activity of hearts pre-treated with FCCP at different concentrations	107
Figure 3:34 Regional ischaemia protocol for infarct size determination.....	108
Figure 3:35 Infarct size and of area at risk of hearts pre-treated with FCCP (100 nM and 250 nM),	109
Figure 3:36 Percentage recovery of cardiac output and total work for hearts pre-treated with FCCP (100 nM and 250 nM)	112
Figure 3:37 ADP and ATP levels of mitochondria from hearts pre-treated with 250 nM FCCP...	114

List of Tables

Table 2:1 Components of the two incubation media used for the mitochondrial analysis	40
Table 2:2 Lysis buffer composition for mitochondrial and heart tissue	45

Table 2:3 BSA serial dilution for Bradford analysis.....	46
Table 2:4 Reagents used for Protein separation and protein transfer.....	47
Table 2:5 Summary of Western blotting information for different proteins analysed.....	49
Table 2:6 Reagents used for HPLC analysis.....	51
Table 3:1 Mechanical data of hearts perfused under baseline perfusions : effects of 3-MA and DMF as a vehicle.....	57
Table 3:2 Mechanical data before ischaemia and after ischaemia for hearts perfused with the autophagy inhibitor 3-MA with DMF as a solvent.....	67
Table 3:3 Mechanical data before ischaemia and after ischaemia for hearts perfused with the autophagy inhibitor 3MA with water as a solvent.....	76
Table 3:4 Mechanical data of hearts before being subjected to 35min regional ischaemia and after ischaemia: effect of pre-treatment with 3-MA (1 mM) in comparison to untreated controls.....	94
Table 3:5 Mechanical data of hearts before and after exposure of hearts to 25 min global ischaemia: effects of different concentrations of FCCP (100 nM to 1000 nM).....	98
Table 3:6 Mechanical data of hearts before and after exposure to 35 min regional ischaemia: effects of FCCP (100 nM).	111
Table 3:7: Comparison of effects of 3-MA vs FCCP..	115

Abbreviations

Units of measurement and symbols

cm	centimetres
°C	degrees Celsius
g	grams
kDa	kilo Daltons
kg	kilograms
mg	milligrams
L	litres
μL	microliters
mL	millilitres
nm	nanometres
mm	millimetres
nM	nano molar
μM	micro molar
mM	millimolar
M	molar
nmol	nano mole
mA	milliamps
min	minutes
OD	optical density
rpm	revolutions per minute
sec	seconds
UV	ultraviolet
V	volts

Chemical Components

3-MA	3 Methyl adenine
ACN	Acetonitrile
APS	Ammonium persulfate
BHT	Butylated hydroxytoluene
BSA	Bovine Serum Albumin
Ca²⁺	Calcium ion
CaCl₂	Calcium chloride
CCCP	Carbonylcynide m-chlorophenylhydrazone
CO₂	Carbon dioxide
CuSO₄	Copper sulphate
dH₂O	Distilled water
DMF	N, N-Dimethylformamide
DMSO	Dimethyl sulfoxide
DNP	2,4-dinitrophenol
DTNB	5,5'-Dithiobis-(2-nitrobenzoic acid)
ECL	enhanced chemiluminescence
EDTA	Ethylenediaminetetraacetic acid
EGTA	Ethyleneglycoltetraacetic acid
FCCP	Carbonyl cyanide 4-trifluoro-methoxy phenylhydrazo
HCl	Hydrochloric acid
KCl	Potassium Chloride
KE	EDTA +KCl
KH₂PO₄	Potassium dihydrogen phosphate
KHB	Krebs-Henseleit buffer

KOH	Potassium hydroxide
MgSO₄	Magnesium sulphate
Na²⁺	Sodium ion
Na₂CO₃	Sodium Carbonate
Na₂S₂O₄	Sodium dithionite
Na₃VO₄	Sodium orthovanadate
NaCl	Sodium Chloride
NaHCO₃	Sodium bicarbonate
NaOH	Sodium hydroxide
O₂	Oxygen
PCA	Pechloric acid
PMSF	Phenyl methyl sulfonyl fluoride
TBAP	Tetrabutylammonium phosphate monobasic
TBS	Tris buffered saline
TCA	Trichloroacetic acid
TEMED	N, N, N', N', - tetramethylethylenediamin
TNB	5-thio-2-nitrobenzoic acid
Tris	tris aminomethane/hydroxymethyl
TTC	2,3,5-triphenyltetrazolium chloride

Proteins and other Compounds

ADP	Adenosine diphosphate
AMP	Adenosine monophosphate
AMPK	Adenosine monophosphate-activated protein kinase
ANT	Adenine nucleotide translocator
ATG	AuTophagy related genes
ATP	Adenosine triphosphate
Bcl-2	B cell lymphoma 2
BH3	Bcl2 homology 3
BNIP3	Bcl-2/adenovirus E1B 19-kDa protein- interacting protein 3
CD 36	Cluster of differentiation 36
CoA	Coenzyme A
CPT 1	Carnitine palmitoyl transferase 1
Cyp-D	Cyclophilin D
ETC	Electron transport chain
FADH₂	Flavin adenine dinucleotide
FFA	Free fatty acids
FUNC1	Fun14 domain containing 1
GTP	Guanosine triphosphate
LC3	Protein 1 light chain protein
MCU	Mitochondrial Ca ²⁺ uniporter
mPTP	Mitochondrial permeability transition pore
mTOR	Mammalian target of rapamycin
NADH	Nicotinamide adenine dinucleotide
NCLX	Sodium calcium lithium exchanger

NCX	Sodium calcium exchanger
NRF-1	Nuclear Respiratory factor 1 (gene)
P62/SQSTM1	Nucleoporin 62/ Sequestosome 1
PARIS	Parkin interacting substrate
PDH	Pyruvate dehydrogenase complex
PGC-1α	Peroxisome proliferator-activated receptor gamma coactivator 1-alpha
Pi	Inorganic phosphate
Pi3k	Phosphoinositide-3-kinase
PI3P	Phosphatidylinositol 3-phosphate
PiC	Phosphate carrier
PINK1	Phosphatase and tensin homolog induced putative kinase 1
SCaMC-3	Ca ²⁺ -sensitive carrier
SMAC	Second mitochondria- derived activator of caspase
TOM70	Translocase outer mitochondrial membrane 70
UBI	Ubiquitin like
UCP2 and 3	Uncoupling protein 2 and 3
ULK1	Unc 51-Like-Kinases 1
Vps	vacuolar protein sorting

Other

20R + 3-MA A. ISCH	3-MA administered after ischaemia or at the onset of reperfusion
20R + 3-MA B. ISCH	3-MA administered before ischaemia followed by reperfusion
20R + FCCP B. ISCH	FCCP administered before ischaemia followed by reperfusion
20R	Perfusion protocol including 20 min reperfusion
25 ISCH + 3-MA	3-MA administered before 25 min of global ischaemia
25 ISCH	25 min global ischaemia
AB	Antibody
ADP/O	Adenosine diphosphate per oxygen atom
ANOVA	Analysis of Variance
C40	Control 40- stabilisation perfusion of 40 min
CVD	Cardiovascular disease
GD	Glucose Deprivation
GFP	Green fluorescent protein
HPLC	High Performance Liquid Chromatography
HRP	Horse radish peroxidase
I/R	Ischaemia/Reperfusion
IHD	Ischaemic heart disease
L	Langendorf e.g. 10'L
LAD	Left anterior descending
POH	Pressure overload hypertrophy
PTM	Posttranslational modification
PVDF	Polyvinylidene fluoride
RCI	Respiratory control index
ROS	Reactive oxygen species

S3	State 3 respiration
S4	State 4 respiration
SDS-Page	Sodiumdodecyl sulphate polyacrylamide gel electrophoresis
SEM	Standard error of the mean
TCA	Tricarboxylic Acid cycle
TEM	Transmission electron microscopy
WH	Working heart mode e.g. 10'WH
WHO	World Health Organisation

Chapter 1

Literature Review

The Role of Mitophagy in Damage Incurred by Myocardial Ischaemia/ Reperfusion

1.1. The heart and cardiovascular diseases

The heart is the first organ to develop in the embryo and throughout our lives it carries the vital task of pumping nutrients and oxygen to the cells of our body along with the removal of waste from cells (Stefan 2015) by means of the blood and vessels. Together these form our cardiovascular system.

The heart is arguably the hardest working muscle in the body, pumping up to approximately 7 500 L of blood per day in 101 000 beats (Watson 2009). However, the ability of the heart to function effectively can be compromised by our lifestyle, genetics, age and other complications leading to consequences such as heart failure. This further highlights the importance of the wellbeing of our heart, as it is core to our vitality.

Disorders of the cardiovascular system include: myocardial infarction, angina (ischaemic heart disease, or coronary heart disease), stroke, hypertension, congestive heart failure and hardening of the arteries, among others. Most deaths from cardiovascular disease (CVD) are as a result of ischaemic heart disease (IHD) (WHO 2014). IHD is characterised by the severe impairment of the coronary blood supply occurring usually as a result of thrombosis or other chronic alterations of coronary atherosclerotic plaques (Buja 2005). This may be triggered by a number of risk factors such as diet, obesity, hypertension, smoking, stress and depression to name a few, although prevalence may vary due to age, sex and geographical location (Yusuf et al. 2004). Impairment of the coronary blood supply results in a decrease in oxygen and nutrients and ultimately the energy supplies to the heart. With a deficient supply of blood to the heart cells i.e. cardiomyocytes, metabolic and cellular processes will be negatively affected. The extent of the negative effects on the cardiomyocytes, tissue and ultimately organ, highly depends on the duration and degree of ischaemia applied. Having mentioned this, one may reason that restoration of blood supply should be administered as soon as possible, to restore normal cellular (metabolic) processes. However immediate restoration of blood supply,

although essential for cardiomyocyte survival, has been reported to have pathological consequences (Kalogeris et al. 2012). This phenomenon of blood flow restoration is known as reperfusion and the damage accompanied by it, is known as reperfusion injury. Worldwide, there is an ongoing quest to understand reperfusion damage and to develop mechanisms to curb the damage incurred by reperfusion of the ischaemic myocardium.

As ischaemic heart disease is a result of a reduction in or lack of oxygen supply to the heart, most of the existing therapies involve increasing the oxygen supply to the heart (revascularisation), or decreasing the demand of the oxygen needed by the heart using e.g. beta (β)-blockers or nitrates, however, these approaches have not seen major clinical use. (Wang & Lopaschuk 2007). The common modalities of revascularisation for restoring blood perfusion to ischaemic myocardium, include percutaneous angioplasty and coronary artery bypass surgery, however, these therapies are not able to promote regeneration of the damaged heart tissue and would be less effective in patients with severe ischaemic cardiomyopathy (Masumoto & Yamashita 2016). In addition to these, are treatments including lifestyle changes, medical devices and more recently, stem-cell based therapies, which aim to ameliorate cardiac dysfunctions. In a recent review it was reported that direct injections of stem cells into ischaemic hearts did not sufficiently improve heart function due to the poor survival support of the grafted cells by the heart (Masumoto & Yamashita 2016). However, improvements on these outcomes are being continuously researched as stem-cell based therapies seem to be a promising strategy. Unlike a few other organs of the body, the heart cannot repair itself fully to its original state after injury (Stefan 2015). Heart transplantation is the only replacement therapy available to date, however, that in itself is limited by the availability of donors. Having mentioned all this, remains the hard reality that CVDs and specifically ischaemic heart disease, have become the leading cause of death in the world today (WHO 2016).

Based on the above, an increase in knowledge and studies of the underlying mechanisms of CVDs are a prerequisite, along with preclinical studies in order to elucidate and manipulate the outcome of CVDs. This may then provide a platform for developing novel therapies or drugs to not only protect against or prevent the development of CVD, but also to protect the heart against reperfusion injury. In the search for new therapies, mitochondria have recently emerged as significant role players. The importance of mitochondria will be discussed at a later stage in this literature survey.

1.1.1. Cardiac Metabolism

Cardiomyocytes are striated in structure and contain smaller subunits known as actin and myosin filaments, which are essential elements of the contraction process. The contraction of the heart is achieved through the sliding of these filaments over one another through the sequential binding and dissociation of myosin to actin, see Figure 1:1. The activation of the process requires adenosine triphosphate (ATP) to generate this force (Fox 2009).

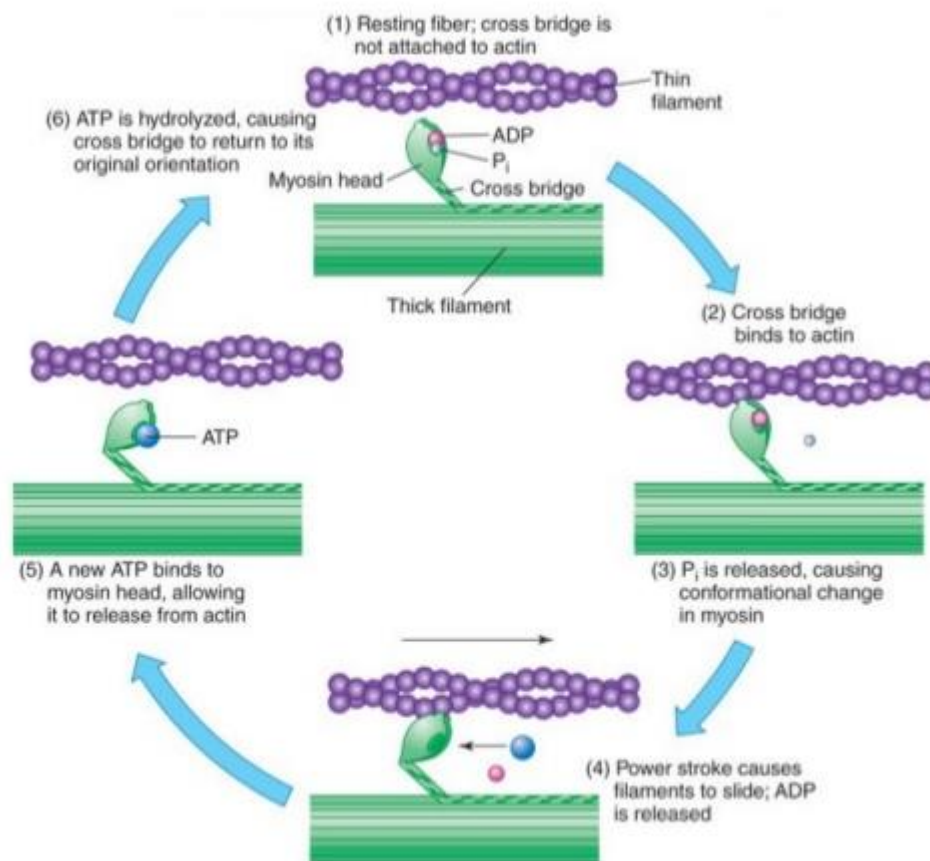


Figure 1:1 Cross-bridge process of sliding filaments. Myosin cross bridges attach to actin filaments through ATP hydrolysis to cause contraction. Relaxation occurs when the filaments detach from each other, this involves ATP attachment to the myosin cross bridges (Fox 2009).

ATP is a nucleoside triphosphate molecule and plays a vital role as an energy carrier molecule. ATP cannot be stored and is mainly derived from the metabolism of substrates such as glycogen, free fatty acids (FFAs) and lactate and is mainly synthesised through the mitochondrial ATP synthase enzyme (F₁F₀-ATPase). ATP drives all energy-mediated cellular activities such as cell division and transportation of substances across the membrane, making its availability central to the survival or death of a cell. As the heart is a continuously

contracting organ, its cells demand a continuous supply of ATP (Nagendran et al. 2013) to enable the processes of the sliding filament to take place.

The heart does not contain large energy reserves as other organs do and as a result, it relies heavily on the transportation of external substrates into the heart as sources to synthesise ATP. For its major sources of energy, the heart alternates between carbohydrates in the fed state and FFAs in the fasted state (Opie 2004). Only a small percentage is contributed by other substrates (Nagendran et al. 2013). However the heart is able to use other substrates such as amino acids and ketone bodies when they become abundantly available et al 2013).

FFA metabolism involves the transportation of long chain fatty acids from the plasma into the cardiomyocytes through protein channels, e.g. cluster of differentiation 36 (CD36) or passive diffusion across the membrane (Stephen et al 2013). Once transported into the cell, FFAs bind to the intracellular fatty acid binding protein before further metabolism (Opie 2004). The FFAs are activated by coenzyme A (CoA) to form fatty Acyl-CoA derivatives. When in excess, fatty Acyl-CoA can be stored as triglycerides. An integral mitochondrial membrane protein known as carnitine palmitoyl transferase 1 (CPT-1) converts the fatty acids to acyl carnitine, by transferring the acyl CoA group of the long chain fatty acid Acyl-CoA to carnitine, found in the mitochondrial matrix to form acyl carnitine, which is converted back to Acyl-CoA in the mitochondrial matrix. The latter compound is then subjected to a series of cleaving of its carbon groups through a process known as beta oxidation (Stanley et al. 2005). The by-products of this cycle are Acetyl-CoA and reduced nicotinamide adenine dinucleotide (NADH), a coenzyme used to assist in the synthesis of ATP (Stanley et al. 2005). Acetyl-CoA is metabolised in a separate process known as the Krebs cycle, the Citric acid cycle or the Tricarboxylic Acid cycle (TCA) (Figure 1:2) (referred to hereafter as the Krebs cycle in this literature survey) - which takes place in the matrix of the mitochondria. NADH is also produced in this cycle and carbon dioxide as a waste product (Fox 2009).

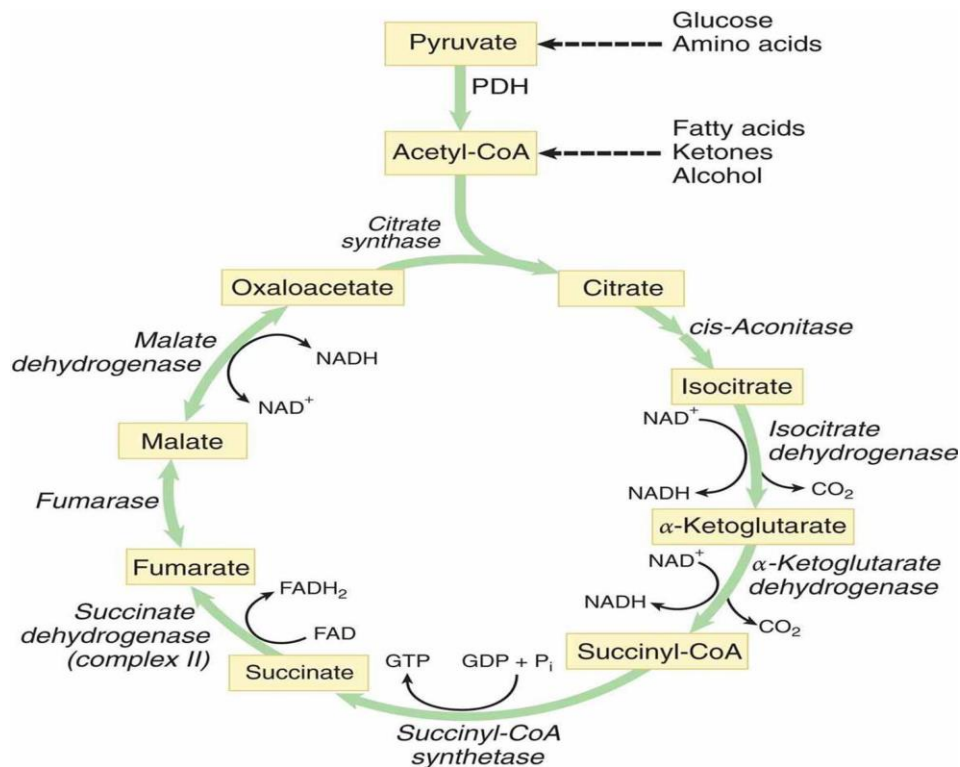


Figure 1:2 Krebs Cycle with the different intermediates in its metabolism. Acetyl-CoA and oxaloacetate are condensed to form citrate through citrate synthase. Citrate is then isomerised followed by a series of conversion reactions involving different enzymes. This is associated with the formation of NADH and FADH₂ and carbon dioxide as a waste product, until the formation of malate. Malate is dehydrogenated to form oxaloacetate along with NADH. Oxaloacetate reacts with Acetyl-CoA forming citrate and repeating the cycle again (Kaplan 2014).

The glycolytic pathway takes place in the cytoplasm of the cell. Glucose is transported into the cell by glucose transporters or Gluts and converted to glucose-6-phosphate, which is further transformed into pyruvic acid (pyruvate) through the process of glycolysis. Pyruvate is either shuttled into the mitochondria via the pyruvate dehydrogenase complex (PDH) where it is further catabolised to form Acetyl-CoA, which will then enter the Krebs cycle to produce substrates for the synthesis of ATP. In the event of insufficient oxygen supply, pyruvate is converted into lactate. The metabolic pathways of both fatty acids and carbohydrates are summarised in Figure 1:3.

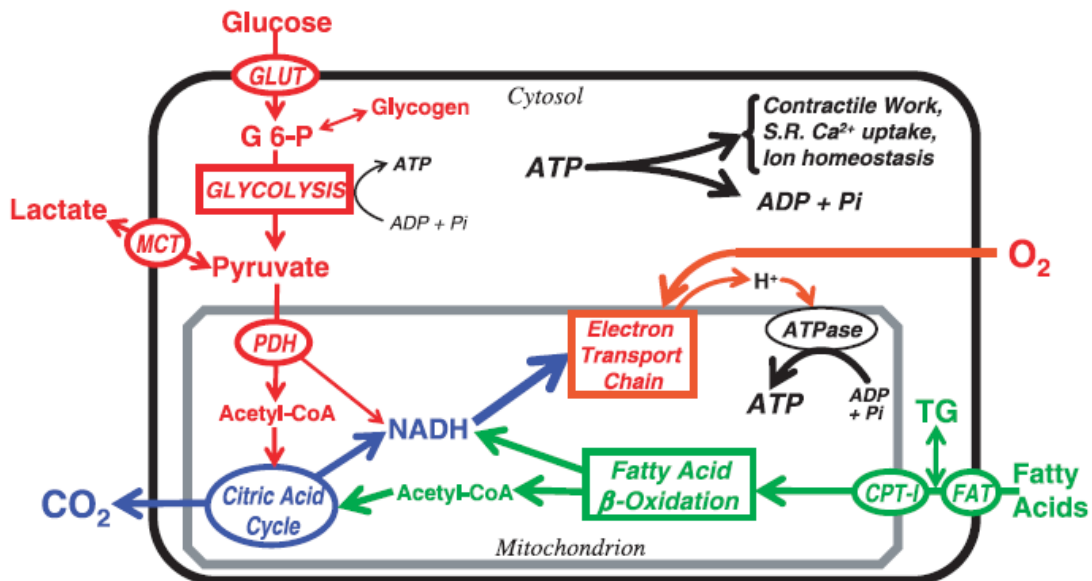


Figure 1:3 Pathways of cardiac fatty acid oxidation in the mitochondrial matrix and glucose metabolism in the cytosol and mitochondria (Stanley et al. 2005).

More than 95% of ATP formation in the heart is produced by the oxidative phosphorylation process in the mitochondria (section 1.1.3). The rest of the ATP production comes from a combination of glycolysis and guanosine triphosphate (GTP) formation in the Krebs cycle (Stanley et al. 2005).

1.1.2. Mitochondria

Mitochondria are organelles found within the cytoplasm of the cells and also considered to be the power house of the cell, as they are the main energy generating system in most eukaryotic cells (Chan 2006). Optimal mitochondrial function is therefore central to the health and function of the specialised cells that host high densities of them. In the heart, mitochondria are either concentrated just beneath the plasma membrane in the vicinity of the ion pumps, or between the myofibrils to be near the site of contraction (Nickel et al. 2013). The mitochondrion is a double membraned organelle which consists of four specialised compartments/regions; the outer membrane, intermembrane space, inner membrane and the matrix (McBride et al. 2006) (see Figure 1:4). The mitochondria have folded internal structures known as cristae found within the matrix of the mitochondria. They are an extension of the inner mitochondrial membrane which is mainly involved in oxidative phosphorylation.

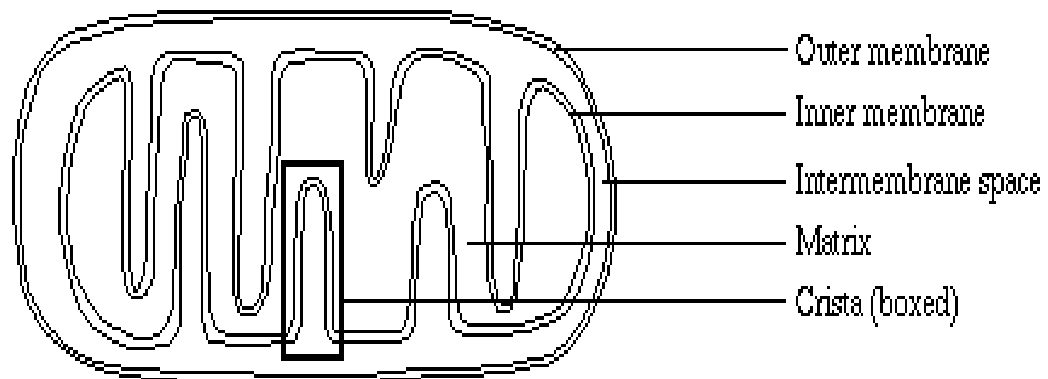


Figure 1:4 Diagram illustrating the five compartments of the mitochondria. The outer membrane, inner membrane, intermembrane space, matrix and the cristae (Caprette 2007).

Apart from producing ATP, the mitochondrion also has other key roles in the cell including fatty acid synthesis, calcium homeostasis, cell death, autophagy, innate immunity (Tait & Green 2012) and similarly are the producers of reactive oxygen species (ROS), the spearheads in oxidative signalling (Canini & Batandier 2016). For the purposes of this study, only the role of mitochondria in calcium homeostasis, cell death and autophagy will be discussed (section 1.2).

1.1.3. Oxidative phosphorylation

Oxidative phosphorylation takes place in the inner membrane of the mitochondria. This is the final stage of the aerobic respiration and it is also the site for the bulk of ATP synthesis in the cell (Stanley et al. 2005). The multistep process primarily consists of four enzyme complexes, embedded in the inner mitochondrial membrane and two mobile electron carrier molecules that pass along electrons generated from NADH or FADH of oxidised fatty acids or glucose (Matti 1999) to molecular oxygen through the enzyme complexes. This phenomenon of a series of electron transfers is also known as the electron transport chain (ETC).

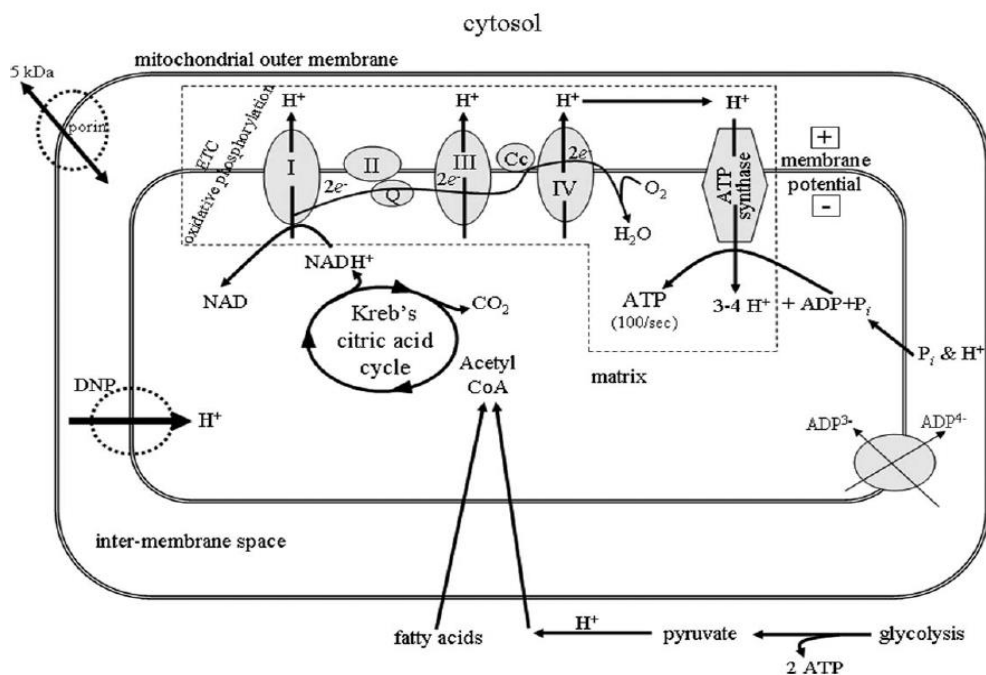


Figure 1:5 Aerobic mitochondrial respiration: NADH and FADH are oxidised by protein complex 1 and complex 2 respectively. The electrons are then transferred through the mobile electron transfer carriers, coenzyme-Q and cytochrome c to the next protein complexes creating a succession of redox reactions until the electrons are finally transferred to oxygen, which is reduced to water (Schultz et al. 2011).

The four complexes involved in mitochondrial respiration include complexes I (NADH dehydrogenase), II (succinate dehydrogenase), III (cytochrome c oxidoreductase) and IV (cytochrome c oxidase). The two mobile electron carriers involved are coenzyme-Q and cytochrome c located on the inner membrane and intermembrane space respectively (Lesnefsky et al. 2001). In respiring mitochondria electron transport is driven by the proton motive force (pmf) (Brand & Nicholls 2011). Substrates such as pyruvate and glutamate lead to the reduction of NAD⁺ and feed two electrons to complex I only. However providing glutamate or pyruvate alone in the absence of malate will not sustain respiration in isolated mitochondria or in permeabilised cells or tissues and ultimately lead to lower oxygen consumption rates (Lin & Scott 2012). Addition of small amounts of malate allows for the formation of oxaloacetate. Oxaloacetate then combines with Acetyl-CoA forming citrate, which is metabolised in the Krebs cycle (Figure 1:2). Malate administration on its own would result in the depletion of the Krebs cycle intermediates (Lin & Scott 2012). Electron transfer in Complex I is coupled to the proton translocation across the membrane into the intermembrane space.

Complex II is also involved in the Krebs cycle and is an inner mitochondrial membrane bound enzyme. The substrate succinate is oxidised to fumarate. The conversion of the substrate transfers electrons to the non-haem group on FAD complex II before being transferred to coenzyme-Q (Chain 2000). Complex III catalyses electron transfer from reduced coenzyme-Q to oxidised cytochrome c. This complex is also involved in the coupling of electron transfer with proton translocation similar to complex I (Lin & Scott 2012). Complex IV forms the concluding step of the electron transport chain, where electrons are finally transferred to oxygen to form water. This complex is also coupled with proton translocation across the inner mitochondrial membrane (Lin & Scott 2012). Proton translocation from complexes I, II and IV occurs from the matrix to the inter-membrane space via the enzyme complexes creating an electrochemical proton gradient in the inter-membrane space (Chan 2006). Complex V, F₁F₀-ATPase, provides a path for the protons to flow down the gradient back into the mitochondrial matrix. By this, energy is generated to phosphorylate ADP using inorganic phosphates and thus synthesising ATP (Lesnefsky et al. 2001).

The rate of oxidative phosphorylation is closely linked to the rate of myocyte energy demand and the utilisation of ATP to ensure a constant availability of ATP (Stanley et al. 2005). Mitochondrial oxygen consumption has been used to determine its bioenergetics with the aid of the standard oxygen electrode developed by Chance and Williams (Chance & Williams 1955). Conventionally, mitochondrial oxygen consumption is measured in the presence of inorganic phosphates alone and is referred to as state 1 respiration of mitochondria. To measure ADP independent respiration, substrates (e.g. glutamate plus malate etc.) would be added to the mitochondria leading to state 2 of mitochondrial respiration. Addition of ADP to mitochondria leads to a rapid increased consumption of oxygen. An increase in ADP, secondary to a rising energy demand would enhance phosphorylation, the processes prior and subsequently the formation of ATP. This is known as state 3 respiration (Lesnefsky et al. 2001). Conversion of all the ADP to ATP or the reduction in the availability of ADP, will ultimately decrease the rate of phosphorylation, resulting in mitochondria to respire as they would in their resting phase or “state 2”, this will also lead to an increased electrochemical potential across the membrane, stimulating the rate of the electron transfer (Lesnefsky et al. 2001). This is known as state 4 respiration (Lin & Scott 2012).

On the one hand state 3 respiration is controlled approximately equally by the ATP turnover and substrate oxidation, which includes the substrate metabolism, processing enzymes and related electron transport chain enzymes. Inhibition of any of these processes would decrease

the state 3 respiration. On the other-hand state 4 respiration is controlled by proton leak (depletion of the electrochemical gradient) and any other agents that affect the ATP synthase and cause the recycling of ATP to ADP (Brand & Nicholls 2011).

State 3 respiration divided by state 4 respiration gives a parameter used to measure mitochondrial function known as the respiratory control index (RCI). High RCI values indicate that mitochondria have a high capacity for substrate oxidation and ATP formation with low proton leak. There are no absolute RCI values for dysfunctional mitochondria as this may vary due to substrate utilisation and the type of tissue mitochondria were isolated from. However, any change in the oxidative phosphorylation procedure will affect the outcome of the RCI value and thus the RCI value remains an advantage as a parameter to measure mitochondrial function (Brand & Nicholls 2011).

The maximum amount of synthesized ATP per oxygen atom consumed during the transfer of electrons in the ETC, is referred to the ADP/O ratio or P/O ratio. This value will be altered if the mitochondria proton translocation is uncoupled from ATP synthesis. Therefore this parameter indicates the coupling efficiency of the mitochondria (Brand & Nicholls 2011).

Thus, the ADP/O parameter together with the mitochondrial respiratory states (i.e. 3 and 4) will be useful indicators of mitochondrial oxidative capacity and hence function.

1.2. Mitochondria in cellular mechanisms

1.2.1. Mitochondria and Calcium

Calcium (Ca^{2+}) is a universal secondary messenger that is involved in several cellular processes such as muscle contraction, fertilisation, cell proliferation and communication as well as driving increased energy demand (Berridge et al. 2000; Bhosale et al. 2015). Calcium is stored in the endoplasmic reticulum of cells and the sarcoplasmic reticulum of muscle cells. At rest, the Ca^{2+} concentrations are on average 100 nM within the cell, but cells become activated when these concentrations rise to approximately 1000 nM (Berridge et al. 2000). The increase in Ca^{2+} concentrations is triggered by stimuli that cause different Ca^{2+} mobilising signals, indicating the crucial role Ca^{2+} has in regulating numerous cellular processes (Berridge et al. 2000). In cardiomyocytes, Ca^{2+} signalling induces contraction amongst others. During an action potential, Ca^{2+} enters the cell through voltage dependent gates and subsequently binds to Ca^{2+} release channels of the sarcoplasmic reticulum, known as ryanodine receptors, leading to release of Ca^{2+} in the cytosol, a process known as the Ca^{2+} induced Ca^{2+} release. (Philipson & Nicoll 2000). Within cardiomyocytes, the mitochondria are closely allied with the SR, creating

a “mitochondrial Ca^{2+} micro-domain” allowing for high concentrations of Ca^{2+} to be created there in order to overcome the inner mitochondrial membrane permeability (Nickel et al. 2013).

Following contraction, an equal amount of Ca^{2+} has to be exported out of the cytoplasm of the cell to ensure muscle relaxation and cellular homeostasis. One of the mechanisms to ensure this regulation is through the sodium-calcium ($\text{Na}^+ - \text{Ca}^{2+}$) exchange transporter (NCX) present in the plasma membrane. This exchanger is mainly for Ca^{2+} efflux and involves the exchange of three Na^+ ions entering the cell for one Ca^{2+} ion leaving the cell (Philipson & Nicoll 2000). Coherent, cytoplasmic Ca^{2+} signalling is also crucial to the cell’s health and disordered signalling leads to cell death as a consequence (Bhosale et al. 2015). The crucial roles displayed by both Ca^{2+} and mitochondria highlight their importance of cellular function and survival.

To date it has become apparent that the majority of the physiological Ca^{2+} signals are associated with mitochondrial Ca^{2+} uptake (Bhosale et al. 2015), typifying a dialogue between Ca^{2+} signalling in the cell and mitochondria, in cell survival. The outer mitochondrial membrane is more permeable than the inner mitochondrial membrane and allows ions, including Ca^{2+} to be freely transported. Ca^{2+} uptake through the inner mitochondrial membrane is regulated by a selective ion channel known as the mitochondrial Ca^{2+} uniporter (MCU) (Tsai et al. 2016). The MCU remains closed when cytosolic Ca^{2+} concentrations are at resting levels (~ 100 nM) (low affinity), but is opened when these concentrations increase (Tsai et al. 2016). A study showed that MCU knockdown in pancreatic islet cells decreased the expression of components of the electron transport chain (Quan et al. 2015; Bhosale et al. 2015) suggesting the role of MCU in mediating increased Ca^{2+} cellular levels to the matrix of the mitochondria (Bhosale et al. 2015). The MCU is also required for cardiac ischaemia/reperfusion injury via the irreversible opening of the mitochondrial permeability transition pore (mPTP) (Bhosale et al. 2015).

The main driving force for Ca^{2+} entry into the mitochondria is the negative potential created from the proton translocation during the ETC (Csordás & Hajnóczky 2009). Ca^{2+} signalling initiates the increase in the mitochondrial bioenergetics productivity through two main processes. The first, as already mentioned above, is mediated through the MCU and is depended on the cytosolic Ca^{2+} concentrations. The second involves the Ca^{2+} -sensitive carrier SCaMC-3, which functions at the outer face of the inner mitochondrial membrane (Bhosale et al. 2015). Both pathways function together in order to increase oxidative phosphorylation. Increased Ca^{2+} activates rate-limiting enzymes in the Krebs cycle i.e. pyruvate, isocitrate and α -ketoglutarate dehydrogenase (Denton R.M 1985; Bhosale et al. 2015) (see Figure 1:2) and

thus upregulating the production of NADH, leading to an increase in the mitochondrial membrane potential and subsequently an increase in ATP synthesis (Bhosale et al. 2015).

Mitochondrial Ca^{2+} efflux is mainly through the plasma membrane family of $\text{Na}^+/\text{Ca}^{2+}$ exchangers i.e. NCLX ($\text{Na}^+/\text{Ca}^{2+} \text{Li}^+$), which is located in the inner membrane of the mitochondria. The Ca^{2+} exchange is driven by the negative membrane potential across the inner mitochondrial membrane and hence the efflux of Ca^{2+} is associated with the net import of positively charged ions into the matrix of the mitochondria (De Stefani et al. 2016). Ca^{2+} theoretically also escapes through the opening of the mPTP in pathological conditions, although efflux of Ca^{2+} in healthy mitochondria through the pore has been questioned as inhibition of the pore in energised mitochondria did not affect the mitochondrial Ca^{2+} uptake/release (Rizzuto et al. 2012).

1.2.2. Mitochondria and cell death

Mitochondria are also central in regulating cell death in response to different stressors such as DNA damage, loss of growth factors, oxidative stress and hypoxia. Cell death initiated by mitochondrial factors is referred to as intrinsic apoptosis (Manuscript & Syndromes 2010). This is mediated through the B-cell lymphoma 2 (Bcl-2) family proteins of the outer mitochondrial membrane or through the opening of the mPTP of the inner mitochondrial membrane (Kubli & Gustafsson 2012). Another form of cell death via mitochondria involves calpains, cysteine proteases localised to the cytosol and mitochondria, and they are known to regulate apoptosis and necrosis (Smith & Schnellmann 2012).

The Bcl-2 family are either anti-apoptotic or pro-apoptotic proteins. Anti-apoptotic proteins promote survival of the cell by inhibiting pro-apoptotic proteins. Pro-apoptotic proteins include the family of BH3 proteins such as Bcl-2/adenovirus E1B 19-kDa protein-interacting protein 3 (BNIP3) (Kubli & Gustafsson 2012). The pro-apoptotic proteins transduce stress indicators from the cytosol to the mitochondria to initiate cell death by binding to and neutralizing the anti-apoptotic Bcl-2 proteins (Kubli & Gustafsson 2012). When this occurs, cofactors like cytochrome c and second mitochondria-derived activator of caspase (SMAC)/Diablo are released into the cytosol and an apoptosome is formed which obligates the cell to programmed cell death (Mammucari et al. 2011).

Due to the electrochemical gradient required for the functioning of the ETC, the inner membrane of the mitochondria needs to be well maintained both structurally and functionally.

Apart from the MCU of the inner mitochondrial membrane, is the mPTP, a dormant non-specific pore (Halestrap & Richardson 2015). Changes in the inner mitochondrial membrane due to different signals could lead to the formation and opening of the mPTP (Manuscript & Syndromes 2010). Opening of the pore results in a loss of the electrochemical gradient across the membrane and as a result, a destruction in the ETC. This will not only ultimately lead to a hindrance in the synthesis of ATP but also a reverse function of the F1F0-ATPase protein (Halestrap 2009). Prolonged exposure of cells to such conditions leads to depletion of ATP levels and cell death via necrosis (Halestrap & Richardson 2015). An open pore also leads to an influx of solutes which will cause internal swelling of the membrane and eventual bursting of the mitochondrial structure. In the process, pro-apoptotic proteins are released into the cytosol of the cell causing cell death to take place (Kubli & Gustafsson 2012). The opening of the pore is primarily moderated by factors that alter its sensitivity to Ca^{2+} , oxidative stress, phosphate levels and membrane potential (Bhosale et al. 2015; Halestrap & Richardson 2015). However, pathological and increased amounts of mitochondrial Ca^{2+} uptake is the main initiator of cell death mediated through the mPTP (Bhosale et al. 2015). Importantly, cyclosporine A (CsA) an immunosuppressant drug prevalent in clinical use, restricts the opening of the mPTP (Bhosale et al. 2015).

The structural composition of the mPTP has not been fully elucidated (Siemen & Ziemer 2013) but it has been suggested to consist of Cyclophilin D (Cyp-D), adenine nucleotide translocator (ANT), mitochondrial F1F0-ATPase with inorganic phosphates and outer mitochondrial proteins as modulators of the pore (Halestrap & Richardson 2015). Due to the role of inorganic phosphates participating in the opening of the pore, phosphate carrier (PiC) along with its interactions with Cyp-D and ANT is proposed to be another structural component of the mPTP (Varanyuwatana & Halestrap 2012; Bhosale et al. 2015). Cyp-D is a matrix soluble protein and has been suggested to be involved in regulating the permeability transition of the mitochondria. It has also been demonstrated to facilitate in the opening of the pore by increasing its permeability to Ca^{2+} (Gonnern & Halestrap 1996). In a study by Nakagawa et al, they showed that mitochondria from mice with knock-out Cyp-D were still prone to apoptotic cell death induced by cytochrome c, while the Cyp-D knock-out did prevent necrotic cell death. They suggest that Cyp-D is involved in some regulation of necrosis but not apoptosis (Nakagawa et al. 2005).

In spite of the uncertainty of the structure of the pore, its role in the setting of ischaemia/reperfusion injury, discussed in section 1.3, has been most evidently defined in a few organs including the heart, where mitochondria are crucial organelles (Bhosale et al. 2015).

As mentioned earlier, cell death via mitochondria can also be induced through calpains. Calpains are activated by Ca^{2+} causing effects including cleavage of the ETC proteins, apoptosis inducing factors (AIF) and voltage channels, all of which could result in cell death, through the damage of mitochondria (Smith & Schnellmann 2012). Studies have also shown that inhibition of calpains during ischaemia/reperfusion resulted in lower apoptosis and infarct sizes (Khalil et al. 2005; Smith & Schnellmann 2012).

1.2.3. Autophagy

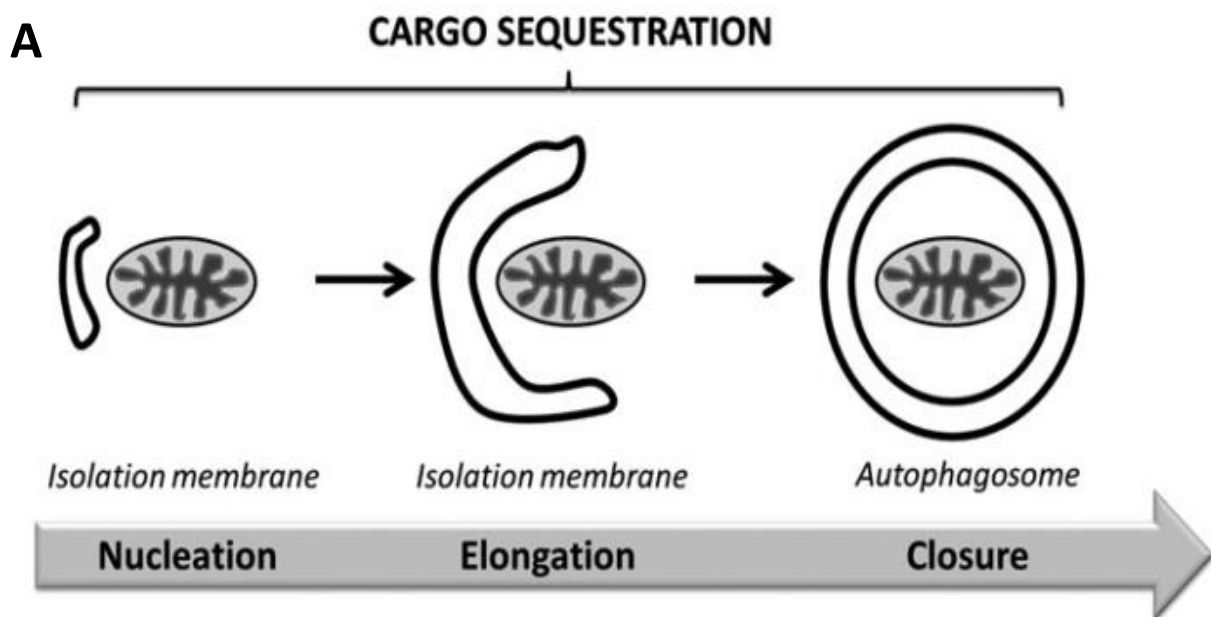
Autophagy is an intracellular degradation process critical to the homeostasis of a cell. The need for degradation may arise to compensate for a depletion in nutrients in the cell or to eliminate harmful substances (Youle & Narendra 2011; Hamacher-Brady 2012). Autophagy involves the removal of damaged cytoplasmic components e.g. pathogens, endoplasmic reticulum and dysfunctional mitochondria that will then be degraded (Manuscript & Protection 2013). This process can either be chaperone mediated or involves the formation of a double-membrane vesicle known as an autophagosome, the latter is the most common (intensely studied) process and is known as macro autophagy (Maejima et al. 2015). As opposed to apoptosis (discussed earlier, section 1.2.2) autophagy is more of a pro-survival mechanism for the cell. The term macro autophagy will be referred to as autophagy hereafter.

It is now known that autophagy can be a selective removal process achieved through specific autophagy receptors. The autophagy receptors can be classified based on their specific cargo binding domains. The different mechanisms of specific binding range from posttranslational modification (PTM) to transmembrane domains (Behrends & Fulda 2012). Ubiquitin binding domains, a form of PTM binding, are involved in protein specific interactions and these ubiquitin domains allow a large selection of proteins for autophagy commitment (Behrends & Fulda 2012). Selective autophagy can also be organelle specific and this is mediated through membrane embedding (Behrends & Fulda 2012). Mitophagy is an example of selective autophagy, specific to mitochondria and will be discussed in section 1.2.4.

Autophagy is initiated by different stimuli, including oxidative stress, caloric restriction and brief episodes of ischaemia and reperfusion (Manuscript & Protection 2013). An

autophagosome [Figure 1:6(A)] is formed from the nucleation of the isolated membrane in the cytosol. This structure is further elongated around the cargo to be sequestered, until the cargo is enclosed in the autophagosome. The autophagosome is then fused with endosomes and finally lysosomes in order to be degraded [Figure 1:6(B)] (Hamacher-Brady 2012).

Regulation of the autophagosome is complex, involving several proteins. AuTophagy (ATG) related genes are required for the formation of the autophagosome. There are several ATG genes, but three groups have been identified to be involved in the core machinery (Xie & Klionsky 2007). The first group being the Atg9 system, which consists of Atg9 and the Atg1 complex (Atg1+Atg13), Atg2 and Atg8. Second is the phosphatidylinositol 3-(OH)-kinase complex which consists of Beclin-1/Atg6 and vacuolar protein sorting (Vps) 34 and 15. The third group is the ubiquitin-like (Ubl) protein system which consists of two Ubl proteins, Atg8 and 12, enzymes and proteases (Xie & Klionsky 2007).



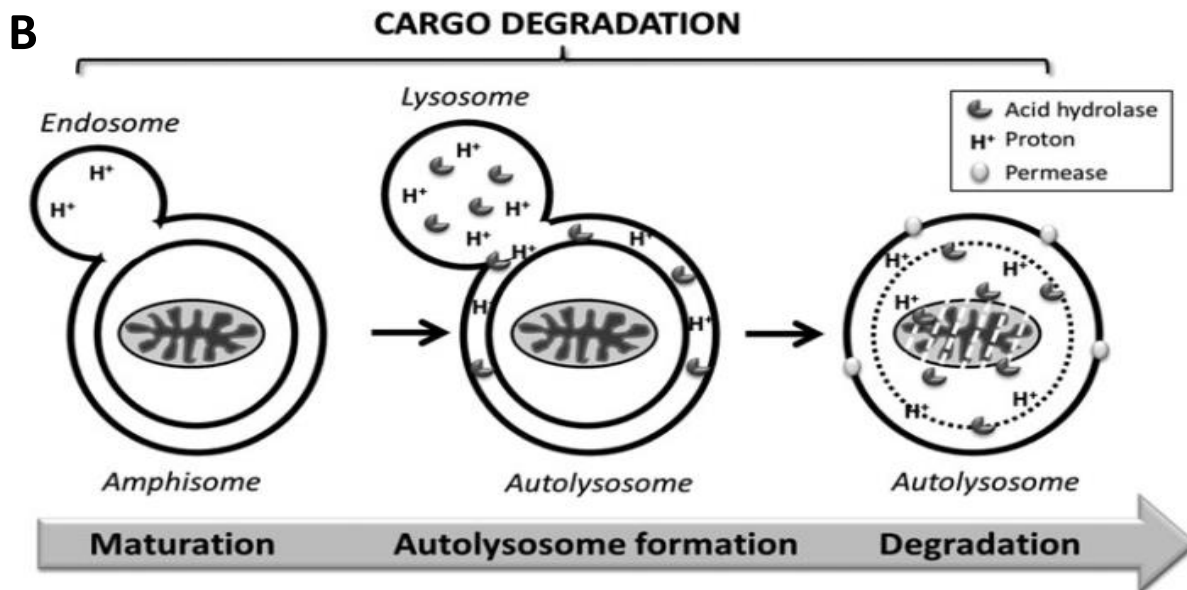


Figure 1:6 Diagram depicting the overview of the autophagic process. In (A) a membrane is formed around the cargo to be degraded, creating an autophagosome. In (B) the autophagosome is fused with enzyme containing lysosomes which will lead to the degradation of the cargo (Hamacher-Brady 2012).

Induction of autophagy is closely controlled by the opposing actions of two groups of PI3Ks (Hamacher-Brady 2012). Class I PI3K negatively regulates autophagy whereas class III PI3K are positive regulators of autophagy (Hamacher-Brady 2012). The mammalian target of rapamycin (mTOR), is a downstream protein target of class 1 PI3K/Akt that senses energy levels and stress levels and regulates cell growth and proliferation. In conditions of growth promoting factors, mTOR promotes anabolism of proteins by activating RNA translation and as a result, prevents autophagy from taking place. In conditions where nutrient levels have been depleted, mTOR is inhibited and autophagy is initiated (Hamacher-Brady 2012)(Matsui et al. 2007a). To initiate the autophagosome, mTOR is dephosphorylated, which will lead to its detachment from the Atg13 complex protein, activating the complex. In its active state Atg13 complex can signal for initiation of autophagy (Hamacher-Brady 2012).

Class III PI3K initiates autophagy when associated with other proteins, such as Beclin-1, to form the core complex for autophagy initiation, phosphatidylinositol 3-phosphate (PI3P). Beclin-1 is a core protein for the formation of this structure (Hamacher-Brady 2012).

Elongation of the autophagosome requires contribution of membrane from other organelles. Ubiquitination reactions are involved with the elongation process of which the protein 1 light chain protein (LC3-I) is a role player (Ravikumar et al. 2010). LC3-I is conjugated in a reaction

to form LC3-II, which is specially directed to elongation of the outer membrane of the autophagosome, where it remains until the structure is fused with the lysosome, forming an autophagolysosome (Ravikumar et al. 2010).

In order to determine the significance of autophagy, quantification of the process would be crucial. An increase in the formation of autophagosomes does not equate to an increase in autophagy, as this could be an indication of a restraint in the downstream processes. The number of autophagosomes is determined by the balance between their formation and the formation of the autophagolysosomes or their degradation by lysosomes- the so called autophagic flux (Maejima et al. 2015). The autophagic flux can therefore be defined as a measure of autophagic formation versus degradation (Agholme et al. 2012).

Different techniques have been used to quantify autophagy. Three common and widely used techniques include Western blotting, fluorescence microscopy and transmission electron microscopy (TEM). Common to all three techniques is the analysis of the LC3-II levels, in the presence or absence of an inhibitor (Loos et al. 2014). As described earlier, LC3-I is conjugated to LC3-II through lipidation and recruited to the membrane of the autophagosome where it is permanently associated with the inner membrane of the autophagosome until the structure is degraded (Loos et al. 2014). This therefore renders LC3-II as a good indicator of the autophagosome amount (Maejima et al. 2015). The degradation of p62/SQSTM1 (referred to as p62), an adaptor protein and ubiquitin binding cargo receptor, is also used as an indicator of whether autophagy is occurring (Behrends & Fulda 2012).

The process of autophagy is an ongoing process and measuring the rate of flux would be a more accurate measurement to quantify the process. Western blotting is a suitable technique to measure the overall change in cell protein levels e.g. up or down regulation but it is not suitable to measure the autophagic flux as it is not able to analyse the protein levels over a period of time (Loos et al. 2014). The same applies for TEM, although one is able to visualise the different stages in autophagy i.e. autophagosome, autophagolysosome etc. Fluorescence microscopy, specifically green fluorescent protein (GFP)-microtubule associated with LC3 is a technique that is able to successfully quantify the autophagic flux (Loos et al. 2014; Maejima et al. 2015). In GFP-LC3 autophagosomes can be counted in the presence or absence of an inhibitor of the formation of the autophagosome e.g. chloroquine (Maejima et al. 2015).

1.2.4. Mitophagy

Mitophagy is a selective form of autophagy for removal of dysfunctional mitochondria. Due to the diverse functions of mitochondria in the cell, including, generation of ROS, cytoplasmic and mitochondrial Ca^{2+} regulation, cell death, ATP synthesis and others, the precise definition of mitochondrial dysfunction would be difficult because of this complex nature of the organelle (Brand & Nicholls 2011). However, because the mitochondria's predominant function involves the synthesis of ATP, a compromising in this process, will be the bases for mitochondrial dysfunction, for the purposes of this study.

The degradation of dysfunctional mitochondria is crucial to cardiomyocytes as they have high densities of mitochondria (Jimenez et al. 2014). There are two mechanisms of mitophagy that have been identified (Shires & Gustafsson 2015). The first and well characterised pathway, is mediated by Parkin and the phosphatase and tensin homolog induced putative kinase 1 (PINK1) [Figure 1:7 (A)].

Parkin is a cytosolic protein and an E3 ubiquitin ligase while PINK1 is a serine/threonine kinase (Kubli & Gustafsson 2012). In basal conditions of a cell PINK1 locates on the outer membrane of the mitochondria in very low concentrations as it is normally translocated into the mitochondria and cleaved by proteases (Derek P Narendra et al. 2010). It has been shown that the translocation of PINK1 into the mitochondria is mediated by the translocase outer mitochondrial membrane 70 (TOM70) (Kato et al. 2013). Upon disruption of the mitochondrial membrane, potentially triggered by cellular stress, Parkin translocates to the mitochondria (Narendra et al. 2008) where it ubiquitinates outer membrane mitochondrial proteins in order for mitophagy to take place (Geisler et al. 2010). In addition to this, PINK1 transportation into the mitochondria is inhibited and it accumulates on the outer membrane. It has been suggested that PINK1 is required for the recruitment of Parkin to the depolarised mitochondrial membrane, however the association is still unclear (Narendra et al. 2008; Kubli & Gustafsson 2012). After proteins are ubiquitinated, p62 binds to them and to LC3 of the autophagosome, for mitophagy to take place (Jimenez et al. 2014).

The second pathway is the mitophagy receptor mechanism [Figure 1:7 (B) and (C)], however it is a less well characterised pathway (Shires & Gustafsson 2015). This pathway does not involve ubiquitination or p62. The protein receptors that have been identified to be involved in this pathway are BNIP3 (Hanna et al. 2012), NIX, also known as BNIP3L (the homologue of BNIP3) (Novak et al. 2010) and Fun14 domain containing 1 (FUNDC1) (Liu et al. 2012; Shires

& Gustafsson 2015). In a study by Hanna et al, BNIP3 was reported to interact directly with the LC3 protein of the autophagosome, through BNIP3's LC3-interacting region (LiR), and thus promoting removal of dysfunctional mitochondria. In addition, disrupting the interaction between BNIP3 and LC3 resulted in lower levels of dysfunctional mitochondrial removal, but did not affect the pro-apoptotic activity of BNIP3 (Hanna et al. 2012). In a separate study by Novak et al, they discovered that BNIP3L/ NIX interacted with Atg8 proteins and LC3A. They also showed that reticulocytes lacking BNIP3L/ NIX had their mitophagy levels restored when BNIP3L/ NIX was overexpressed (Novak et al. 2010). Both BNIP3 and BNIP3L/ NIX possess BH3- only sequence homology of the Bcl-2 family proteins (Imazu et al. 1999), however, they differ in their mode of mechanism to initiate cell death and are also weaker inducers of the opening of the mPTP (Imazu et al. 1999; Rikka et al. 2011). FUNDC1 is the most recently identified mitophagy receptor, and has been recognised to activate mitophagy in a dephosphorylated state, under hypoxic conditions or when the mitochondrial membrane potential has been lost (Chen et al. 2014).

However, in a study by Lee and colleagues, they found a cross talk between the two pathways of mitophagy. Induction of mitophagy via BNIP3 was associated with the recruitment of Parkin to mitochondria and this was dependent on the mitochondrial fission dynamic process (Lee et al. 2011). However, they propose further investigations to understand the interaction between Parkin and BNIP3.

As the PINK1/Parkin mediated mitophagy is the better characterised pathway, it will be the pathway analysed in our studies.

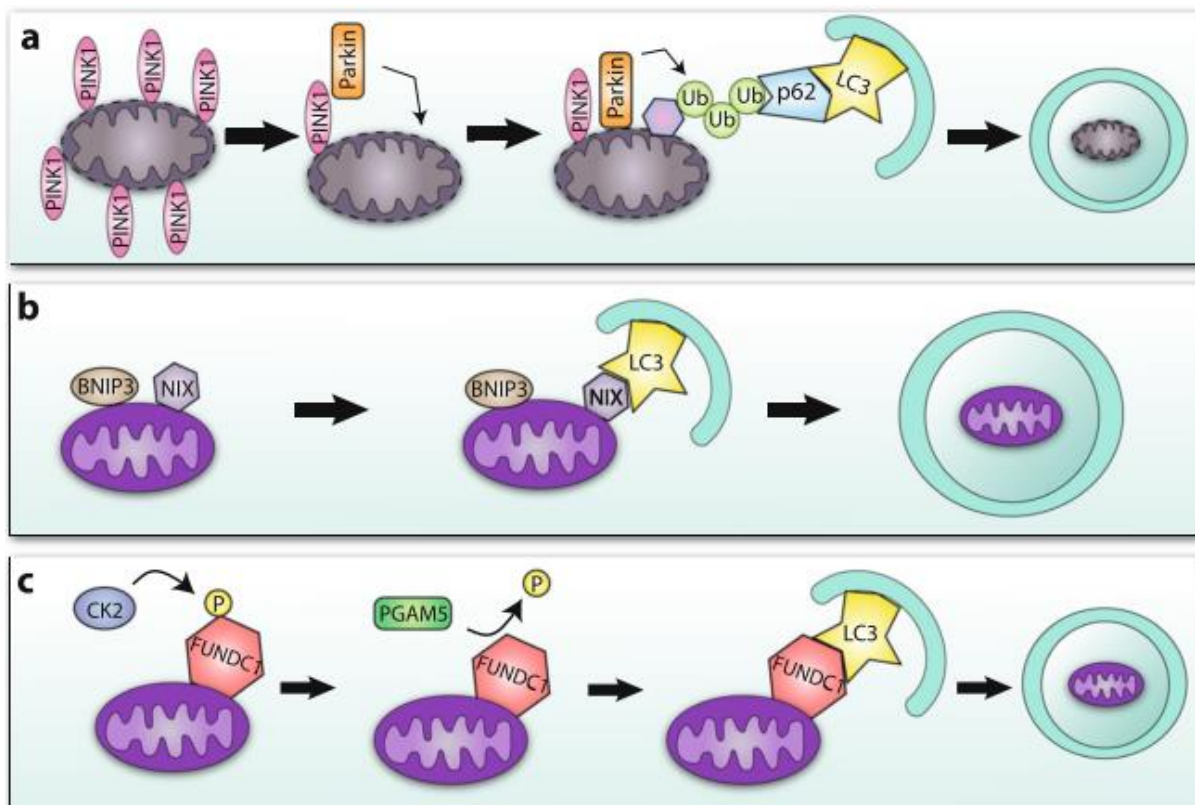


Figure 1:7 Scheme of PINK1/Parkin and receptor mediated mitophagy. In (A) PINK1/Parkin regulate mitophagy, upon exposure to stress, a loss of membrane potential occurs, leading to the accumulation of PINK1 on the outer mitochondrial membrane, followed by ubiquitination by Parkin, interaction with p62 and LC3 and the formation of the autophagosome and finally degradation. In (B) LC3 of the autophagosome interacts with BNIP3 and NIX through their LiR. In (C), under starvation conditions, FUNDC1 is dephosphorylated allowing for its interaction with LC3 (Shires & Gustafsson 2015).

1.2.5. Mitophagy and the heart

Removal of dysfunctional mitochondria has been increasingly recognised as an essential mechanism in order to sustain a healthy pool of mitochondria for the cell (Lee et al. 2011). Elimination of dysfunctional mitochondria can be of benefit to the heart as dysfunctional mitochondria produce elevated levels of ROS, which can affect neighbouring mitochondria and thus contaminate the mitochondrial pool with mutated DNA. (Jimenez et al. 2014; Maejima et al. 2015). Dysfunctional mitochondria also result in the release of pro-apoptotic proteins. Additionally, it has also been reasoned that dysfunctional mitochondria can consume cellular

ATP, diminishing the cellular levels (Gottlieb & Mentzer 2013). In view of that, the heart is particularly vulnerable to stresses that damage mitochondria. In a study by Kubli et al, they showed that impaired mitophagy from Parkin knock-out myocytes, resulted in the accumulation of dysfunctional mitochondria after infarction. This was also associated with impaired recovery after myocardial infarction, thus suggesting the crucial role of Parkin in myocardial stress adaptation through mitophagy (Kubli et al. 2013).

In a separate study on PINK1 knock-out mice, the results showed that the mice developed left ventricular dysfunction as well as increased oxidative stress levels, indicated by increased lipid peroxidation (Billia et al. 2011). The knock-out of PINK1 also resulted in damage to the mitochondria including increased susceptibility of ROS-dependent mitochondrial membrane potential depolarisation and as a result, a decrease in the oxidative phosphorylation potential of the mitochondria. Mitochondrial swelling was increased and the ability of mitochondria to replicate was decreased. This was also associated with alterations in the mitochondrial protein expressions (Billia et al. 2011). In view of these studies, it is clear that the removal of dysfunctional mitochondria is needed to optimise the overall health and function of mitochondria and cardiomyocytes.

On the other hand, this raises the question of the replacement of dysfunctional mitochondria. PGC-1 α (PGC-1 α) is one of the main regulators of mitochondrial biogenesis. PARIS, an inhibitor of PGC-1 α is also a substrate of Parkin, required to initiate mitophagy, as stated above. PARIS represses the expression of the transcriptional coactivator, PGC-1 α and the PGC-1 α target gene, NRF-1, by binding to insulin response sequences in the PGC-1 α promoter (Lin & Scott 2012). Parkin mediated mitophagy would then lower PARIS levels and subsequently increase PGC-1 α levels to upregulate mitochondrial biogenesis. Therefore in normal conditions, homeostasis would lead to a preservation of mitochondrial levels and function of cardiomyocytes (Gottlieb & Mentzer 2013). This may not be the same in a diseased heart.

1.3. Ischaemia reperfusion

As defined earlier, ischaemic heart disease is characterised by the severe impairment of the coronary blood supply, usually as a result of thrombosis or other chronic alterations of coronary atherosclerotic plaques (Buja 2005). Deprivation of nutrients and oxygen to the heart results in pathophysiological effects on the myocardium known as ischaemic injury, caused by changes in the metabolic and biochemical processes shown in Figure 1:8

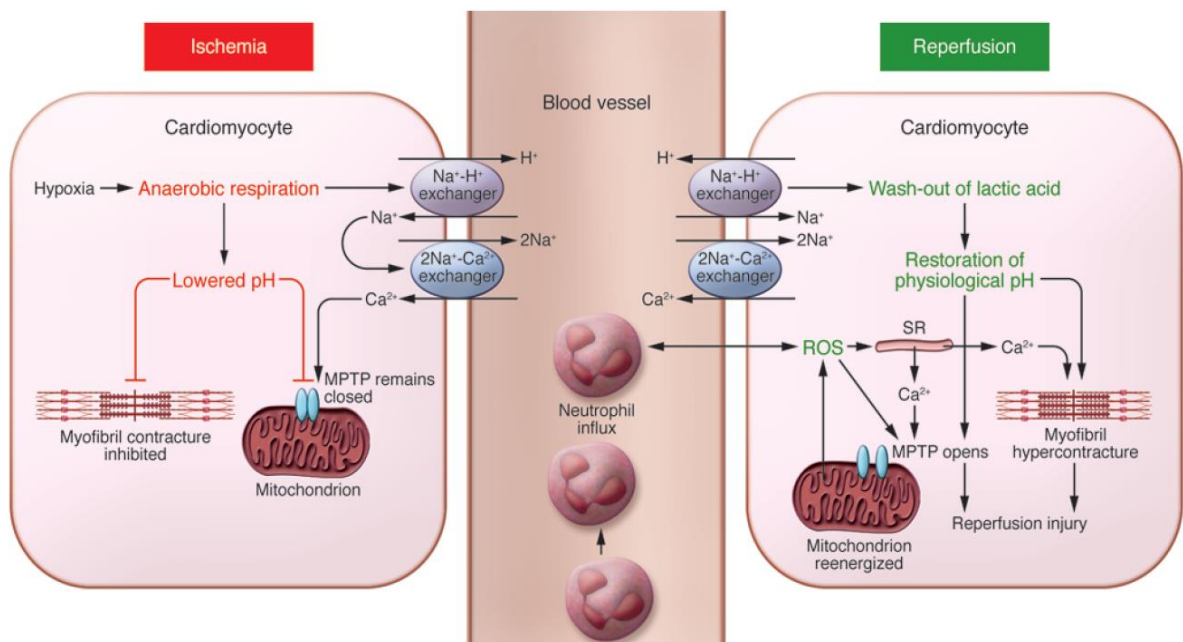


Figure 1:8 Diagram illustrating the main metabolic changes during ischaemia and reperfusion. Due to hypoxia anaerobic respiration begins to take place, this leads to a decrease in the intracellular pH levels which leads to the activation of the $\text{Na}^+\text{-H}^+$ exchanger and prevents myofibril contracture and the opening of the mPTP. In reperfusion the pH levels are restored and this is followed by an increase in Ca^{2+} levels leading to reperfusion injury through the opening of the mPTP and hypercontracture activation (Hausenloy & Yellon 2013).

Myocardial substrate metabolism is tightly controlled in response to exogenous substrate availability and the pathophysiological state of the heart (Lesnefsky et al. 2001). During ischaemia, the uptake of both fatty acids and glucose is initially increased in order to maintain energy levels, however their metabolism by mitochondria is decreased (Nickel et al. 2013). In addition to this, a reduction in oxygen supply will also result in discontinued mitochondrial oxidative phosphorylation and consequently a depletion of cellular ATP (Buja 2005). To compensate for this reduction in energy levels, anaerobic respiration is increased leading to an accumulation of lactic acid and hydrogen ions, resulting in a reduction of intracellular pH, a state known as acidosis (Buja 2005). An increase in hydrogen ions causes an induction of the $\text{Na}^+\text{-H}^+$ exchanger to extrude the H^+ ions. As a result, intracellular Na^+ ions increase. This in turn activates the $\text{Na}^+\text{-Ca}^{2+}$ exchanger (NCX) to function in reverse to extrude Na^+ ions while Ca^{2+} ions enter the cell. Consequently, Ca^{2+} cellular levels rise leading to a Ca^{2+} overload (Hausenloy & Yellon 2013). A decrease in pH levels also leads to myofibril contracture and

prevents the opening of the mitochondrial permeability transition pore mPTP see Figure 1:8 (Hausenloy & Yellon 2013).

Mitochondrial morphology is affected during ischaemia, for example, features such as swelling, disrupted cristae and a reduction in the expression of the mitochondrial proteome i.e. fatty acid oxidation proteins and the subunits of the electron transport chain, have been observed (Nickel et al. 2013). Changes in mitochondrial morphology have been observed in rat hearts after ischaemic durations as short as 10 min (Edoute et al. 1983).

The effect of myocardial infarction (injury) is dependent on the length of time of coronary artery occlusion as well as the severity of the insult. Damage can be reversible or irreversible. Usually occlusion for more than 30 min in rat hearts is irreversible (Duncker et al. 1998) and myocardial function will not recover. However, the recovery of myocardial function after exposure to ischaemic conditions may not always be immediate despite the lack of irreversible damage and the restoration of normal flow (Duncker et al. 1998). This phenomenon is referred to as stunning and the cellular mechanisms are discussed below.

Restoration of nutrients and oxygen to the heart after ischaemia, albeit essential for functional recovery, also induces damage at a cellular level, referred to as reperfusion injury. Histologic characteristics of reperfused ischaemic canine myocardium have been reported to show features including cell swelling, contracture of myofibrils and the appearance of intramitochondrial phosphate particles (Jennings et al. 1960; Yellon & Hausenloy 2007). Several factors as discussed below have been identified that contribute to the phenomenon of reperfusion injury.

ROS produced by several organelles leads to oxidative stress which mediates cell death and injury. Sources of reactive oxygen species include endothelial cells, endoplasmic reticulum neutrophils and mitochondria which have their oxidative phosphorylation capacity restored at the onset of reperfusion. Implications of oxidative stress include the opening of the mPTP which leads to cell death and mediates the malfunction of the sarcoplasmic reticulum. Opening of the pore results in a loss of the electrochemical gradient across the inner mitochondrial membrane and as a result a disruption in the ETC. This will not only ultimately lead to a hindrance in the synthesis of ATP but also a reverse function of the ATPase protein (Halestrap 2009). Prolonged exposure of cells to such conditions leads depleted ATP cell levels and cell death via necrosis (Halestrap & Richardson 2015).

Although Ca^{2+} overload of the cytoplasm and mitochondria is initiated during ischaemia, this is further amplified during reperfusion. Amongst others, this is due to disruption of the sarcoplasmic reticulum, as a result of oxidative stress as well as restoration of the mitochondrial membrane potential which allows for the entry of Ca^{2+} ions (Hausenloy & Yellon 2013; Bhosale et al. 2015) and consequently the opening of the mPTP, leading to cell death.

At the onset of reperfusion pH, levels are rapidly restored as the previously formed lactic acid is washed out and the function of the $\text{Na}^+\text{-H}^+$ exchanger is restored. This cellular change contributes to cell death and injury as it leads to the opening of the mPTP and hypercontracture of the myofibrils (Hausenloy & Yellon 2013). A study showed that the opening of the mPTP during reperfusion is dependent on pH in hepatocytes: normal pH levels (7.4) during reperfusion led to the opening of the pore and cell death, whereas treatments with a lower pH (6.3) during reperfusion prevented cell death due to a closed mPTP (Qian et al. 1997).

Stunning and therefore the reperfusion injury is mainly as a result of different cellular events that lead to cell death through the opening of the mPTP (Bhosale et al. 2015).

1.3.1. Ischaemia/Reperfusion: Mitochondria and the electron transport chain

Mitochondria are known to be very fragile during the early stages of reperfusion (Jennings 2013). Under normal circumstances, the mitochondria consume oxygen and reduce it to water through the series of enzymes of the electron transport chain (section 1.1.3). However, in the event of ischaemia and concomitant reduction in oxygen supply and stimulation of anaerobic respiration, ATP is broken down to ADP and in some instances AMP, resulting in an accumulation of inorganic phosphates, which leads to the permeabilization of the inner mitochondrial membrane. This could also be contributed to by the accumulation of Ca^{2+} levels in the cytosol (Castilho 1996). Increased permeability leads to the entry of water, resulting in swelling of the matrix and subsequently rupturing of the mitochondria. Following this, proapoptotic mitochondrial proteins are released into the cytosol, resulting in apoptosis (Crompton 1999; Antwerp 2004). Prolonged ischaemia will also result in a decrease in the activity of the electron transport chain complexes, specifically complexes I and IV (Antwerp 2004). This will in turn influence the production of ATP and hence the energy levels of the cell. Impairment of the complexes of the ETC leads to electron leak and, upon reperfusion, the formation of superoxides from O_2 is aggravated as oxygen levels are increased (Baker & Kalyanaraman 1989; Antwerp 2004). In addition to these changes during reperfusion, ROS are formed due to

the liberation of ferrous irons from the ETC proteins with sulphur centres. Enzymes involved in the ETC as well as the Krebs cycle are susceptible to ROS-induced inactivation (Nickel et al. 2013) contributing to the dysfunction of the mitochondria.

The leak of protons across the inner mitochondrial membrane results in the uncoupling of mitochondria to ATP production (Nickel et al. 2013). Mitochondrial uncoupling can also be induced by uncoupling proteins such as uncoupling protein 2 and 3 (UCP2 and UCP3) which are the two isoforms expressed in the heart and thought to be activated by free fatty acids and ROS (Busiello et al. 2015). However, UCP3 has been suggested to play a role in prevention of mitochondrial oxidative induced damage (Busiello et al. 2015).

1.3.2. Autophagy in the setting of I/R

As described earlier, autophagy is a cellular process involved in the degradation of damaged proteins or organelles triggered by different stimuli. Basal levels of autophagy in cardiomyocytes are essential for structure, function and quality control of organelles. In the event of ischaemia/reperfusion, autophagy is activated due to oxidative stress and the depletion of energy levels (Ma et al. 2015).

When energy supply does not meet its demand, the enzyme adenosine monophosphate-activated protein kinase (AMPK) senses this drop in energy levels and initiates autophagy directly through Unc-51-Like Kinases1 (ULK1). AMPK is reported to be upregulated during the initial phase of ischaemia when autophagy takes place while reduced AMPK levels is accompanied by downregulation of autophagy (Matsui et al. 2007b; Takagi et al. 2007). During the degradation process of autophagy, free fatty acids and amino acids are released and recycled in order to generate more ATP through the Krebs cycle to compensate for the depletion in energy levels (Ma et al. 2015).

In reperfusion, the main mediator of autophagy activation is Beclin-1 (instead of AMPK), activated by ROS. Beclin-1 is a key protein involved in the formation of the autophagosome and its subsequent processing (Ma et al. 2015). Although autophagy is a beneficial cellular process, excessive autophagy can be harmful and contributes to cardiomyocyte cell death. For example, it has been shown that inhibition of autophagy by 3-methyl-adenine (3-MA), or inhibition of Beclin-1 using siRNA, resulted in a decrease in cell death in I/R injury (Valentim et al. 2006; Ma et al. 2015). Aggressive autophagy, or the cross talk between autophagy and apoptosis, is also another possibility of harmful effects of autophagy in a pathological condition

such as I/R. Autophagy can either be a partner, agonist or enabler of apoptosis (Bialik et al. 2009).

1.3.3. Mitophagy in the setting of I/R

Excessive or prolonged stress on mitochondria can ultimately lead to the dysfunction and damage of mitochondria (Marín-García & Akhmedov 2016). Mitophagy is a quality control mechanism and is essential to the homeostasis of the cell. For cardiomyocytes, containing high levels of mitochondria, maintaining a constant healthy population of mitochondria is essential (Shires & Gustafsson 2015).

Mitophagy induced by stress is protective as it results in the removal of dysfunctional mitochondria (Ma et al. 2015) and therefore contributes significantly to the heart's adaption to mild stress (Marín-García & Akhmedov 2016). Increased mitophagy however may not always be protective, for example, under severe stress conditions. This can be detrimental to cardiomyocytes as this consequently leads to either an impairment of mitophagy and an accumulation of harmful proteins and ROS that will result in cell injury or death, or aggressive response of mitophagy that reduces the number of functional mitochondria and subsequently functional cardiomyocytes (Marín-García & Akhmedov 2016). The effects of increased or decreased mitophagy are summarized in the diagram below (Figure 1:9).

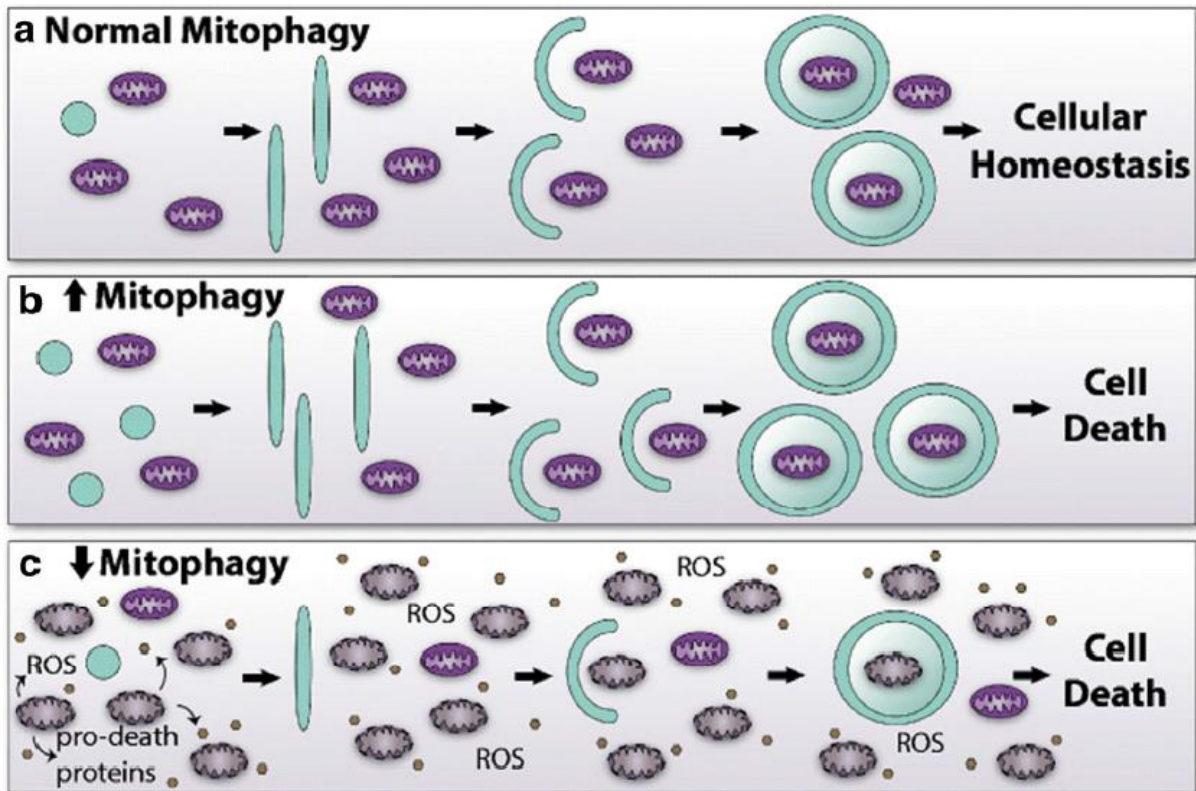


Figure 1:9 Diagram illustrating the outcome of mitophagy in (A) normal (B) upregulated and (C) downregulated conditions. Normal levels of mitophagy are required for homeostasis, whereas an increase or decrease in mitophagy is harmful and leads to cell death (Shires & Gustafsson 2015).

1.4. Pharmacological Tools

1.4.1. FCCP and Mitophagy

Mitophagy is induced by dysfunctional mitochondria due to a loss of membrane potential. Uncouplers are one way to disturb the membrane potential of the mitochondria as they weaken the coupling between substrate (fuel) oxidation and ATP synthesis (Lou et al. 2007). Uncouplers are usually weak lipophilic acids which are able to pick up protons, and translocate them across the inner mitochondrial membrane into the matrix, and in this manner, short-circuiting the usual proton flow in oxidative phosphorylation (protonophore). The proton gradient is therefore collapsed and this leads to a decrease in ATP synthesis. In the matrix they deprotonate and exit as anions, which enables them to pick up more protons and thus repeat the cycle again. In addition to this, uncouplers cause an increase in energy expenditure mainly through the generation of heat (Lou et al. 2007). Different pharmacological uncouplers are available for research purposes, examples include 2,4-dinitrophenol (DNP), butylated hydroxytoluene (BHT), benzoic acid, carbonylcynide m-chlorophenylhydrazone (CCCP) and Carbonilcyanide p-trifluoromethoxyphenylhydrazone (FCCP), to name a few. For the purposes of this study, only research done on FCCP will be discussed.

FCCP is an uncoupler that has been commonly used to study mitochondria. A study that aimed to test the effect of low concentrations of FCCP and establish if it elucidated cardio protection in Langendorff perfused hearts, showed that concentrations of 100 nM FCCP was cardio protective when administered for 5 mins before global ischaemia, as left ventricular developed pressure (LVDevP) was increased from 14.7 +/- 1.9% in control hearts to 57.8 +/- 5.1% in treated hearts. ATP levels during administration of FCCP were no different when compared to those of control groups, but these levels declined greatly during ischaemia. Concentrations of 300 nM conferred no protective effect (17.9 +/- 5.8%) and this concentration completely eradicated the contractility of the heart during the 5 min of drug administration prior to ischaemia, increasing ischaemic injury (Brennan, Southworth, et al. 2006).

It is suggested from this study that the protection of FCCP (100 nM) is dependent on ROS formation as treatment was associated with increased ROS production (Brennan, Southworth, et al. 2006). This therefore suggests the possible activation of mitophagy, which is triggered by dysfunctional mitochondria (increased ROS production from dysfunctional mitochondria) and therefore the resultant cardio protection that was observed.

In a separate study by the same group, 100 nM FCCP caused significantly less uncoupling of mitochondria when compared to hearts treated with higher concentrations of FCCP (≥ 300 nM) (Brennan et al. 2006). Both concentrations also were noted to cause mitochondrial oxidation of substrates, however, 100 nM was not associated with mitochondrial depolarisation whereas the higher concentrations were. Based on these results the authors concluded that cardio protection via mitochondrial uncoupling has a “small window” where mild uncoupling activates protection but higher levels of uncoupling leads to cell death (Brennan et al. 2006).

A study by Narendra and colleagues showed that administration of 100 nM FCCP for 5 or 15 min to Langendorff perfused hearts from wild type and PINK1 knock-out mice, surprisingly resulted in increased Parkin levels in both groups, contrary to other studies which showed the need of PINK1 for Parkin recruitment (Narendra et al. 2010) (Geisler et al. 2010). This was also noted in their *in vivo* studies where mice were injected with FCCP (1 mg/kg) prior to perfusions (Kubli et al. 2015). These observations suggested that PINK1 is not required for Parkin engagement toward depolarised mitochondria. These findings were also associated with increased expression of LC3-II autophagic proteins, indicating induction of mitophagy via FCCP.

In addition to the above, studies were carried out using rotenone, a mitochondrial complex I inhibitor, in wild type and PINK1 knock-out mice and results similar to the FCCP studies were observed, namely, an increase in Parkin levels. This suggested that PINK1 accumulation on dysfunctional mitochondria is not immediate (does not occur in the short time frame utilised) and that Parkin recruitment can take place prior to PINK1 accumulation. They also suggested that other kinases may be involved to compensate for loss of PINK1, implying that an alternative pathway of mitophagy may be involved (Kubli et al. 2015)

1.4.2. 3-Methyl-Adenine (3-MA) and Autophagy

3-MA has been widely used to inhibit autophagy. The mechanism of 3-MA is known to have an inhibitory effect on phosphoinositide-3-kinase (PI3K), which is essential for autophagy initiation. The inhibitor targets both class I and III of PI3K. Via class III 3-MA prevents the production PI3P essential for recruitment of the isolation membrane to form the autophagosome (Wu et al. 2010). However 3-MA has persistent effects on class I PI3K, but brief suppressive effects on class III of PI3K (Wu et al. 2010).

In a study carried out to determine the effects of PI3K inhibitors, 3-MA and wortmannin, on autophagy under both nutrient rich and deprived conditions, it was shown that prolonged exposure of 3-MA (9hrs) promotes autophagy rather than inhibiting it under nutrient rich conditions while in contrast, wortmannin was able to inhibit autophagy despite the nutrient conditions. Higher levels LC3 were observed in nutrient rich treated cells when compared to the starved cells (Wu et al. 2010). They suggested from this study that 3-MA may have dual roles in modulating autophagy under prolonged nutrient rich conditions.

In a separate study, cardiomyocytes under glucose deprivation (GD), to mimic ischaemic conditions, were treated with 3-MA (10 mmol/L) for 24hrs. Results showed a decrease in LC3 II/LC3 I levels and GFP-LC3 dots were not observed via fluorescence. This showed that starvation induced autophagy was inhibited by 3-MA. In addition to this the GD cardiomyocytes showed a reduction in ATP levels which further reduced when cells were treated with 3-MA. They correlated their findings with the higher ATP levels during GD in comparison to the ATP levels when cells were treated with 3-MA, to be consistent with the idea that autophagy preserves ATP levels during GD (Matsui et al. 2007b).

From these studies one can infer that 3-MA is effective in Inhibiting autophagy at low concentrations after ischaemic or nutrient deprived conditions. Mitophagy however, is a specialised form of autophagy and is a highly selective process. Mitophagy may not necessarily be induced or inhibited by the same pharmacological agents as autophagy (Sargsyan et al. 2015) as it depends on other factors such as the loss of mitochondrial membrane potential with specific proteins involved (Narendra et al. 2008; Kubli & Gustafsson 2012).

Chloroquine is another pharmacological tool that has been used to inhibit autophagy and mitophagy. It acts by inhibiting the lysosomal reaction in the process of autophagy by altering the pH of the vacuole and the lysosome, preventing the fusion process of the autophagosome and lysosome (Zhang 2013). High concentrations of chloroquine in pressure overload hypertrophy (POH), can be toxic, as shown in a study by Antione and colleagues. When rats were treated with 40 mg/kg/day for two weeks, their hearts showed a regression in hypertrophy, however, this was associated with reduced contractility and impaired relaxation when echocardiograms were carried out. In addition to this, chloroquine further increased the ultrastructural damage of the mitochondria compared to the untreated rats (also exposed to POH). Their results showed a prominence of collapsed and fragmented mitochondria and collapsed cristae. Chloroquine, however, seems to be a more favourable inhibitor of mitophagy,

as its mode of action will be able to successfully interfere with the pathway of mitophagy. However, lower concentrations of chloroquine can be administered, as higher concentrations have led to detrimental outcomes. Chloroquine was not used in the current study due to its cytotoxic effects on hearts during perfusion.

1.5. Concluding Remarks

Despite intense research over many decades, Ischaemic heart disease remains the leading cause of death worldwide. Although our knowledge regarding events in the ischaemic myocardium as well as the changes induced by reperfusion, has increased exponentially since the first reports on the phenomenon of ischaemic preconditioning, there are still several aspects that need to be clarified in order to effectively prevent cell death. It has been known for many years that the reduction in the supply of oxygen and nutrients leads to a decrease in mitochondrial oxidative phosphorylation capacity, leading to a reduction in tissue ATP levels and finally an imbalance between the energy demand and supply of the heart. This influences, amongst others, the metabolic processes and contractility of the heart. It is not surprising therefore that the mitochondrion eventually became the centre of interest in the quest to find interventions to protect against cell death. Recent work focused on the role of the mitochondrial permeability transition pore in this regard.

In view of the role of the mitochondrion in the death or survival of the cardiomyocyte, attention has recently shifted to the role of the removal of damaged mitochondria or mitophagy in cell survival. To our surprise, it became clear that there are several caveats in our current knowledge regarding the association (if any) between the well-known ischaemia-induced reduction in mitochondrial oxidative phosphorylation function and the mitophagy process. This is particularly important if the size of the mitochondrial population in the heart muscle is taken into account.

In evaluating the role of mitophagy in the outcome of ischaemia/reperfusion damage, it was surprising that despite the level of sophistication applied in the study of the mitophagic process, surprisingly little is known about its significance in mitochondrial oxidative phosphorylation function and ultimately contractility of the heart when exposed to ischaemia/reperfusion.

In view of the above, we posed the research question, *is mitophagy cardioprotective or detrimental in the outcome of ischaemia and reperfusion?* We hypothesised that mitophagy is cardioprotective in the outcome of ischaemia and reperfusion.

We aimed to evaluate the mitophagic process in the setting of I/R injury, using the isolated perfused working rat heart and mitochondrial oxidative phosphorylation measurements as experimental models. The significance of mitophagy in the outcome of I/R was further evaluated by the use of a specific activator and inhibitor of this process.

Objectives of study:

1. Characterization of the mitophagic process in the heart when exposed to ischaemia alone and the effect of reperfusion
2. Determination of the importance of mitophagy in the outcome of I/R by use of an inhibitor (3-MA) and activator (FCCP)
3. Correlation of the function, cell survival, mitochondrial oxidative phosphorylation capacity and signalling events associated with mitophagy in hearts exposed to ischaemia/reperfusion.

Chapter 2

Methods

In this study we aimed to determine the significance of mitophagy in the setting of ischaemia/reperfusion injury. Mitophagy was therefore either (i) inhibited or (ii) stimulated in hearts subjected to ischaemia/reperfusion during isolated working heart perfusions.

Animals

Male Wistar rats weighing 230-250 g were used throughout the study. The rats were obtained from the Stellenbosch University Central Research Facility, Faculty of Medicine and Health Sciences, Tygerberg. Animals had free access to water and food before experimentation. The study was approved by the Ethical Committee for Animal Research of the Faculty of Health Sciences, Stellenbosch University (Ethics Approval number: SU-ACUM-1400039).

2.1. Perfusion technique of the isolated rat heart

Reagents: 3 - Methyl Adenine (3-MA) (Sigma Aldrich) and Carbonyl cyanide 4-trifluoro-methoxy phenylhydrazone powder (FCCP) (Sigma Aldrich) were used as the inhibitor and stimulant respectively of mitophagy. 3-MA (1 mM) was prepared with 14.9 mg of 3-MA dissolved in 1.49 mL of distilled water (dH₂O) or N, N- dimethylformamide (DMF) (Sigma Aldrich), diluted to 100 mL of Krebs-Henseleit buffer (KHB) see below. A stock solution of FCCP was prepared (1M in DMSO) (Sigma Aldrich) and diluted in 500 mL of KHB, as required. Evans blue (0.01% aqueous solution) was used to outline viable tissue.

Procedure: Rats were anaesthetised with sodium pentobarbitone (Bayer) (160 mg/kg body weight) by intraperitoneal injection. Deep anaesthesia was determined through the loss of the pedal pain withdrawal reflex (foot pinch). Surgical harvesting of the heart began with a skin incision performed at the xyphoid-sternum and was extended to the lateral ends of the left and right costal margins. Following this an incision was made through the ribs at the right and left axillary lines to create a clamshell thoracotomy (Bell et al. 2011). The chest was deflected upwards and the pericardium was opened. The heart was then removed and arrested in cold KHB.

Hearts were mounted onto an isolated working heart perfusion apparatus via cannulation of the aorta and pulmonary vein. KHB was used as perfusate for the heart. The buffer contained 118.46 mM NaCl, 24.995 mM NaHCO₃; 4.748 mM KCl; 1.185 mM KH₂PO₄; 1.19 mM MgSO₄·7H₂O; 1.25 mM CaCl₂·2H₂O and 10 mM glucose. The buffer was gassed with 95% oxygen and 5% carbon dioxide to obtain a pH of 7.4. To stabilise the heart and wash out the blood, the hearts were perfused in the

retrograde (Langendorf) mode in a non-recirculating manner and a constant hydrostatic pressure (100 cm H₂O). After stabilisation, hearts were perfused in the working mode at a preload of 15 cm H₂O and an afterload of 100 cm H₂O. To monitor temperature, a temperature probe was inserted into the pulmonary artery. The temperature was thermostatically regulated at 36.5 °C during ischaemia and 35.5-37 °C during working mode. Hearts were then either subjected to global or regional ischemia with or without drug administration as demonstrated in the protocols discussed below. Drug interventions were applied during Langendorf perfusion through a separate arm into the aortic cannula.

2.1.1. Global ischaemia

To induce global ischaemia, aortic and pulmonary vein (arterial) cannulas were occluded after stabilisation leading to cessation of coronary perfusion. Drug intervention was administered prior to or post ischaemia. Temperature was maintained at 36.5 °C for 25 mins before the aortic cannula was opened again to initiate reperfusion. Hearts were sampled at different time points during the protocol, for mitochondrial isolation or Western blotting, as indicated in Figure.2:1-2:2. The protocols were as follows:

- Control 40 (**C40**): Protocol used in preliminary studies, to determine effects of drugs and solvent (Figure 2:1); 10 min Langendorf perfusion, 10 min in working heart perfusion; 10 min again in Langendorf perfusion and 10 min in working heart perfusion (Figure 2:1).
- Control 40 (**C40**): 40 min of stabilisation (10 min in Langendorf perfusion, 20 min in working heart perfusion and 10 min again in Langendorf perfusion with no drug intervention included) (Figure 2:2 (A))
- 25 min ischaemia (**25 ISCH**): 40 min of stabilisation followed by 25 min of global ischaemia with no drug intervention included (Figure 2:2 (B)).
- 25 min ischaemia plus 3-MA (**25 ISCH + 3-MA**): 40 min of stabilisation with drug intervention during the last 10 min of stabilisation, followed by 25 min of global ischaemia (Figure 2:2 (C)).
- 20 min reperfusion (**20R**): 40 min stabilisation, followed by 25 min of global ischaemia and 20 min of reperfusion (10 min in Langendorf perfusion and 10 min working heart mode). No drug intervention included (Figure 2:2 (D)).
- 20 min reperfusion plus 3-MA administered *before ischaemia* (**20R + 3-MA B.ISCH or 20R + FCCP B.ISCH**): 40 min of stabilisation with drug intervention (3- MA or FCCP) during the last 10 min of stabilisation, followed by 25 min of global ischaemia and 20 min of reperfusion (Figure 2:2 (E)).

- 20 min reperfusion plus 3-MA administered *after ischaemia* (**20R + 3-MA A.ISCH**): 40 min of stabilisation followed by 25 min of global ischaemia and 20 min of reperfusion with drug intervention during the first 10 min of reperfusion. No drug intervention was included prior to ischaemia (Figure 2:2 (F)).



Figure 2:1 Baseline perfusion protocol for preliminary studies (A) without drug intervention and (B) with drug intervention indicated with the red block

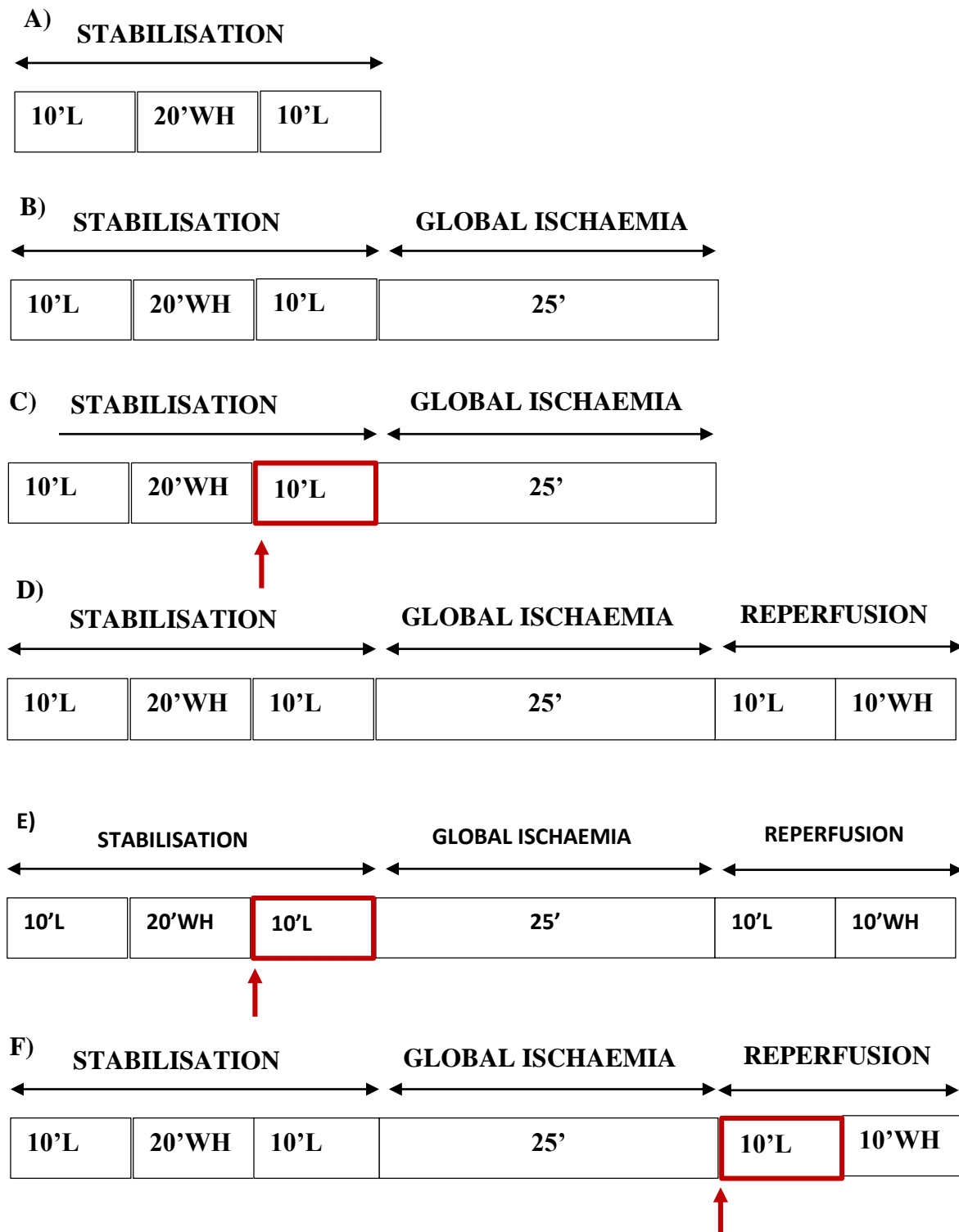


Figure 2:2 Outline of baseline, global ischaemia and reperfusion perfusion protocols. (A) Untreated baseline perfusion (B) untreated ischaemia, (C) ischaemia with pre-treatment of drug indicated by the red arrow and block (D) untreated reperfusion protocol (E) Reperfusion with drug administration before ischaemia and (F) at the onset of reperfusion, indicated by the red arrow and block. Hearts were sampled at the end of each perfusion protocol.

2.1.2. Regional Ischaemia

For evaluation of myocardial function and infarct size determination, a regional ischaemia protocol was used (see Figure 2:3). Ethicon silk suture (3/0, 26 mm ½ Taper, Johnson and Johnson Medical (PTY) LTD, South Africa) was used to induce ischaemia by occluding the left anterior descending (LAD) coronary artery at the end of the stabilisation period. The LAD was occluded for 35 min with the temperature maintained at 36.5 °C. Indication of adequate regional ischaemia was shown by a decrease of ~ 40% in the coronary flow when compared to the pre-ischaemic coronary flow. After ischaemia the suture was released and the heart reperfused for 60 min. At the end of the protocol, hearts were stained with 1 mL Evans blue (Sigma Aldrich), by slowly infusing the solution into the heart through the aortic cannula, during Langendorf perfusion. Hearts were then frozen away at -20 °C. Myocardial function was recorded prior to and post ischaemia.

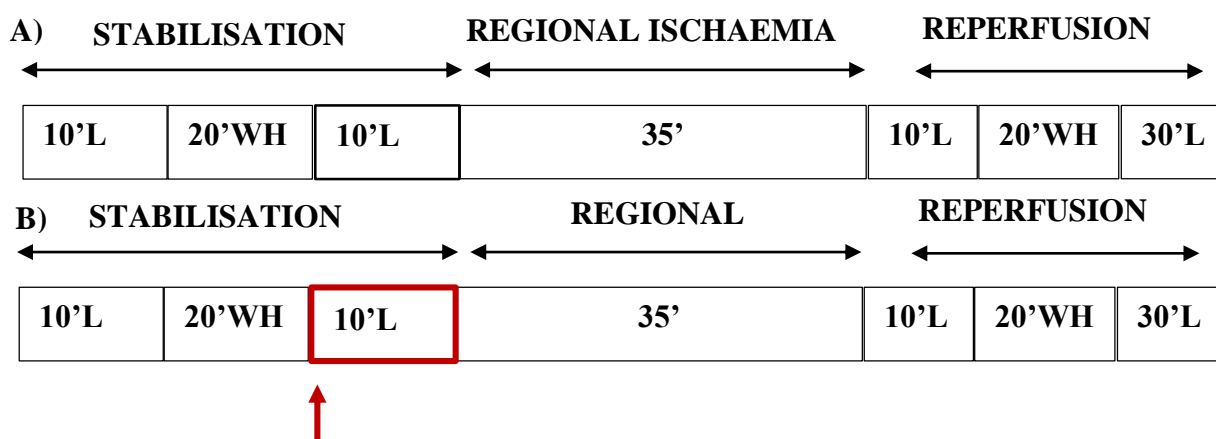


Figure 2:3 Outline of regional ischaemia perfusion protocol. (A) untreated control and (B) pre-treatment with drug intervention before ischaemia, indicated by the red arrow and block. Hearts were sampled at the end of each perfusion protocol.

Infarct size determination

2,3,5-triphenyltetrazolium chloride (1% in a phosphate buffer Na_2PO_4), pH 7.4, 10% formaldehyde; (TTC) was used for infarct size determination. This method is based on the fact that TTC binds to intracellular dehydrogenases and the preserved NADPH of viable cells, with reducing potential, are stained brick-red while necrotic cells, with no intact sarcolemmal membranes and washed out membranes appear pale/white (Bell et al. 2011)

Frozen hearts were sliced into 2 mm slices and immediately placed in the TTC solution for 15 min at room temperature. To fix the staining of the separate regions, the heart tissues were placed in 10% formaldehyde at room temperature for an hour. For each slice the left ventricle area at risk and the

infarcted areas were determined using computerized planimetry (UTHCSA Image Tool programme, University of Texas Health Science Center at San Antonio, TX, USA).

2.2. Mitochondrial Isolation

To determine the oxidative phosphorylation potential of mitochondria, a polarographic measure of mitochondrial respiration was carried out using a Hansatech Clark-type oxygen electrode (Hansatech Instruments) which measures the oxygen tension.

Reagents: 0.18 M Potassium Chloride (KCl) (Merck KGaA), 0.01 M Ethylenediaminetetraacetic acid (EDTA), lysis buffer (see Western blotting, section 2.3), 10 % Trichloroacetic acid (TCA).

Procedure: After a perfusion protocol was completed, the heart muscles (ventricles) were divided longitudinally and both halves were used to isolate mitochondria. Ventricles were minced separately in Sorvall tubes containing ice cold KE buffer (consisting of 0.18 M KCl and 0.01 M EDTA). Hearts were further homogenised on ice with a polytron (Heidolph silent crusher M Polytron) for a few seconds (4 sec) at 12000 rpms in two bursts. Hearts were then centrifuged (Sorvall SS34 rotor) for 10 min at 4 °C at 2500 rpms. The pellet was discarded and the supernatant was decanted and centrifuged for another 10 min at 12500 rpms at 4 °C. From the second spin, the supernatant was removed and the pellet was gently suspended using a Glass-Teflon homogenizer (Teflon® pestle PYREX® Potter-Elvehjem tissue grinders) in 0.26 mL KE buffer. 50 µL of the suspension was precipitated in 1 mL 10% TCA for protein determination with a Lowry assay (Schagger et al. 1994), while 50 µL was stored at -80°C for determination of the citrate synthase activity. The rest of the mitochondrial suspension was used for measurement of function in an oxygraph (Hansatech Clark-type oxygen electrode – Hansatech Instruments). The mitochondrial pellet obtained from the other half of the ventricles was suspended in 200 µL lysis buffer for Western blotting.

2.2.1. Mitochondrial Oxidative Phosphorylation

Reagents: Glutamate plus malate and palmitoyl-L-carnitine plus malate substrate media (shown in Table 2.1), 1.25 M stock sucrose (Merck Pty Ltd), 100 mM stock Tris-HCl, 85 mM stock potassium dihydrogen phosphate (KH_2PO_4), 50 mM stock glutamate, 20 mM stock malate, 4.5 mM stock palmitoyl-L-carnitine, 50% KCl, sodium dithionite ($\text{Na}_2\text{S}_2\text{O}_4$) (Merck Pty Ltd), 300-400 nM of adenosine-5'-diphosphate monopotassium salt hydrate (ADP) (Sigma-Aldrich) (0.02 g in 5 mL of distilled water- final concentration determined using a Ultra Violet (UV) spectrophotometer at 259 nm, with an extinction coefficient of 15.4 OD, 6% perchloric acid (PCA), universal pH indicator, 40% KOH-KCl and 0.2 M Tris-HCl

Table 2:1 Table showing the components of the two incubation media used for the mitochondrial analysis: (A) represents the glutamate (carbohydrate) medium and (B) the palmitoyl-L-carnitine (fatty acid) medium

A)	Reagent	Volume of stock used (mL)	Final Concentration in incubation medium (M)
	Sucrose	2	0.25
	Tris-HCl	1	0.01
	KH ₂ PO ₄	1	0.0085
	Glutamate	1	0.005
	Malate	1	0.002
	dH ₂ O	4	n/a
	Total	10	Adjust to pH 7.4 before use
B)	Reagent	Volume used (mL)	Concentration Molar (M)
	Sucrose	2	0.25
	Tris-HCl	1	0.01
	KH ₂ PO ₄	1	0.0085
	Palmitoyl-L-Carnitine	1	0.00045
	Malate	1	0.002
	dH ₂ O	4	n/a
	Total	10	Adjust to pH 7.4 before use

Oxygraph setup: Drops of 50% KCl (electrolyte) were added to the cathode at the top of the electrode as well as the surrounding anode beneath the dome. Paper spacer and an oxygen permeable membrane were positioned over the cathode and dome and secured with an O-ring using an applicator shaft. An outer O-ring was used to seal the electrode disk into the oxygen electrode chamber. The electrode was standardised before experiments were run. To standardise electrode, 650 μ L of incubation medium and a small magnetic stirrer were added to the oxygraph chamber. Temperature of the system and speed of the magnetic stirrer were set to 25 °C and 100 respectively. The oxygraph was then calibrated in the liquid phase and oxygen levels were left to equilibrate to ambient levels as 100%. After stabilisation a few grains of Na₂S₂O₄ was added to remove all oxygen within the chamber to register for zero oxygen levels. The chamber was then thoroughly rinsed with distilled water before replacing with fresh 650 μ L of incubation medium.

Procedure: Substrates were used in separate chambers. 650 μ L of incubation medium was added to the chamber and allowed to equilibrate to ambient oxygen (temperature 25 °C). 100 μ L of mitochondria suspension in KE buffer, was added to the chamber, the system was closed and the recording allowed to run for several seconds. This represented state 2, the respiration of the mitochondria in the presence of the substrate alone (see Figure 2:4). Thereafter, 50 μ L of known

concentrations of ADP was slowly added to the chamber using a Hamilton syringe to ensure no air bubbles were present. In this phase, mitochondria were allowed to convert the ADP to ATP (state 3 respiration). After mitochondria converted all the ADP to ATP, they returned to their normal respiration (state 4). State 4 respiration was allowed to progress for 60 sec. To simulate hypoxia, 50 μ L of 10x ADP concentration (\pm 3500 nM) was then added to the chamber and the mitochondria converted as much ADP to ATP until all oxygen in the system was consumed. The mitochondria were then subjected to anoxia for 20 min followed by re-oxygenation and the state 3 respiration rate determined again.

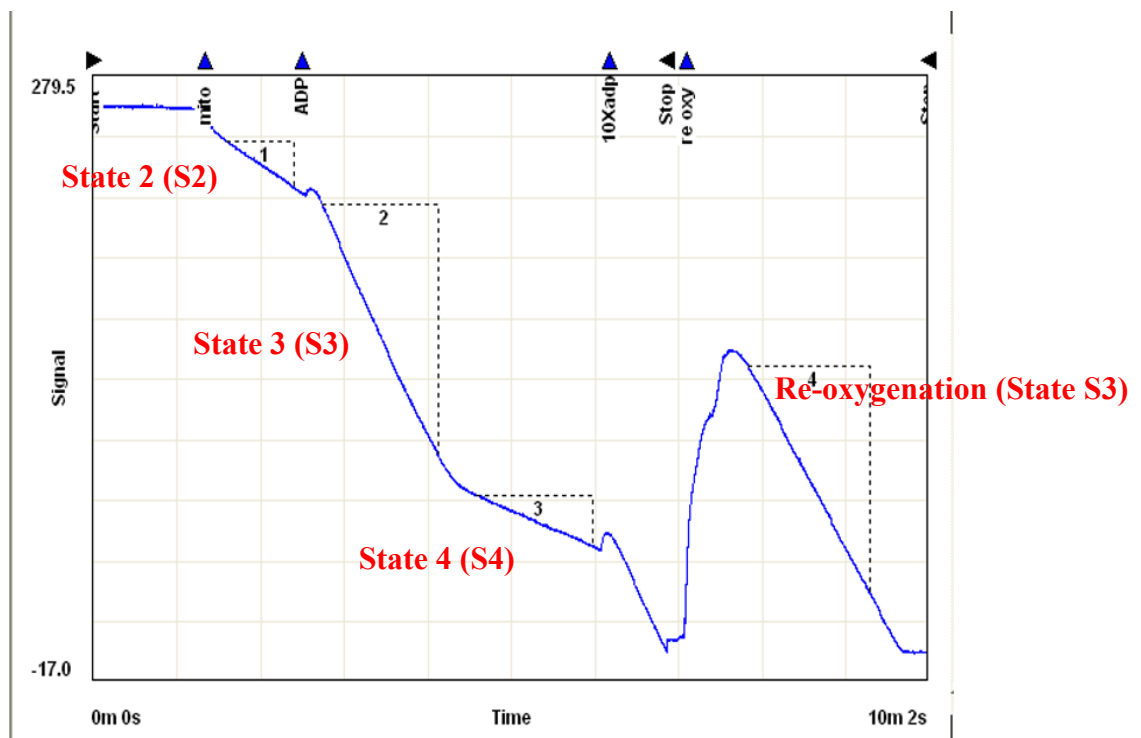


Figure 2:4 Illustration of mitochondrial registration generated by the oxygraph. The image shows the three states (labelled in red) of mitochondrial respiration. State 2 represents respiration of mitochondria in the presence of the substrate alone. State 3 represents mitochondrial respiration in the presence of ADP (oxidative phosphorylation) and state 4 represents mitochondrial respiration after ATP formation. Re-oxygenation state 3 respiration represents mitochondrial respiration after 10x concentrated ADP was added to the oxygraph followed by 20 min hypoxia.

From the graph generated by the oxygraph, the following parameters were calculated, in addition to the protein concentrations determined with the Lowry assay, in order to deduce the function of the mitochondria;

- ADP/O: The coupling efficiency of the mitochondria: ratio of ATP production to total oxygen uptake during state 3 (nmoles ATP/nAtom of oxygen consumed)
- QO_2 (state 3): nAtoms oxygen uptake in the presence of ADP /mg mitochondria protein/min

- QO_2 (State 4): nAtoms oxygen uptake in the absence of ADP/mg mitochondria protein/min
- RCI (respiratory control index): $QO_2(S3)/ QO_2/(S4)$
- Oxidative Phosphorylation rate: $QO_2 (S3) \times ADP/O$ (nmoles ATP produced/mg mitochondria protein /min)
- Oxidative Phosphorylation rate: $QO_2(S4) \times ADP/O$ (nmoles ATP produced/mg mitochondria protein /min)

For samples to be analysed for ATP levels, the reaction mixtures of the mitochondria were removed from the oxygraph chambers soon after stage 4 and placed in 1 mL of 6% perchloric acid (PCA) and allowed to precipitate for 30 min. This was followed by centrifugation at 4000 rpms for 10 min at 4 °C. 1 mL of the supernatant was added to 5 µL of the universal pH indicator transforming the solutions to a purple appearance. A neutralising solution of 40% KOH-KCL and 0.2 M Tris-HCL (2:3 ratio) were gradually added to the samples (10 µL at a time) and mixed by inversion until the samples were neutralised i.e. pH 7.0 giving the samples a light green appearance. Samples were centrifuged again at 4000 rpms for 3 min at 4 °C and 80 µL of the supernatant was stored at -80 °C for subsequent analysis of ATP and ADP levels using HPLC.

2.2.2. Lowry Assay

Lowry assay is a protocol commonly used for protein determination by the Folin reaction. Proteins are initially pre-treated with copper ions in alkali solution, the treated samples, specifically the aromatic amino acids, reduce the phosphomolybdic-phosphotungstic acid in the Folin Ciocalteus reagent, resulting in a blue appearance (Schagger et al. 1994). Protein levels are therefore determined from the amount of reduced Folin Ciocalteus reagent by reading the absorbance at 750 nm. A standard curve of selected Bovine Serum Albumin (BSA) concentrations was used to calculate the protein concentrations in the samples.

Reagents: 2% Na_2CO_3 in dH_2O (20g/1L), 2% Na-K-Tartrate in dH_2O (2 g/100 mL), 1% $CuSO_4 \cdot 5H_2O$ in dH_2O (1 g/100 mL), Folin Ciocalteus reagent, 1N NaOH, 0.161 mg/mL BSA, 0.332 mg/mL BSA, 0.644 mg/mL BSA. 0.5 mLs each of Na-K-Tartrate and $CuSO_4 \cdot 5H_2O$ were added to 49,5 mL of Na_2CO_3 . A Folin solution was made up in a ratio of 1:2 with dH_2O .

Procedure: Precipitated mitochondrial samples in 10% TCA were centrifuged (Heraeus Megafuge 16R Centrifuge, Thermo Fischer Scientific) at 3000 rpms for 10 min at 4 °C. The supernatant was discarded and the samples were allowed to air dry. 1N NaOH (0.5 mL) was added to each sample and placed in a 60 °C water bath to allow the proteins to dissolve. 0.5 mL of dH_2O were then added to the samples (final NaOH concentration 0.5N). Samples and standards (50 µL) were assayed in triplicate.

50 μL of 0.5N NaOH was used as a blank. 1 mL of Na-K-Tartrate- CuSO_4 - Na_2CO_3 solution was added to each tube at 10 sec intervals. The samples were left for the reaction to take place for 10 min. Following this 100 μL of Folin solution (diluted 1:2 with dH_2O) was similarly added. This reaction was allowed to develop for 30 min before OD readings were obtained from the spectrophotometer (spectronic 20 Genesys spectrophotometer set at 750 nm). A standard curve was generated and used to determine the protein concentration of the mitochondrial samples.

2.2.3. Citrate Synthase Assay

Citrate synthase is the initial enzyme in the Krebs cycle. It catalyses the reaction between acetyl coenzyme A (acetyl CoA) and oxaloacetic acid forming citric acid (see Chapter 1, Figure 1:2). The hydrolysis of the thioester of acetyl CoA results in the formation of CoA with a thiol group (CoA-SH) (Morgunov & Sreere 1998). In the assay the thiol reacts with 5,5'-Dithiobis-(2-nitrobenzoic acid) (DTNB) to form 5-thio-2-nitrobenzoic acid (TNB) a yellow product, which can be observed spectrophotometrically at 412 nm. The citrate synthase activity is used as an indicator of intact mitochondria (Holloszy et al. 1970).

Reagents: CellLytic M Sample buffer, 1x Assay buffer for Citrate synthase, 30 mM Acetyl CoA, 10 mM Oxaloacetate (OAA), 10 mM DTNB, positive control citrate synthase. All components were obtained from Sigma-Aldrich in kit form and used as directed by the manufacturer's instructions.

Procedure: 200 μL of CellLytic M sample buffer was added to 50 μL of stored mitochondrial samples. 10 μL of this mixture was transferred to clean tubes. To this, was added 930 μL of assay buffer, 10 μL of Acetyl CoA and 10 μL of DTNB. Absorbance of samples were read every 20 sec for 1.5 min. 50 μL of oxaloacetate was then added to the samples and absorbance values were similarly re-read, summarised in Figure 2:5. The net citrate synthase activity was calculated by subtracting the change in absorbance of the endogenous activity ($\Delta A_{412}/\text{minute}$) from that of the total activity i.e. after addition 10 mM OAA. The citrate synthase activity was expressed as $\mu\text{mole}/\text{mL}/\text{min}$.

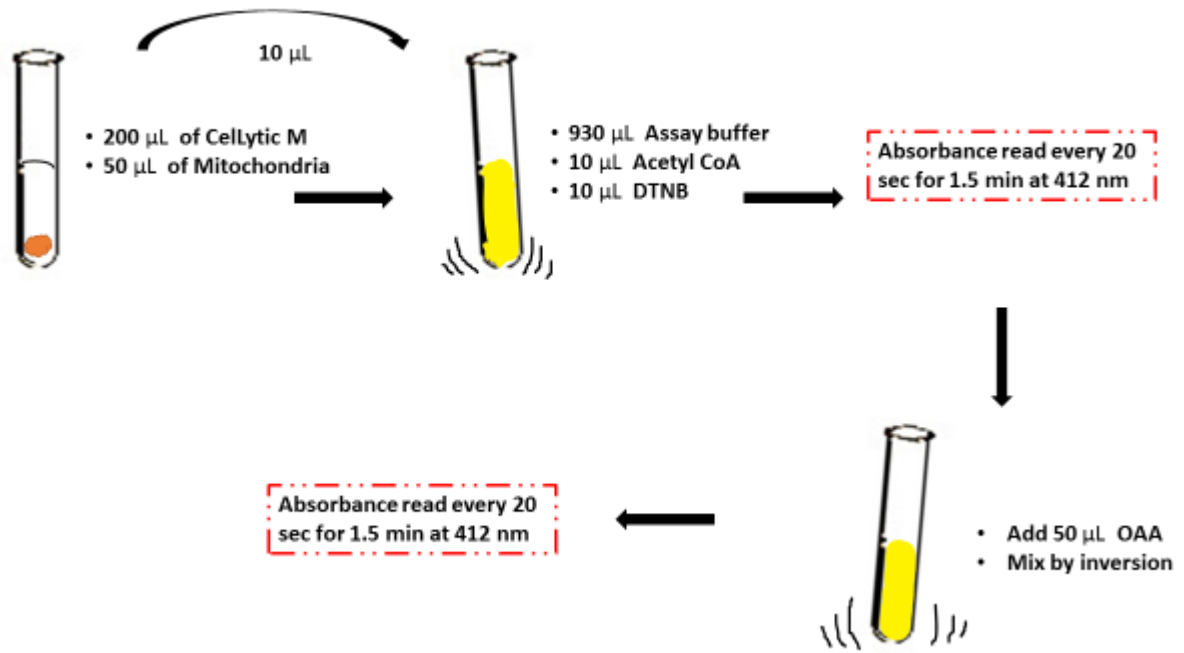


Figure 2:5 . Summary flow diagram of citrate synthase assay described above.

2.3. Western Blotting

2.3.1. Protein extraction

Reagents:

Table 2:2 Lysis buffer composition for mitochondrial and heart tissue

Reagent	Stock	Content	Amount for 30 mL
Tris-HCl EGTA (pH 7.5)	200 mM	20.0 mM	3 mL
EDTA	100 mM	1 mM	300 μ L
NaCl	1 M	150 mM	4.5 mL
B-glycerol-phosphate	-	1 mM	0.006 g
Sodium pyrophosphate	-	2.5 mM	0.03 g
Na₃VO₄	10 mM	1.0 mM	3 mL
Leupeptin	10 μ g/ μ L	10 μ g/ μ L	30 μ L
Aprotinin	10 μ g/ μ L	10 μ g/ μ L	30 μ L
PMSF	100 nM	50 μ g/mL	30 μ L
dH₂O			Fill up to 30 mL

Heart Tissue extraction

Frozen heart tissue from perfusions were pulverized and ~300 mg of pulverised tissue was weighed into Sorval tubes containing 800 μ L of lysis buffer. Each tissue sample was then homogenised on ice using the Heidolph Silent Crusher M at 9 rpms for 5 sec, for two episodes or until well mixed. Homogenate samples were then transferred to Eppendorf tubes. Samples were centrifuged (Sigma 1-14k benchtop refrigerated centrifuge) for twenty minutes at 15000 rpm at 4 °C. After centrifuging, the supernatant was transferred into fresh Eppendorf tubes and kept on ice for protein determination using Bradford analysis (Bradford 1976). (Described later).

Mitochondrial extract from samples stored in 200 μ L of lysis buffer after mitochondrial isolation for Western Blotting

Samples were thawed on ice, followed by homogenisation by adding a scoop of 0.15 nm Zirconium oxide beads and placing samples in a Bullet blender ® (Next Advanced Inc., USA) at 4 °C for 3 min at speed 5. Homogenates were left to stand on ice for 15 min before being centrifuged (Sigma 1-14k

benchtop refrigerated centrifuge) for 20 min at 15000 rpms at 4 °C and prepared for protein determination according to the method of Bradford (Bradford 1976), discussed below.

Bradford Protein determination

Reagents: 100 mg of Coomassie Brilliant Blue G-250, 50 mL 95% Ethanol, 100 mL 85 % (w/v) Phosphoric Acid, 850 mL dH₂O (Bradford Reagent), Bovine serum albumin (BSA).

A 5x Bradford dilution of 100 mL was prepared and filtered through a double layer of Whatman filter paper. BSA stock solution (5 mg/mL dH₂O) was used for the standard curve. Prior to the protein determination the BSA stock solution was diluted 5x (100 µL BSA stock and 400 µL of dH₂O). The diluted BSA was then serially diluted in duplicate test tubes (Table 2.3), generating concentrations ranging from 1-50 µg in 100 µL volume.

Table 2:3 BSA serial dilution for Bradford analysis

Diluted BSA µL	dH ₂ O µL
0 (blank)	100
5	95
10	90
20	80
40	60
60	40
80	20

5 µL of the supernatant of the centrifuged samples were diluted in a 10x dilution (to 100 µL) with dH₂O. 5 µL of the 10x dilution was assayed in a total volume of 100 µL per tube.

900 µL of diluted Bradford reagent was then added to each test tube, beginning with the blank and standard tubes followed by the test tubes of the samples. All tubes were then vortexed and left to incubate for 20 min at room temperature before measuring the absorbance. The absorbance was measured at 595 nm using a spectrophotometer (Spectronic® 20 Genesys™ Spectrophotometer, Thermo Fisher Scientific Inc., RSA). A standard curve was generated from the readings of the spectrophotometer and used to calculate the protein concentrations of each sample. Lysis buffer was then added to the samples in order to dilute the samples to equal concentrations i.e. 30 µg/12 µL, this

was followed by adding a mix of 850 μL Laemmli sample buffer and 150 μL mercaptoethanol to the samples in a volume equal to half of the lysis buffer and sample. Samples were boiled for 5 min and stored in -80°C fridge for future analysis using Western blotting.

2.3.2. Protein separation and transfer

Reagents

Table 2:4 Reagents used for Protein separation and protein transfer

REAGENT	COMPOSITION
12% Fast cast kit resolving gel	3 mL TGX Stain-Free™ FastCast™ Resolver A and B, 30 μL 10% APS, 3 μL TEMED per gel
12% Fast cast kit stacking gel	1 mL TGX Stain-Free™ FastCast™ Stacker A and B, 10 μL 10% APS, 2 μL TEMED per gel
Running buffer	192 mM Glycine, 0.1% SDS, 25 mM Tris-HCl
Trans Blot Turbo Buffer	200 mL Ethanol, 200 mL Trans Blot® Turbo™ buffer 600 mL dH_2O
TBS-Tween Buffer Solution pH 7.6	137 mM NaCl, 20 mM Tris-HCl, 0.1% Tween-20
Ponceau Red (Sigma-Aldrich)	5 mL acetic acid, 0.5 g ponceau/ 100 mL dH_2O

Pre-cast gels

A Midi-protean® TGX Stain-Free or non-stainfree precast gradient gel of 4-20%, purchased from Bio-Rad, was used to run the samples. Gels were placed in a Midi-protean® dual system (Bio-Rad Laboratories Inc., USA) and filled with running buffer in the demarcated tanks. 10 μL of the PageRuler™ Prestained Protein Ladder, Thermo Scientific (for proteins <100 kDa) was loaded in the first well followed by 12 μL of each sample containing 30 μg of protein. A sample prepared from an un-perfused heart or baseline perfusion, where appropriate, was loaded in the first well as an internal control, to be used later for normalisation of blots. With the use of the sodium dodecyl sulphate polyacrylamide gel electrophoresis (SDS-PAGE), proteins were separated. Gels were run for 10 min at 100 V and 200 mA, followed by a 40 min run at 200 V and 200 mA. After separation, gels were

activated in the ChemiDoc™ MP system (Bio-Rad Laboratories Inc., USA). Non-stainfree precast gels were not activated in the ChemiDoc™ MP system.

FastCast gels

Fast cast gels were prepared by adding 3 mL each of 12% resolver gels solutions A and B followed immediately by 1 mL each of 12% stacker A and B (Table 2.4) into Bio-Rad hand cast glass plates, stabilised by plastic cassettes. A plastic comb was aligned and inserted into the gels. Gels were allowed to set for 45 min. Glass plates containing gels were placed in a Mini-protean® dual system and filled with running buffer in the demarcated tanks. 5 µL of the PageRuler™ Prestained Protein Ladder, Thermo Scientific (for proteins <100 kDa) was loaded in the first well followed by 12 µL of each sample containing 30 µg of protein. A sample prepared from an un-perfused heart or baseline perfusion, where appropriate, was loaded in the first well as an internal control, to be used later for normalisation of blots. Gels were run and activated as described above.

Transfer of proteins

After activation of the gels, proteins were transferred to polyvinylidene fluoride (PVDF) membranes, with the use of the Trans-Blot® Turbo™ Transfer (semi-dry) system (Bio-Rad Laboratories Inc., USA) for 7 min at 25 V and 1 mA. Membranes were then visualised in the Chemi Doc™ to ascertain transfer and document the amount of proteins transferred to the membrane. Non-stain free gels had their membranes immersed in ~ 2 mL of Ponceau Red reversible stain (Sigma-Aldrich) for 30 sec to 1 min. The Ponceau Red dye was gently rinsed off with very little dH₂O and membranes were visualized in the ChemiDoc under a Ponceau setting. Both stain free and ponceau membrane images were saved for later use of quantification of blots. Following visualisation, membranes were blocked with a 5% fat free milk TBS-Tween solution for two hours on a shaker, lab rotor V1.00, to ensure blocking of non-specific binding sites. Membranes were then washed with TBS-Tween for 30 min (3 x 10 min replacing with fresh buffer in between each wash) before being probed with gentle shaking, lab rotor V1.00, overnight at 4 °C with a 1:1000 dilution of different antibodies. See Table 2.5 for different antibodies used in the present study.

Table 2:5 Summary of information on protein analysed, molecular weight of protein, gel percentage used for protein separation, primary and secondary antibody dilution, percentage of milk used to block membrane, duration of ECL incubation and exposure time for protein bands to develop in the ChemiDoc.

Protein	MW (kDa)	Gel (%)	Protein loaded (μg)	Primary AB dil. Factor	Secondary AB dil. Factor	Milk % for secondary AB	Duration of ECL incubation prior to exposure (min)	Exposure time in Chemi Doc (min)
PINK 1	60, 50	4-20	30	1: 1000	1: 4000	2.5	5	10-15
PARKIN	52	4-20	30	1: 1000	1: 4000	2.5	5	10-15
p62/SQSTM1	60	4-20	30	1: 1000	1: 4000	0	2	2-3
TOM70	70	4-20	30	1: 1000	1: 4000	0	3	1-2
LC3A/B	14, 16	12	30	1: 1000	1: 4000	0	2	2-3
Beclin-1	60	12	30	1 :1000	1: 4000	0	5	15
BNIP3L/Nix	38, 76	12	30	1: 1000	1: 4000	0	5	15

2.3.3. Immunodetection of protein using secondary antibody

Primary antibodies were washed off with TBS-tween for 30 min (3 x 10 min replacing with fresh buffer in between each wash) the following day and membranes were then incubated with diluted secondary anti-mouse or anti-rabbit immunoglobulin G, horse radish peroxidase (HRP) coupled antibody for an hour at room temperature on the lab rotor shaker V1.00. Secondary antibody binds to the primary antibody for visualisation aid. Membranes were washed again with TBS-Tween for 30 min (3 x 10 min replacing with fresh buffer in between each wash) on the lab rotor shaker V1.00 and visualised using Bio Rad Clarity™ enhanced chemiluminescence (ECL) substrate in the Chemi Doc. See Table 2.5 for information about the dilution of the secondary antibody and the exposure time of the membranes to visualize the protein bands of interest.

Visualisation and normalisation using the Bio-Rad ChemiDoc™ MP

Exposure time, detection sensitivity for intense or faint bands and number of images to be developed were set prior to visualising the membranes. Stainfree and non stainfree membranes with ECL were placed in the ChemiDoc system and membranes were allowed to develop over the set time. Images were saved for quantification of the blots.

The optimum image of the developed membranes was normalised for the density of the protein bands against the total protein per lane transferred to the respective PVDF membranes which were saved earlier after the protein transfer step. The densities were expressed relative to the internal control to be able to compare one blot to another. All blots were analysed using the Bio Rad ChemiDoc Image Lab 5.0 series software.

Stripping of membranes

Membranes to be stripped were incubated with dH₂O for 2 x 5 min, followed by incubation with 0.2 M NaOH for 1 x 7 min and again another 2 x 5 min with dH₂O. Incubation steps were carried out on the rotor shaker V1.00. Membranes were then probed with the antibody of interest, following the procedures described above. Membranes that were stripped were only stripped once.

2.4. High Performance Liquid Chromatography

HPLC was used to identify and quantify the high energy phosphates (ATP and ADP) from our mitochondrial samples.

- HPLC Aligent 1100,
- Column: Aligent Eclipse (PN 993967-906; SN USRK007728)
- Detector wave length: 254 nm
- Injection volume: 5 μ L

Table 2:6 Reagents used for HPLC analysis

REAGENT	COMPOSITION
Mobile phase	257 mM KH_2PO_4 , 1.18 mM TBAP, 12% HPLC graded Methanol
Buffer/Solvent pH 5.6	5 mM Acetonitrile (ACN)
Adenosine triphosphate (ATP) final concentrations/ 10 μL	0.45 nmol, 0.9 nmol, 1.8 nmol and 3.6 nmol
Adenosine di-phosphate (ADP) final concentrations/ 10 μL	0.60 nmol, 1.20 nmol, 2.41 nmol and 4.82 nmol

Procedure: Each standard concentration of ATP and ADP was injected into the HPLC before the mitochondrial samples were run. Mitochondrial samples that were stored at $-80\text{ }^\circ\text{C}$ for ATP analysis were thawed on ice and filtered through a $0.45\text{ }\mu\text{m}$ filter paper 2 min prior to being injected into the HPLC. Using the areas under the curve from the chromatographs, a standard curve was generated and used to determine the mitochondrial ATP and ADP levels. The following formulas together with each sample's chromatograph area readings were used to determine the amount of ADP and ATP concentrations. Values determined were expressed as nmoles of ATP formed / mg of mitochondrial protein or nmoles of ADP not converted to ADP/ mg mitochondrial protein.

$$\text{a) } \frac{\text{Area of sample}}{\text{Area of standard}} \times \frac{\text{concentraion of standard}}{1} = \text{concentration of sample nmol per } 10\text{ }\mu\text{L}$$

$$\text{b) } \text{sample concentration (a)} \times \frac{1000+\text{neutralisation vol.}}{10\text{ }\mu\text{L}} \times 1.8$$

$$\text{c) } \frac{\text{value from (b)}}{\text{mg mitochondrial protein}}$$

2.5. Statistical Analysis

Graph Pad Prism 5 was used for the statistical analysis of all the data. Values were expressed as Mean \pm Standard error of the mean (SEM). One-way Analysis of Variance (ANOVA), followed by Bonferroni post-hoc test was used to determine difference between perfusion groups with or without drug administration. A two-way ANOVA was used to determine differences between the combined reperfusion protocols versus the combined ischaemic protocols. A *p value* of less than 0.05 was considered significant.

Chapter 3

Results

In view of the aims of this study, namely to manipulate the mitophagic process and to determine its effects on mitochondrial function and the response of the heart to ischaemia/reperfusion injury, two sets of preliminary experiments were required: (i) standardization of the Western blotting technique to determine expression of markers of mitophagy for example PINK1 and p62/SQSTM1 (shortened to p62); (ii) establishment of the optimal concentration of 3-methyl adenine (3-MA) to be used for inhibiting autophagy (mitophagy) in a perfused heart model.

Preliminary data

3.1. Standardisation of Western blotting technique

In this set of experiments, we aimed to standardise the Western blotting technique for the mitochondrial markers of mitophagy namely PINK1, Parkin and p62. For this purpose, isolated hearts were perfused for either 40 min under baseline conditions or exposed to 20 min global ischaemia. Mitochondria were subsequently isolated and lysates for Western blotting prepared, using the techniques described in Chapter 2, section 2.3. The following data was generated from experiments carried out by Dr Karthik Dhanabalan from our laboratory. Using the dilutions indicated in Chapter 2 (Table 2.5) satisfactory blots were obtained for the mitophagy markers and the technique was employed in the subsequent experiments on mitochondria. The results obtained so far showed that exposure to 20 min global ischaemia showed a strong indication of increased, although not significant, mitochondrial PINK1 while a significant increase in p62 expression ($p=0.026$, $n=5$) was observed (see Figure 3:1).

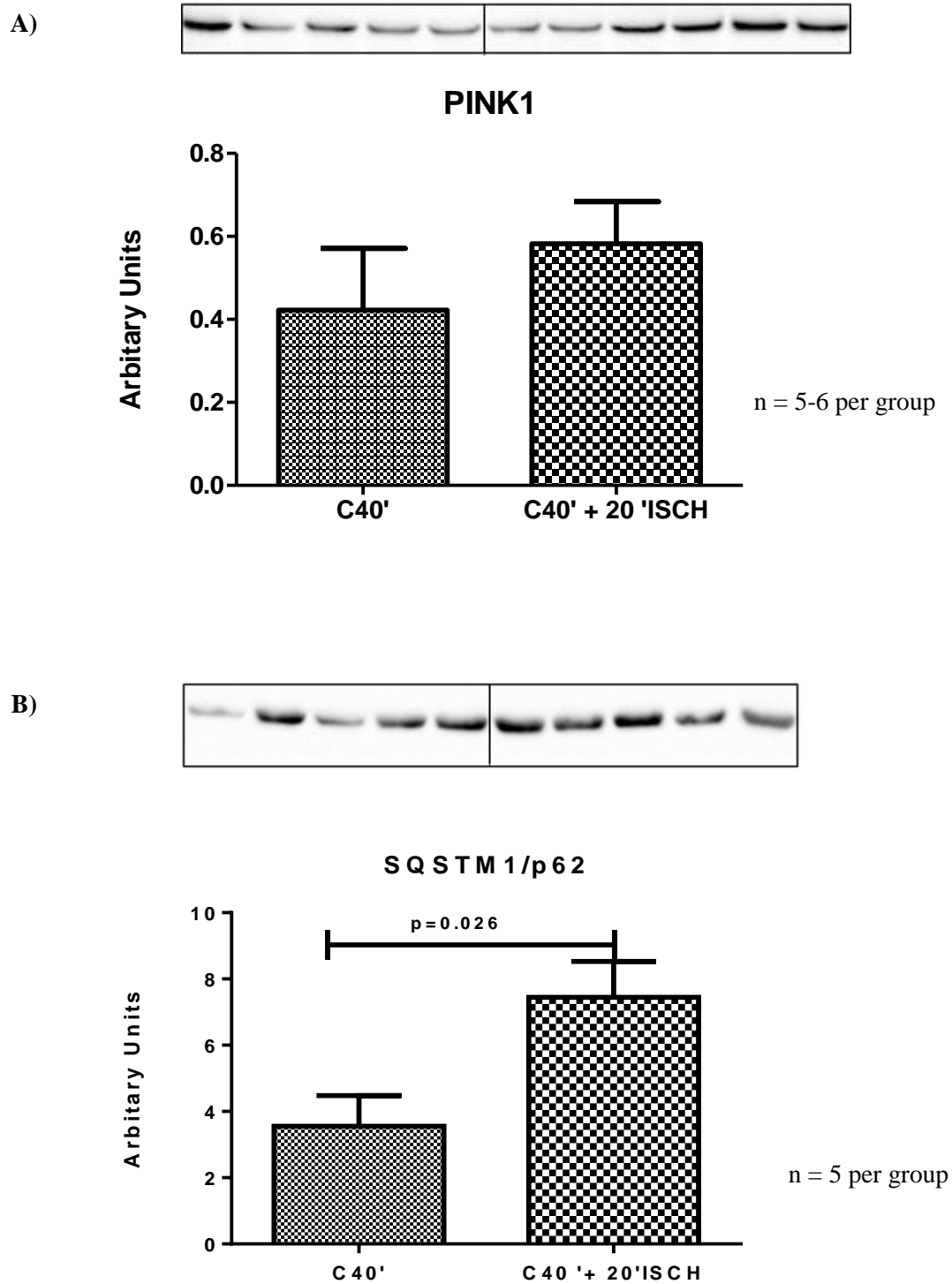


Figure 3:1 Mitochondrial levels of (A) PINK1 and (B) p62 of hearts from baseline perfusion (C40') and hearts exposed to 20 min of global ischaemia

3.2. Standardisation of autophagy markers under baseline conditions: effect of 3-methyl-adenine (3-MA) and N, N-dimethylformamide (DMF)

In these sets of experiments, we aimed to standardise the Western blotting technique for the autophagy markers, LC3A/B, Beclin-1 (D40C5) and BNIP3L/Nix (D4R4B) using *tissue* obtained from hearts perfused under baseline conditions. Since the autophagy inhibitor 3-MA was used to manipulate mitophagy in subsequent experiments, it was necessary to determine whether 3-MA at a concentration of 1 mM was sufficient to inhibit autophagy. Parallel to this, we also determined the effect of DMF as a vehicle on mitochondrial and heart function, in these initial experiments. The results described in this section were obtained using DMF as a solvent for 3MA.

The following perfusion protocols were used: hearts perfused for 40 min in the absence of drugs (C40) or with exposure to DMF (C40+DMF) or 3-MA (C40+3-MA) for 10 min, followed by washout (see Fig 3:2)

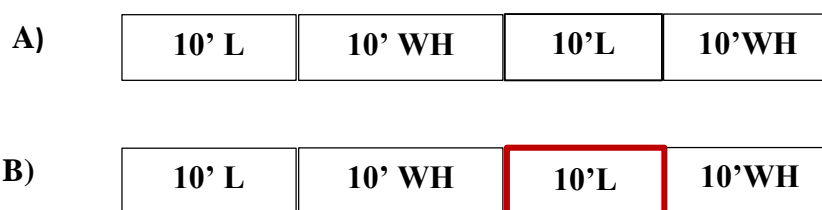


Figure 3:2 (A) perfusion protocol for untreated baseline (C40) hearts and (B) hearts treated with 3-MA and DMF as a vehicle, 10 min before final working heart period, indicated by the red block

Blots as well as stain free (SF) technology or ponceau membranes are shown with the Western blotting data throughout the present study results.

The two drugs when added during baseline perfusion conditions affected myocardial function: 3-MA and DMF, when added for a period of 10 min had lower, but not significant aortic and cardiac output and thus Total work (TW), but had no effect on peak systolic pressure and heart rate (Table 3:1). These observations indicated that the effects of the interventions persisted after a washout period of 10 min.

Tissue LC3A/B-I levels were significantly reduced in all three baseline stabilisation protocols with or without drug intervention (*C40*, *C40 +DMF* and *C40+3-MA*) when compared to the un-perfused hearts $p=0.0070$. However, there were no changes between the LC3A/B-I levels of tissue from hearts which were perfused for 40 min in the absence or presence of the drugs [Figure 3:3(A)]. LC3-II levels were increased for hearts perfused with DMF in comparison to the un-perfused hearts $p = 0.0043$ (*C40 + DMF* vs *UP*). However, LC3 A/B -II levels were decreased for hearts treated with 3-MA in

comparison to hearts treated with DMF $p = 0.0443$ (C40 +3-MA vs C40 + DMF). No changes were observed between the treated hearts and the baseline perfusion. The LC3-II/LC3-I ratios were also lower from hearts treated with 3-MA in comparison to hearts treated with DMF alone $p = 0.0415$ (Figure 3:4). Hearts treated with DMF had higher LC3-II/LC3-I ratios in comparison to the un-perfused hearts $p = 0.0009$. Again, no differences were observed between the hearts treated with DMF or 3-MA in comparison to the hearts from the baseline perfusions.

DMF $p = 0.0322$, as well as the combination of DMF and 3-MA $p = 0.0132$, reduced the expression levels of Beclin-1(D40C5), whereas DMF only reduced the BNIP3L/Nix (D4R4B) expression levels, $p = 0.0235$, when compared to the un-perfused hearts (Figure 3:5). However, a combination of DMF and 3-MA lead to a significant Increase in the BNIP3L/Nix (D4R4B) levels $p = 0.0386$ in comparison to DMF only treated hearts.

The results obtained in these preliminary experiments indicated that the combination of 3-MA at a concentration of 1 mM plus the vehicle inhibited autophagy in the heart perfused under basal conditions.

Table 3:1 Mechanical data of hearts perfused under baseline perfusions for 40 min: effects of 3-MA and DMF as a vehicle. No significant differences were observed between the groups. n= 3 per group.

TIME	PARAMETERS	C40	C40 + DMF	C40 + 3MA
40 min	Coronary Output (mL/min)	13.8 ± 1.4	12.1 ± 1.6	13.9 ± 2.7
	Aortic Output (mL/min)	42.3 ± 3.3	26.5 ± 5.1	27.2 ± 6.2
	Cardiac Output (mL/min)	55.4 ± 4.1	38.5 ± 5.0	41.1 ± 5.2
	Peak Systolic Pressure (mm Hg)	83.5 ± 1	79.4 ± 1.6	85.8 ± 3.2
	Heart Rate (BPM)	320.8 ± 13.6	322 ± 11.4	339.8 ± 40.6
	Total Work (TW)	10.5 ± 0.8	6.9 ± 1.0	7.82 ± 1.3

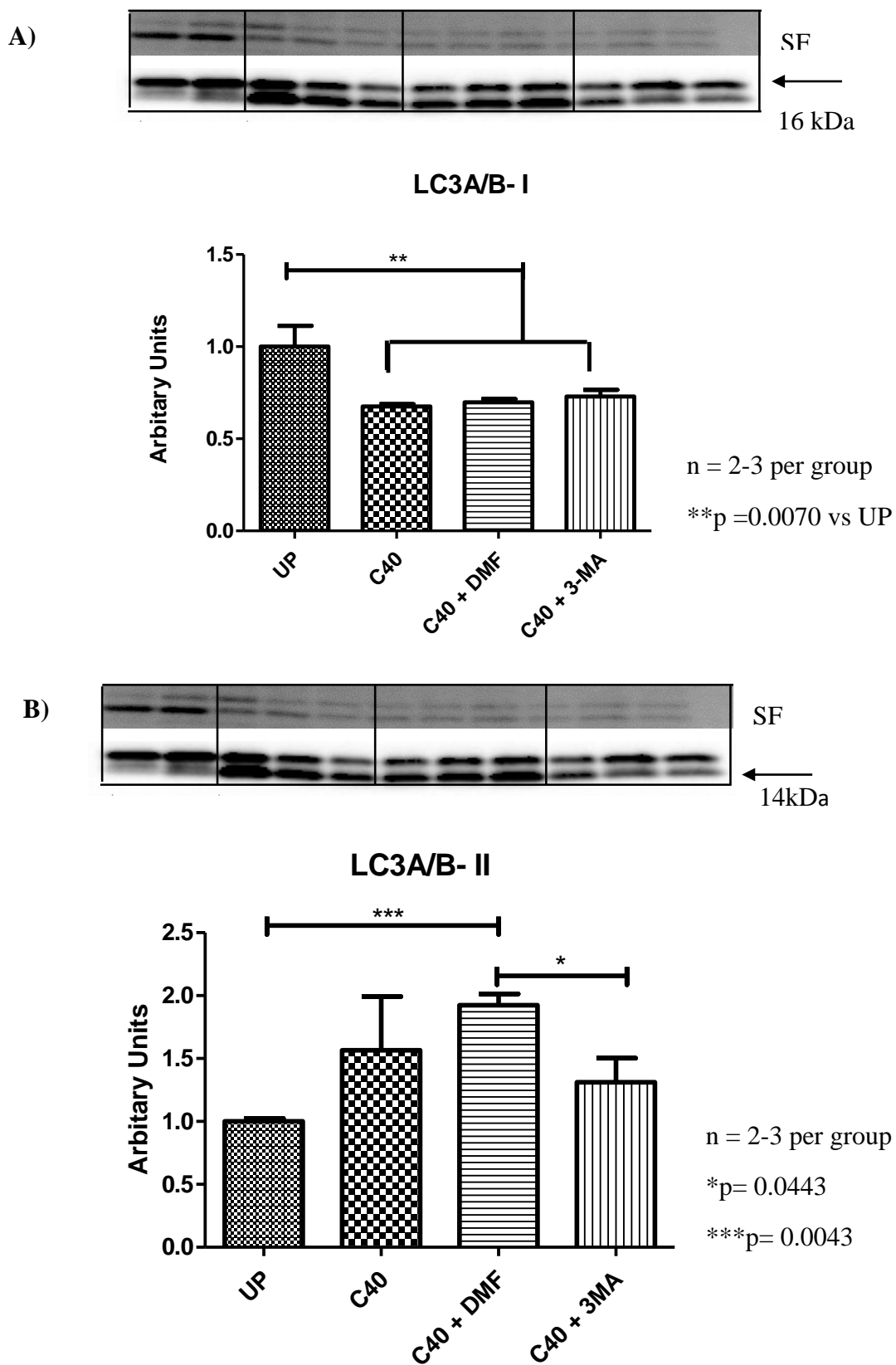


Figure 3:3 (A) LC3 A/B-I level and (B) LC3 A/B-II levels of tissue from un-perfused hearts and hearts perfused with or without 3-MA and DMF as a vehicle. SF= Stain Free

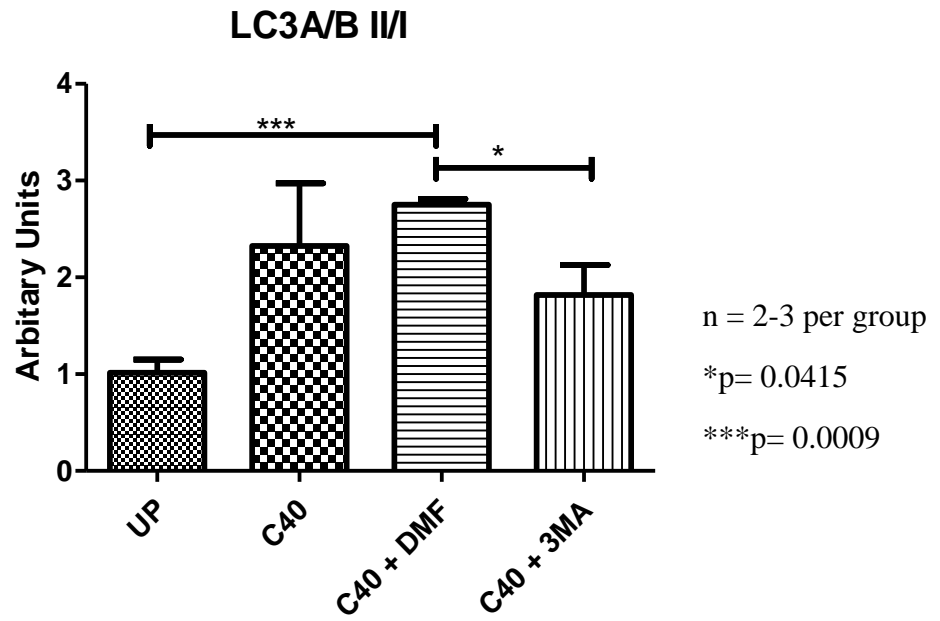


Figure 3:4 LC3A/B-II/I ratio of tissue from un-perfused and perfused hearts treated with or without 3-MA and DMF

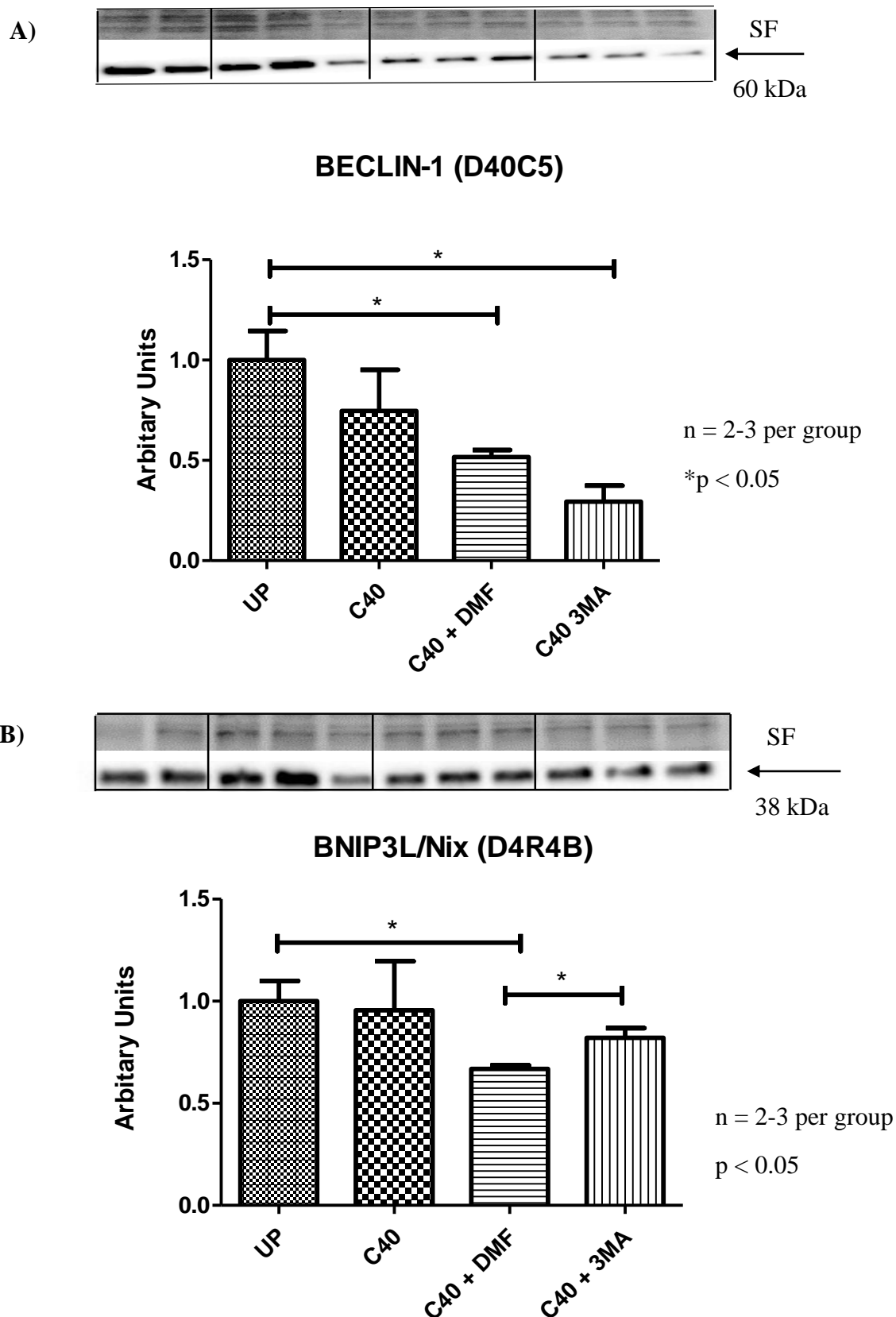


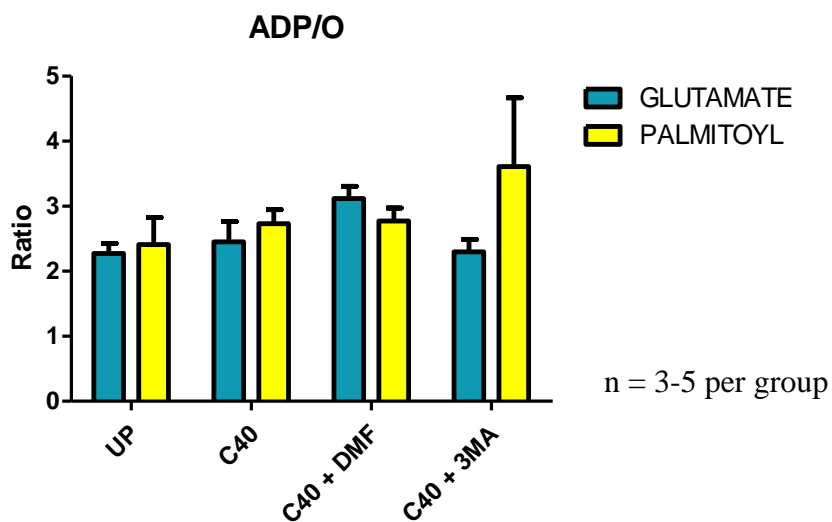
Figure 3:5 (A) Beclin-1 (D40C5) levels and (B) BNIP3/Nix (D4R4B) levels of tissues from unperfused and perfused hearts treated with or without 3-MA and DMF. SF= Stain free

3.2.1. Effect of 3-MA and DMF on mitochondrial oxidative phosphorylation function of hearts perfused under baseline conditions

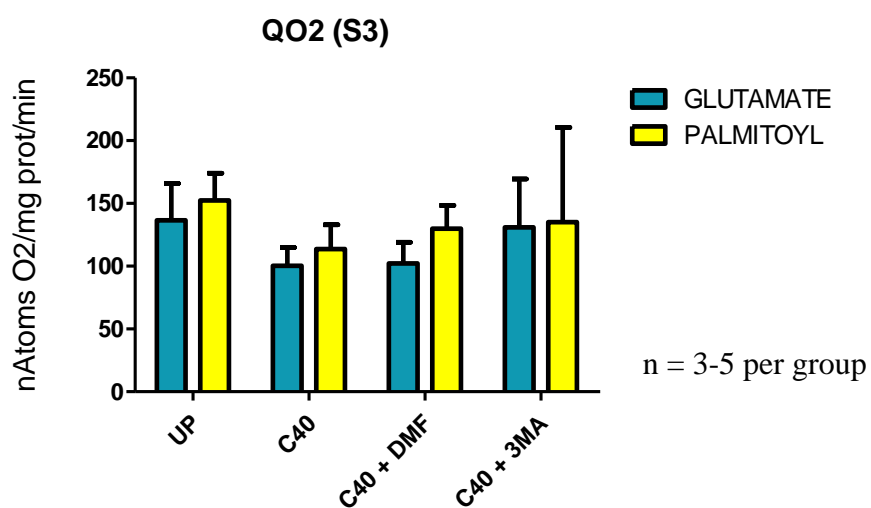
At the end of 40 min stabilization, mitochondria were prepared from heart tissue for analysis of the effects of 3-MA on the oxidative phosphorylation function. The parameters measured included the ADP/O ratio, states 3 and 4 respiration, the respiratory control index (RCI), oxidative phosphorylation rates for states 3 and 4. To assess the recovery potential of mitochondria, samples were exposed to 20 min anoxia in the oxygraph chamber, reoxygenated and State 3 respiration (in the presence of excess ADP) determined. Glutamate plus malate and palmitoyl-L-carnitine plus malate were used as substrates. The protocols used for these studies are the same as described above (see Figure 3:3).

There were no significant changes in any of the mitochondrial parameters in both media with the exception of the RCI (Figure 3:6D). There was a significant decrease in the RCI levels of mitochondria in the glutamate plus malate substrate medium for the untreated stabilisation protocol (C40) $p = 0.0333$ and with 3-MA (C40 + 3-MA) $p = 0.0098$ in comparison to the un-perfused hearts.

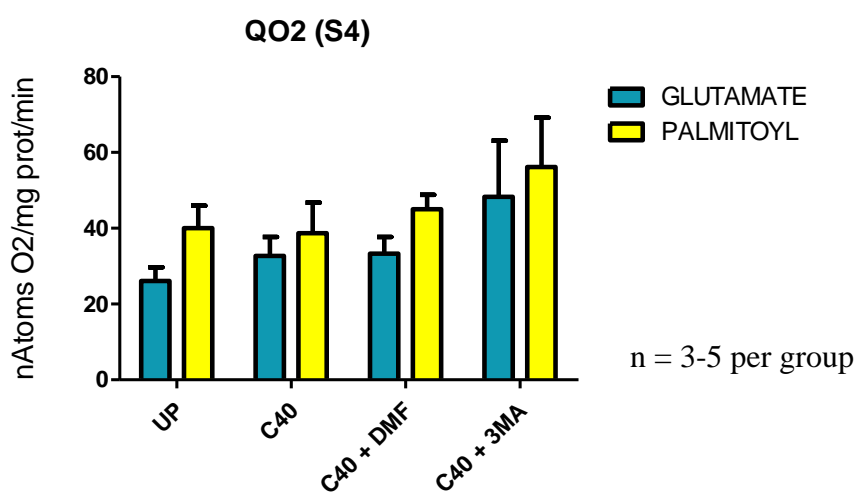
A)



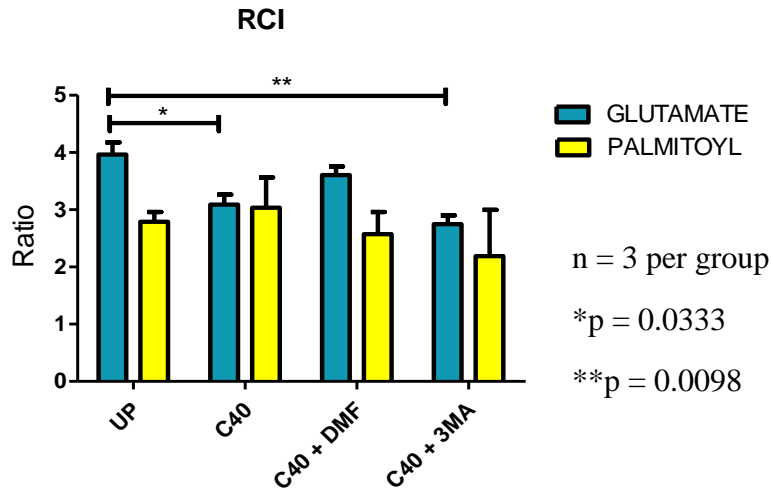
B)



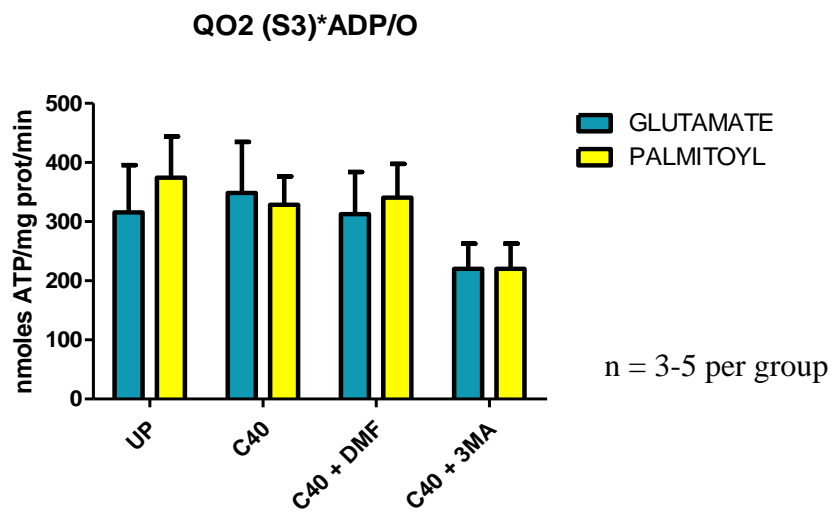
C)



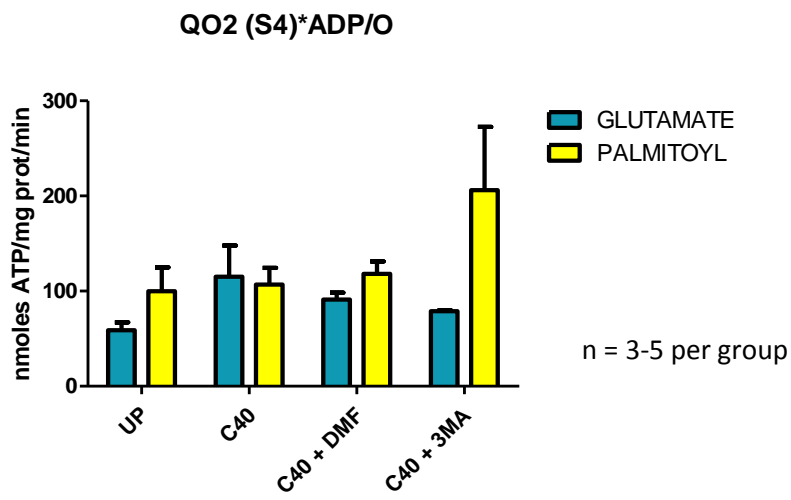
D)



E)



F)



G)

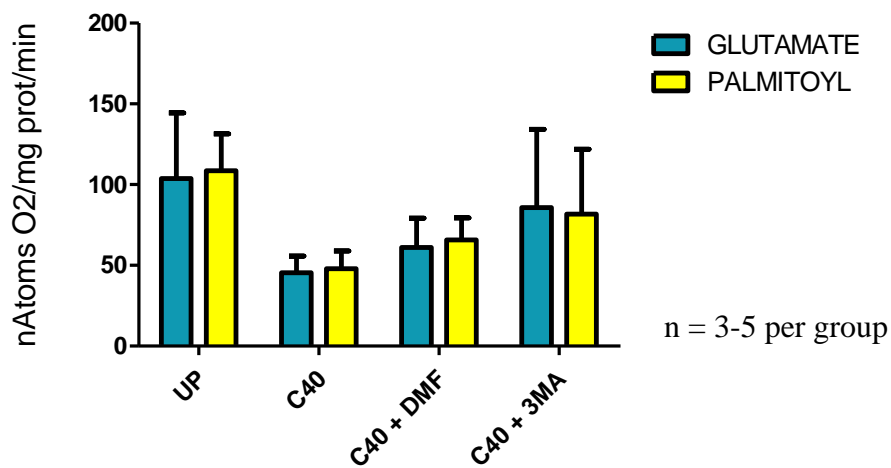
RE-OXYGENATION QO₂ (S3)

Figure 3:6 (A) ADP/O ratio, (B) QO₂ (state 3) respiration, (C) QO₂ (state4) respiration of mitochondria, (D) RCI, (E) oxidative phosphorylation rate (State3), (F) oxidative phosphorylation rate (State 4) and (G) Re-oxygenation QO₂ (S3) respiration, of mitochondria in glutamate plus malate or palmitoyl-L-carnitine plus malate substrate media, isolated from un-perfused hearts and baseline perfused hearts, treated with or without 3-MA with DMF as a vehicle.

3.3. Autophagic markers of hearts exposed to ischaemia or reperfusion with or without 3-MA and DMF as a vehicle

In these sets of experiments, we aimed to determine the effects of inhibiting autophagy with 3-MA before 25 min of global ischaemia and at the onset of 20 min of reperfusion on functional recovery of the heart, as well as the expression of autophagy markers, LC3A/B, Beclin-1 (D40C5) and BNIP3L/Nix (D4R4B) in heart tissue using Western blotting (for protocols see Figure 3:7)

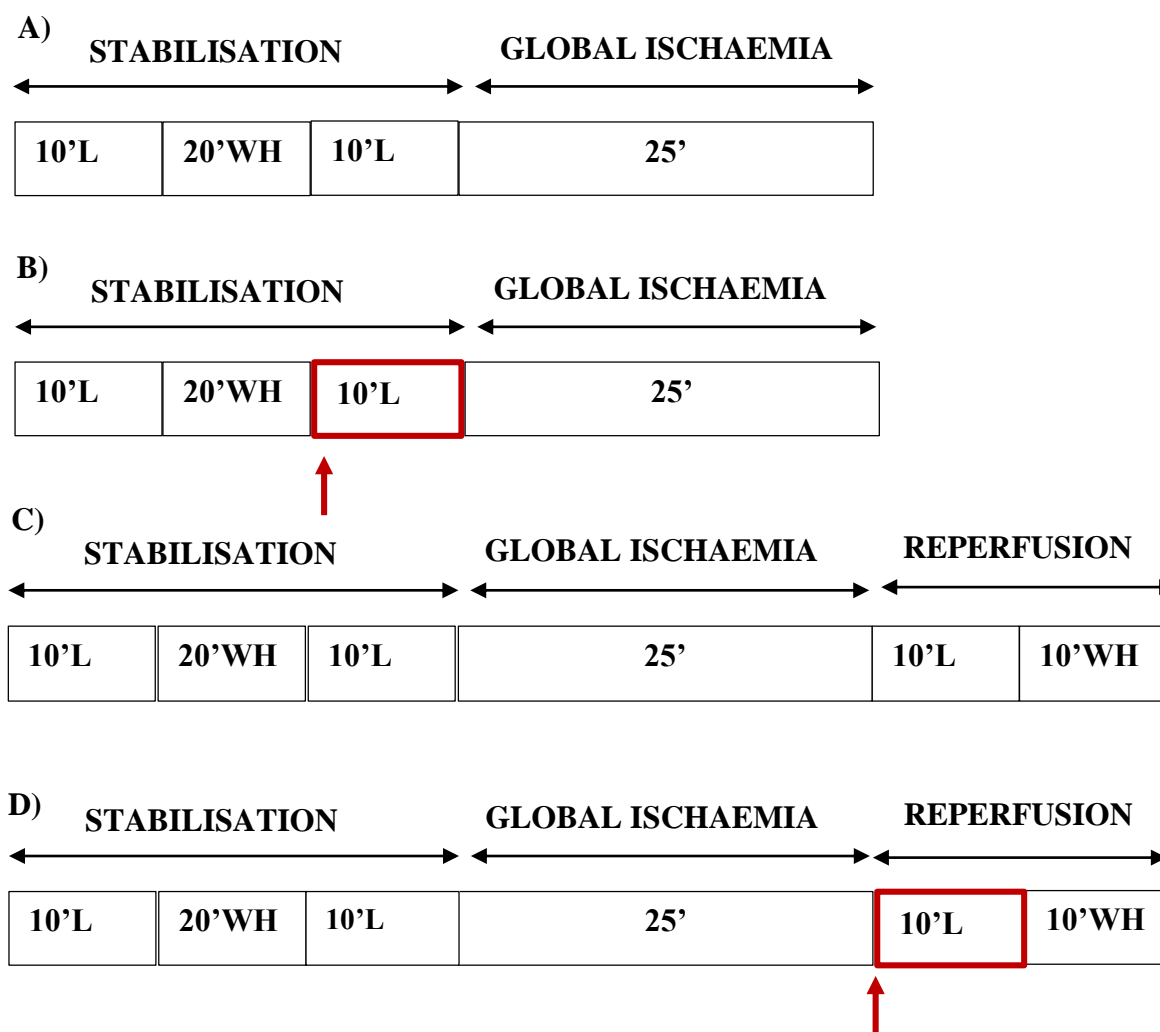


Figure 3:7 Perfusion protocols of hearts exposed to (A) untreated 25 min of global ischaemia (25 ISCH) or (B) pre-treated for 10 min with 3-MA or DMF before 25 min of global ischaemia (25 ISCH + 3-MA or 25 ISCH + DMF) represented with a red arrow and red block. (C) Hearts exposed to an un-treated 25 min global ischaemia followed by 20 min of reperfusion (20R) and (D) hearts treated with DMF or 3-MA (in combination with DMF) in the first 10 min of reperfusion (20R +3-MA or 20R +DMF), indicated with the red block and arrow

In the mechanical data untreated reperfused hearts functioned poorly during reperfusion whereas hearts treated with either DMF or 3-MA at the onset of reperfusion did not produce aortic output during reperfusion in comparison to pre-ischaemic function $p < 0.0001$ (Table 3.2 A and B). The untreated ischaemia and reperfusion did not have any effect on BNIP3L/Nix (D4R4B) and Beclin-1 (D40C5) levels (Figure 3:8 and 3:9 respectively). 3-MA and DMF similarly did not affect these protein levels. LC3 A/B-I levels (Figure 3:10) were generally significantly lower in reperfused hearts treated with 3-MA or DMF in comparison to the hearts of the ischaemic protocols with the same drug conditions $p = 0.0015$. However, LC3 A/B-I levels were significantly increased when 3-MA was added pre-ischaemia in comparison to the untreated ischaemic hearts (25 ISCH + 3-MA vs 25 ISCH) $p = 0.020$. Similarly, with the LC3 A/B-II levels, hearts from the reperfusion protocols had significantly lower levels in comparison to the ischaemic protocols $p = 0.0031$ (Figure 3:11). In the LC3 A/B-II/I ratio (Figure 3:12), expression levels were significantly higher in the untreated ischaemic protocol in comparison to when DMF or 3-MA was administered before ischaemia $p = 0.0279$ and 0.0495 respectively.

Table 3:2 Mechanical data before ischaemia (A) and after ischaemia (B) for hearts perfused with the autophagy inhibitor 3-MA with DMF as a solvent. n = 4-15 per group (variance in sample size due to repetition of control experiments). ***p <0.0001 between functional parameters before vs after ischaemia, of individual protocols.

A)	TIME	PARAMETERS	25 ISCH (n=11)	25 ISCH + DMF (n=4)	25 ISCH + 3MA (n=4)	20 R (n=15)	20R + DMF (n=10)	20R + 3MA (DMF) (n=4)
	Before ischaemia	Coronary Output (mL/min)	13.4 ± 0.8	13.1 ± 0.9	13.1 ± 0.9	12.9 ± 0.5	15.4 ± 0.9	13.9 ± 0.4
		Aortic Output (mL/min)	46.5 ± 2.3	44.5 ± 5.3	44.5 ± 5.3	43.5 ± 1.9	43.2 ± 2.1	38 ± 3
		Cardiac Output (mL/min)	59.9 ± 2.5	57.1 ± 6.2	57.1 ± 6.2	56.3 ± 2.1 ***	59 ± 2.7 ***	51.9 ± 3.2***
		Peak Systolic Pressure (mm Hg)	84.4 ± 1	84 ± 1.8	84 ± 1.8	84 ± 0.7	86.6 ± 1.1	83 ± 0.7
		Heart Rate (BPM)	297 ± 5.8	285 ± 28.4	285 ± 28.4	301.6 ± 8.9	352 ± 20.7	320.3 ± 10.5
		Total Work (mW)	11.3 ± 0.6	10.9 ± 1.2	9.6 ± 0.6	10.9 ± 1.2 ***	11.3 ± 0.5***	9.4 ± 0.6***

B)

TIME	PARAMETERS	25 ISCH (n=11)	25 ISCH + DMF (n=4)	25 ISCH + 3MA (n=4)	20 R (n=15)	20R + DMF (n=10)	20R + 3MA (DMF) (n=4)
After ischaemia during Reperfusion	Coronary Output (mL/min)	n/a	n/a	n/a	3.2 ± 1.4	0	0
	Aortic Output (mL/min)	n/a	n/a	n/a	0.3 ± 0.3	0	0
	Cardiac Output (mL/min)	n/a	n/a	n/a	3.5 ± 1.6***	0***	0***
	Peak Systolic Pressure (mm Hg)	n/a	n/a	n/a	9.5 ± 6.7	0	0
	Heart Rate (BPM)	n/a	n/a	n/a	40.4 ± 27.5	0	0
	Total Work (mW)	n/a	n/a	n/a	0.4 ± 0.3***	0***	0***

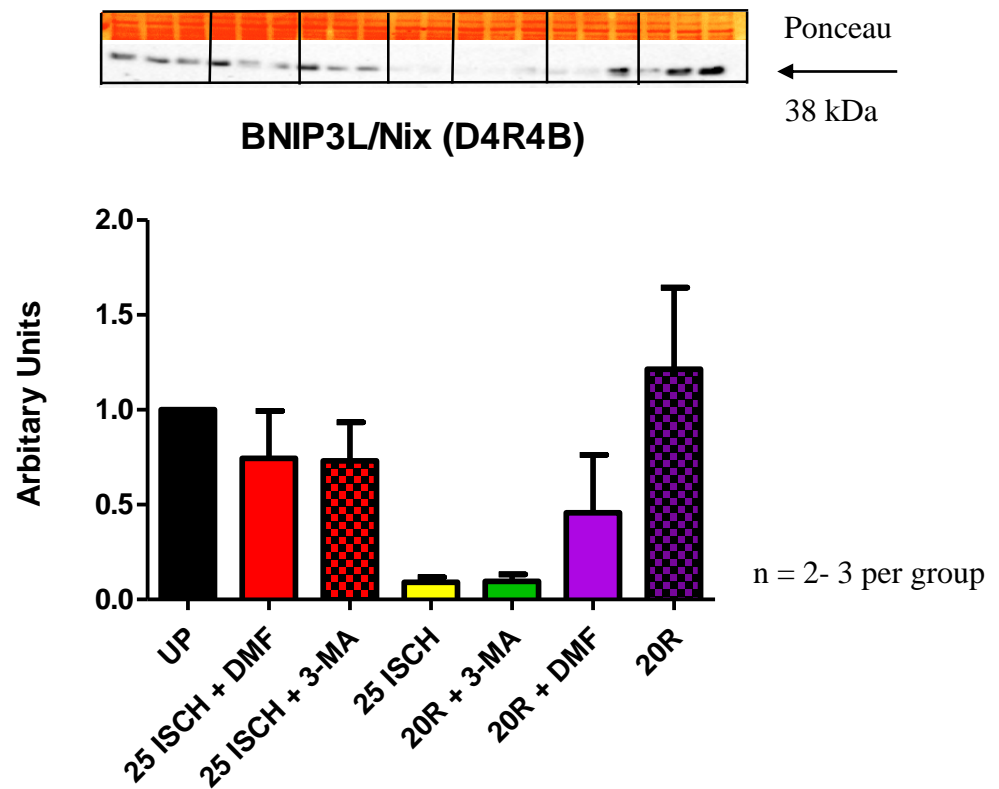


Figure 3:8 BNIP3L/Nix (D4R4B) levels of heart tissue exposed to ischaemic and reperfusion protocols treated with or without 3-MA and DMF as a vehicle

c

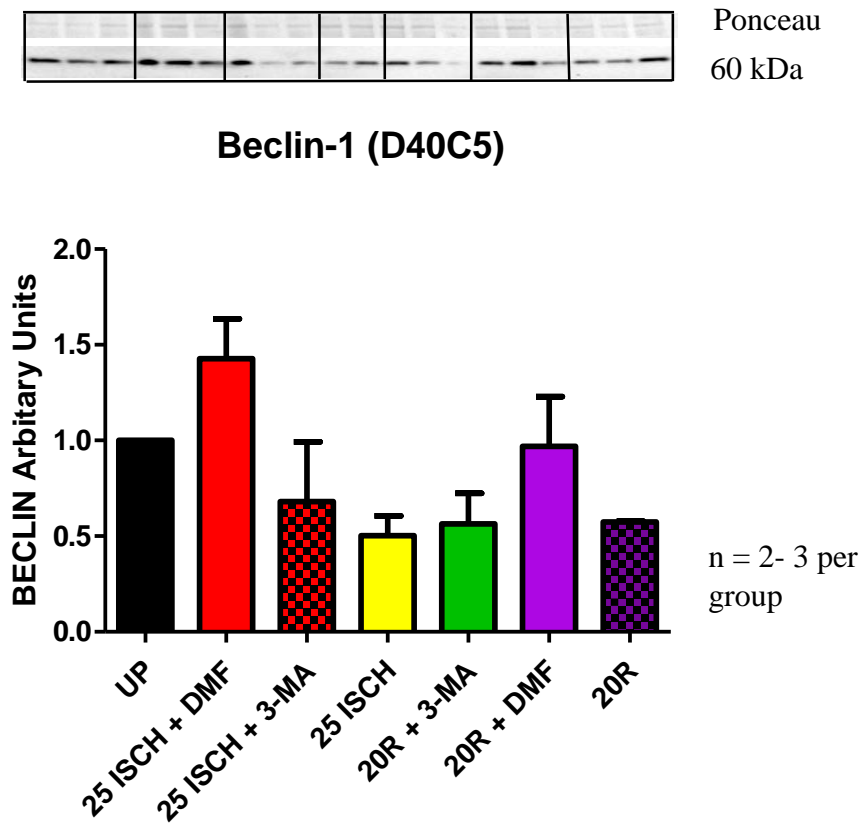


Figure 3:9 Beclin-1 (D40C5) levels of heart tissue exposed to ischaemic and reperfusion protocols treated with or without 3-MA and DMF as a vehicle. Ponceau saved in grey colour image.

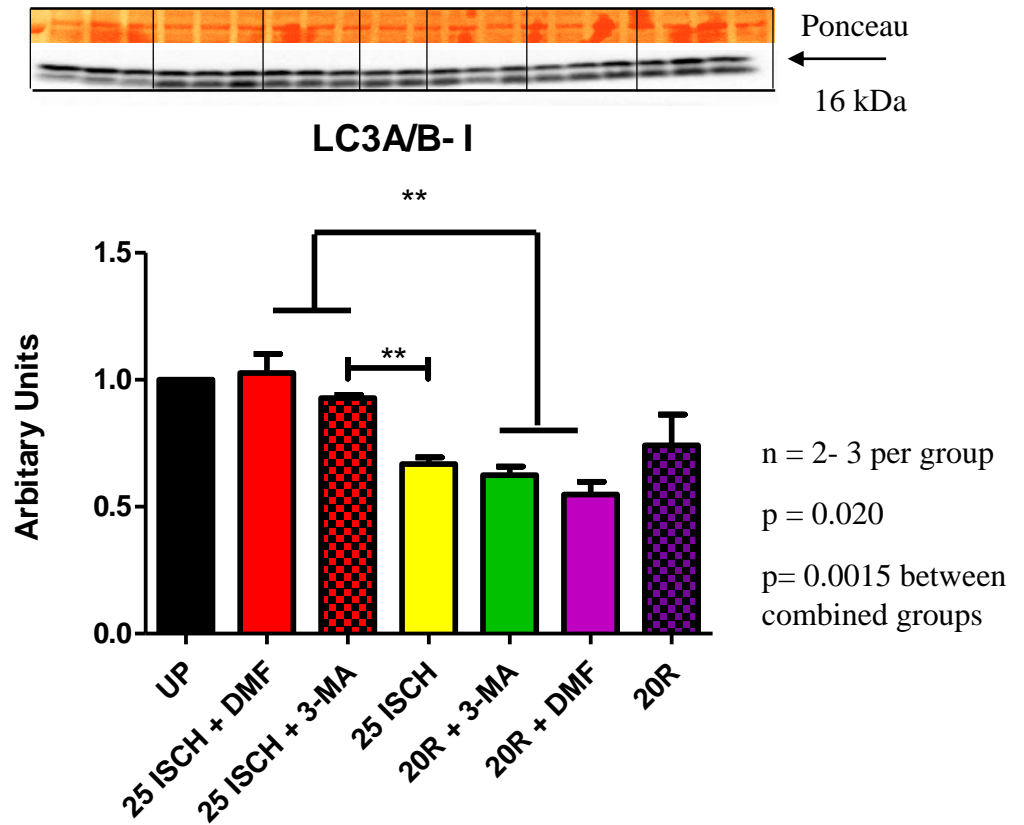


Figure 3:10 LC3A/B-I levels of heart tissue exposed to ischaemic and reperfusion protocols treated with or without 3-MA and DMF as a vehicle

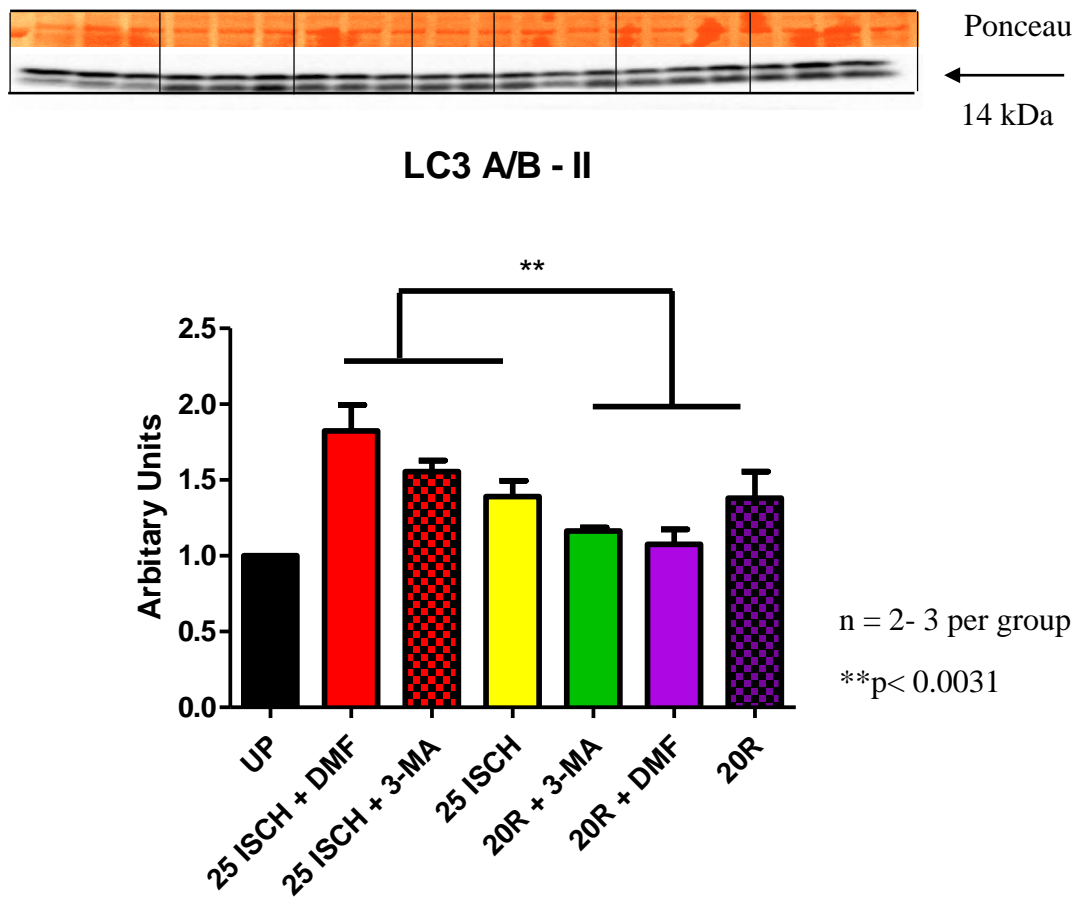


Figure 3:11 LC3A/B-II levels of heart tissue exposed to ischaemic and reperfusion protocols treated with or without 3-MA and DMF as a vehicle

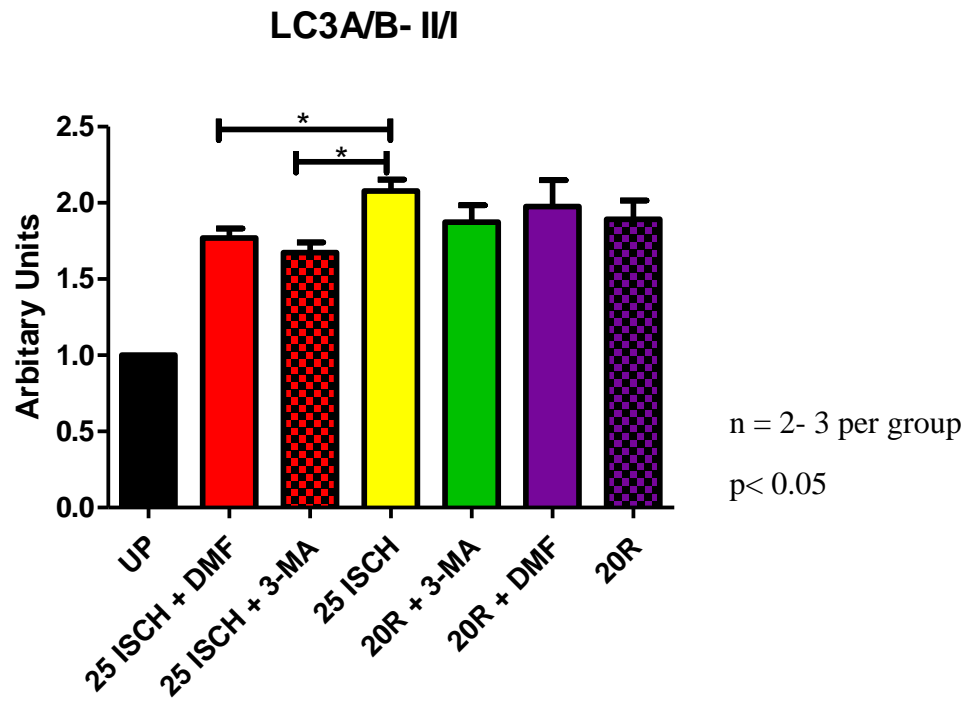


Figure 3:12 LC3 A/B-II/I ratio levels of heart tissue exposed to ischaemic or reperfusion protocols with or without 3-MA and DMF as a vehicle

3.4. Autophagic markers of hearts exposed to ischaemic or reperfusion protocols treated with or without 3-MA and H₂O as a vehicle

In these sets of experiments, we aimed to determine the effect of the autophagy inhibitor, 3-MA dissolved in distilled water (dH₂O) as DMF as a solvent appeared to be toxic to the hearts and led to heart failure during reperfusion. In fact, the data indicate that the effects seen in most experiments were due to the vehicle DMF, rather than 3-MA since similar observations were made in these groups. In these sets of experiments hearts were exposed to 25 min of global ischaemia or 20 min reperfusion with or without drug intervention (see Figure 3:13.). The expression of LC3A/B, Beclin-1 (D40C5) and BNIP3L/Nix (D4R4B) were determined using Western blotting on heart tissue from the perfused hearts.

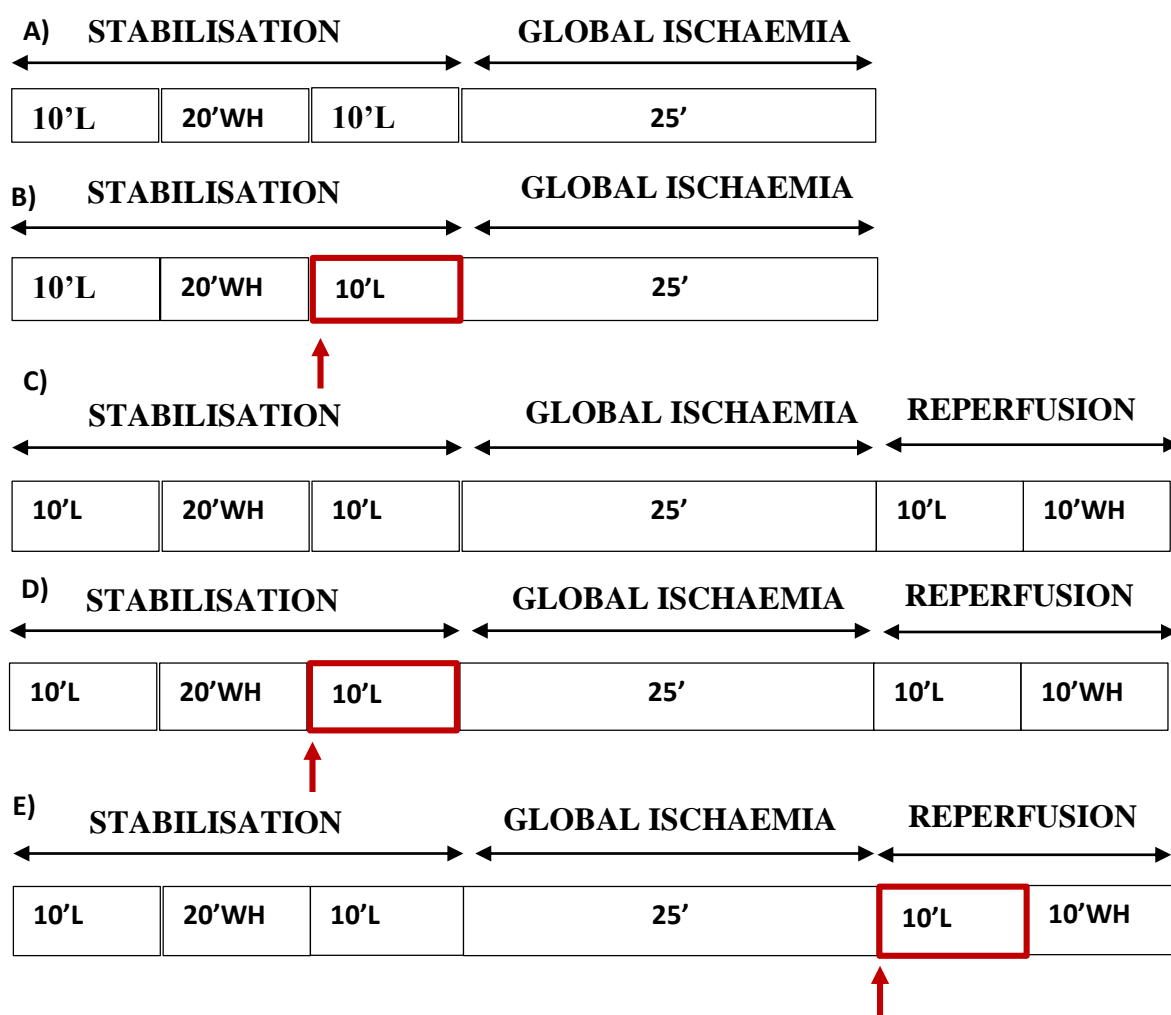


Figure 3:13 Perfusion protocols for hearts exposed to (A) untreated 25 min of global ischaemia (25 ISCH), (B) pre-treated with 3-MA before ischaemia (25 ISCH + 3-MA), (C) untreated 20 min of reperfusion (20R), (D) 3-MA treatment before ischaemia and reperfusion (20R +3-MA B. ISCH) and (E) 3-MA post-treatment at the onset of reperfusion/after ischaemia (20R + 3-MA A. ISCH).

There was a slight recovery from hearts pre- or post-treated with 3-MA during reperfusion compared to hearts pre-treated with DMF (Table 3.3b vs Table 3.2b). However, the post-ischaemic function was significantly lower than that of the pre-ischaemic function $p < 0.0001$. Hearts exposed to ischaemia or reperfusion with or without 3-MA did not affect the expression levels of Beclin-1 (D40C5) (Figure 3:14). Hearts from reperfusion together with hearts from reperfusion with 3-MA pre-ischaemic treatment yielded higher BNIP3L/Nix (D4R4B) levels than hearts from untreated and pre-treated ischaemic protocols $p = 0.0417$ (Figure 3:15). There were no significant changes in the LC3 A/B-I and II levels in any of the protocols with or without 3-MA. LC3A/B-II/I levels of hearts were reduced when exposed to ischaemia in comparison to hearts from the baseline perfusion $p = 0.014$. These levels were further reduced in the reperfusion protocols $p = 0.0009$ (Figure 3:18). 3-MA had no effect on this ratio of the proteins levels in any of the perfusion protocols.

Table 3:3 Mechanical data (A) before ischaemia and (B) after ischaemia for hearts perfused with the autophagy inhibitor 3MA with water as a solvent n = 4-15 per group. All groups were followed by mitochondrial preparation. ***p <0.0001 between functional parameters before vs after ischaemia, of individual protocols.

A)	TIME	PARAMETERS	C40 (n=15)	25 ISCH (n=11)	25 ISCH + 3MA (n=9)	20 R (n=15)	20R + 3-MA B. ISCH (n=11)	20R + 3MA A. ISCH (n=12)
Before ischaemia		Coronary Output (mL/min)	14 ± 0.6	13.4 ± 0.8	10.8 ± 1	12.9 ± 0.5	16.1 ± 1.7	13.5 ± 1
		Aortic Output (mL/min)	44.5 ± 1.6	46.5 ± 2.3	41.3 ± 2.5	43.5 ± 1.9	37.8 ± 2.8	43.8 ± 1.9
		Cardiac Output (mL/min)	58.5 ± 1.8	59.9 ± 2.5	52.2 ± 3	56.3 ± 2.1***	53.9 ± 3.1	57.6 ± 2.2***
		Peak Systolic Pressure (mm Hg)	83.3 ± 0.5	84.4 ± 1	83.6 ± 1.8	84 ± 0.7	84.4 ± 0.9	84.4 ± 0.5
		Heart Rate (BPM)	307 ± 9.7	297 ± 5.8	270 ± 12.2	301.6 ± 8.9	282.6 ± 13.1	285 ± 12.7
		Total Work	10.8 ± 0.4	11.3 ± 0.6	9.6 ± 0.6	10.5 ± 0.4***	10.1 ± 0.6	10.9 ± 0.7***

B)	TIME	PARAMETERS	C40 (n=15)	25 ISCH (n=11)	25 ISCH + 3MA (n=9)	20 R (n=15)	20R + 3-MA B. ISCH (n=11)	20R + 3MA A. ISCH (n=4)
		Coronary Output (mL/min)	n/a	n/a	n/a	3.2 ± 1.4	6.3 ± 2.0	4.2 ± 1.4
		Aortic Output (mL/min)	n/a	n/a	n/a	0.3 ± 0.3	-	3.8 ± 3.8
	After ischaemia during reperfusion	Cardiac Output (mL/min)	n/a	n/a	n/a	3.5 ± 1.6***		11.6 ± 4.9***
		Peak Systolic Pressure (mm Hg)	n/a	n/a	n/a	9.5 ± 6.7	-	53.5 ± 18.9
		Heart Rate (BPM)	n/a	n/a	n/a	40.4 ± 27.5	-	223.3 ± 74.8
		Total Work	n/a	n/a	n/a	0.4 ± 0.3***	-	1.9 ± 1***

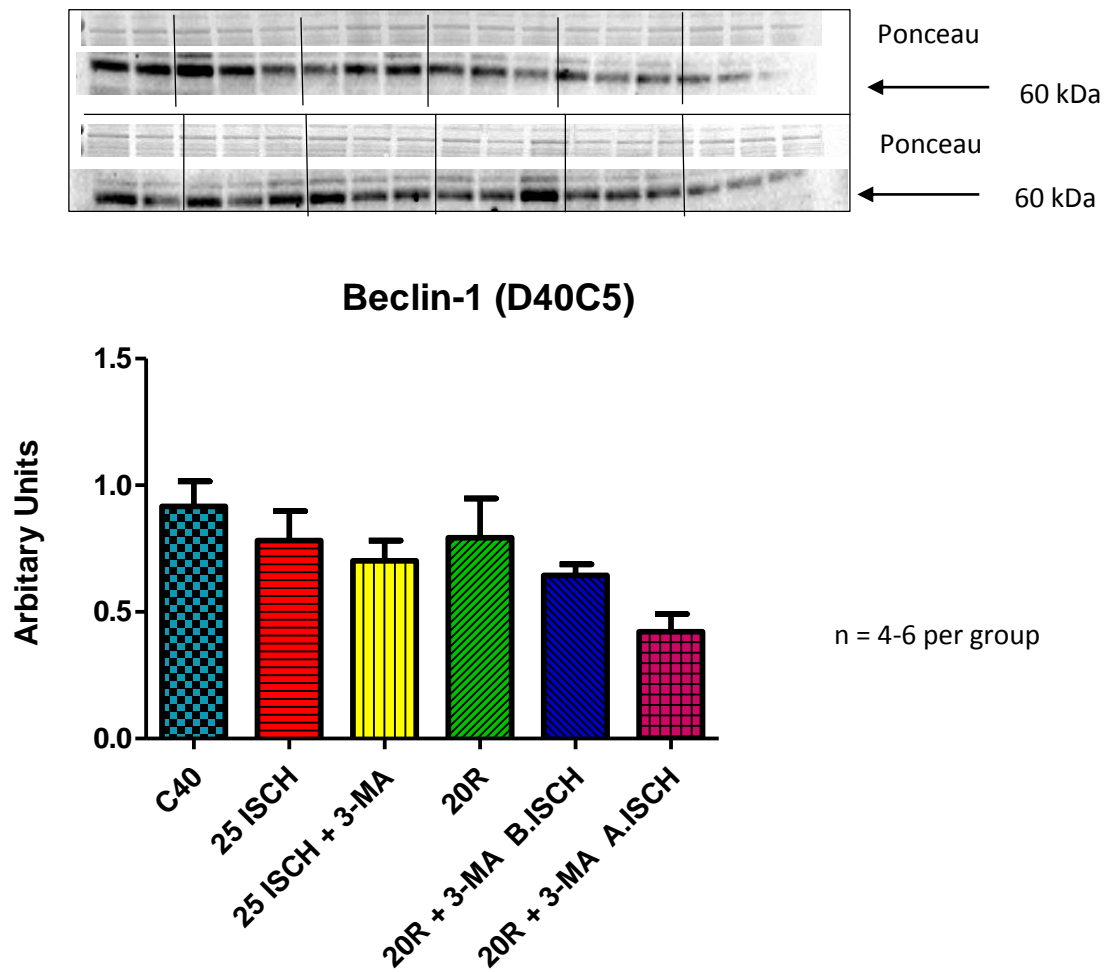


Figure 3:14 Beclin-1 (D40C5) levels of heart tissue from ischaemic or reperfusion protocols treated with or without 3-MA. Ponceau saved in grey colour image.

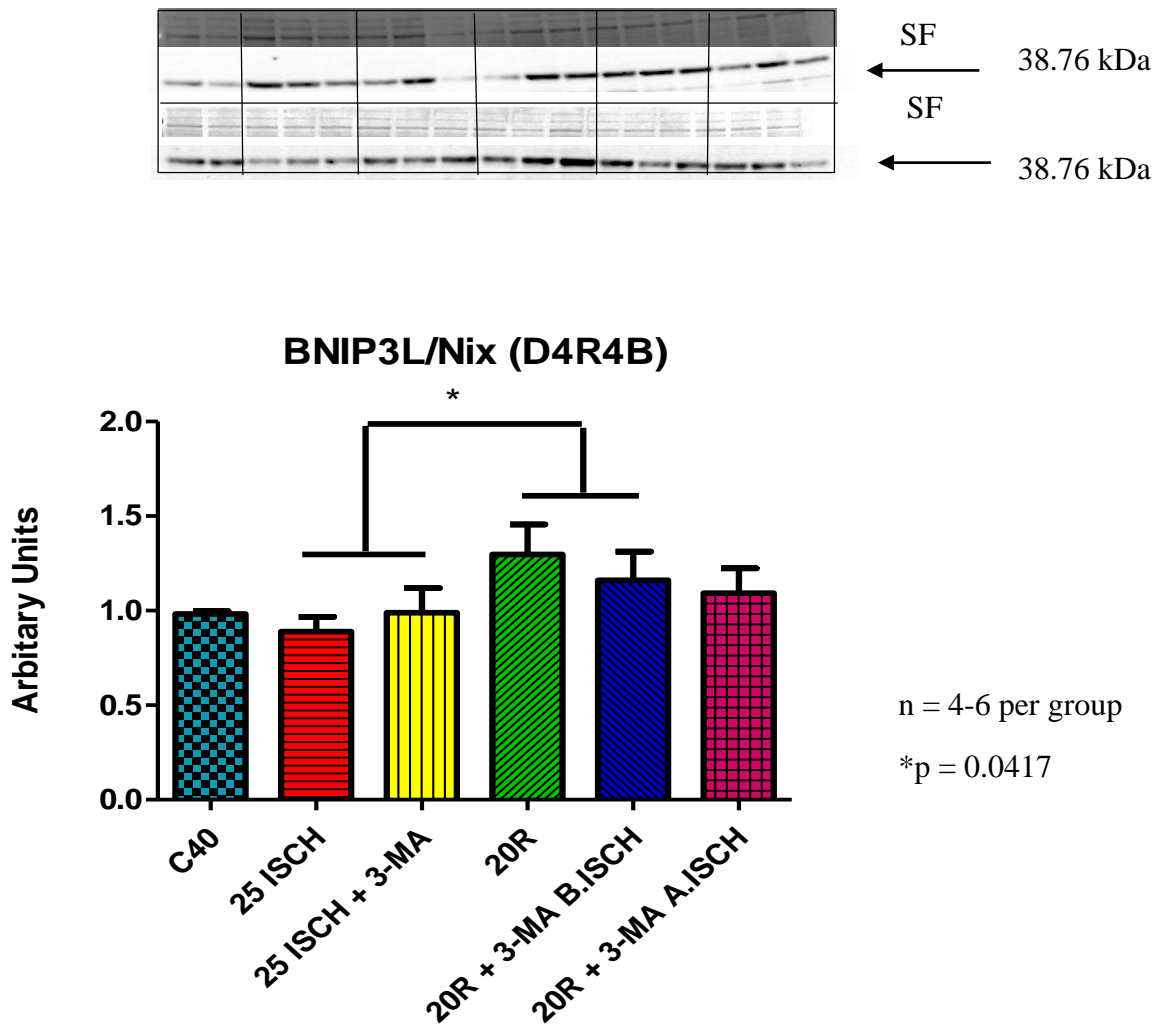


Figure 3:15 BNIP3L/Nix (D4R4B) levels of heart tissue from ischaemic or reperfusion protocols treated with or without 3-MA. SF= Stain Free

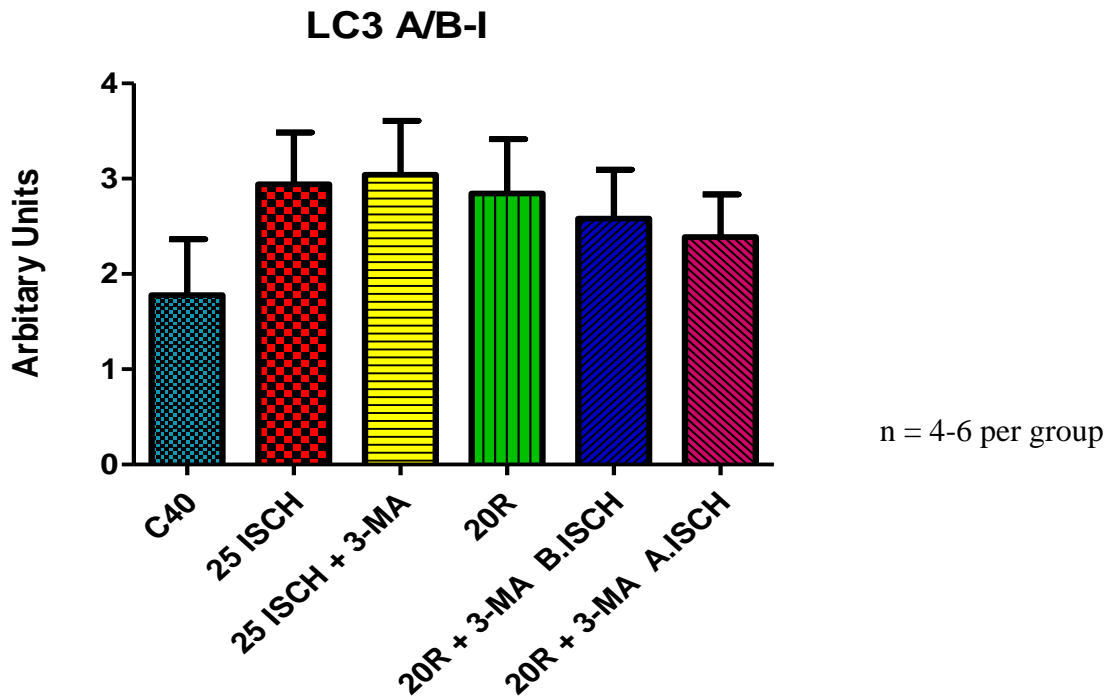
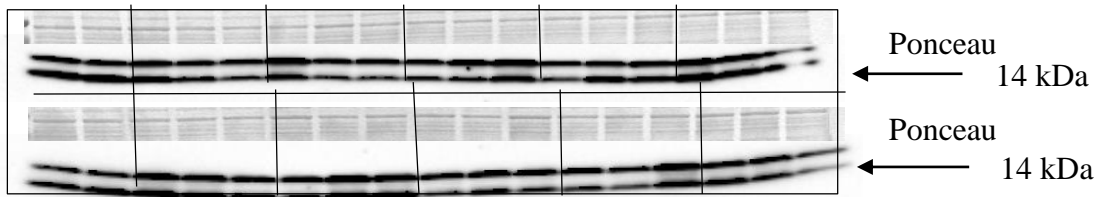


Figure 3:16 LC3A/B- I levels of heart tissue from ischaemic or reperfusion protocols treated with or without 3-MA. Ponceau saved in grey colour image

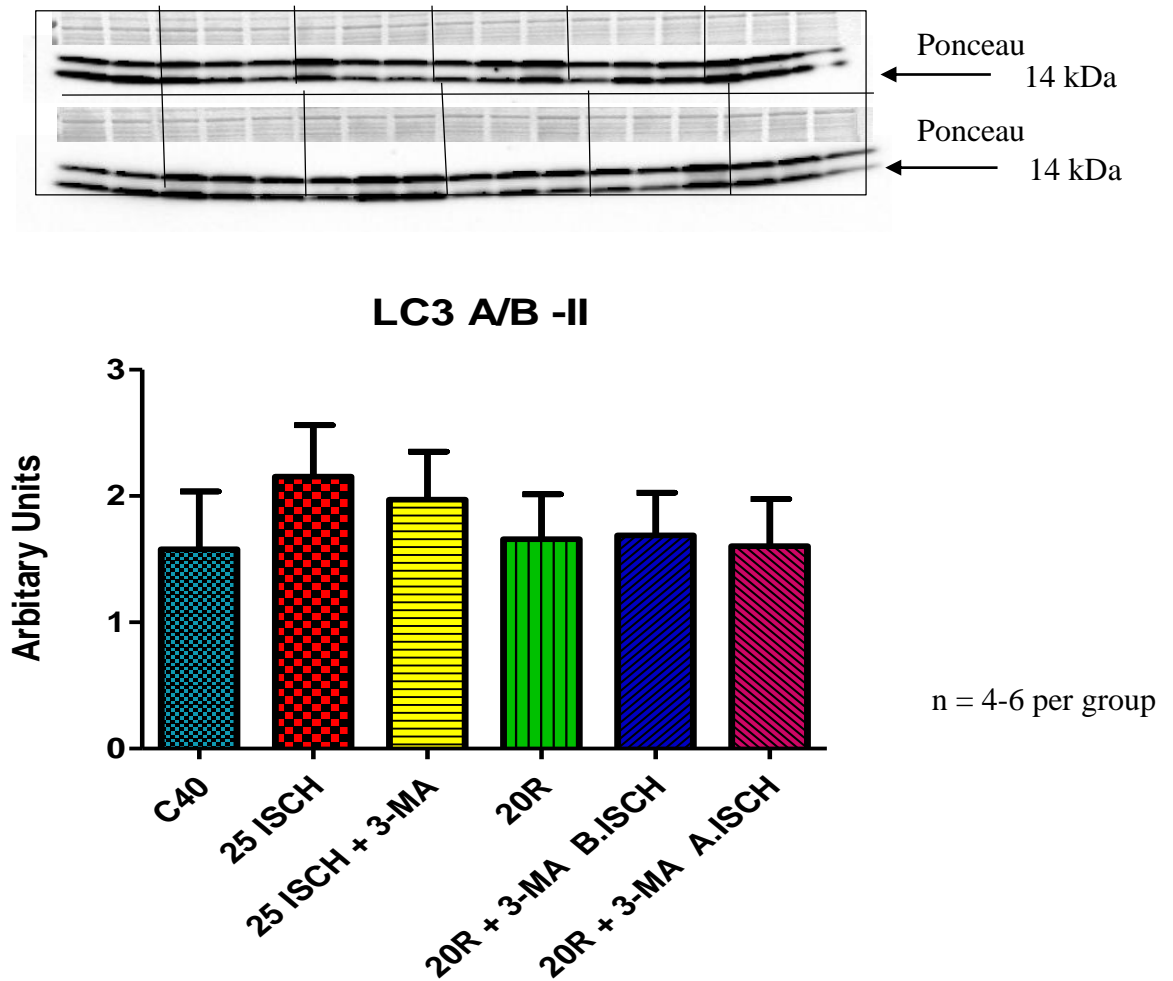


Figure 3:17 LC3A/B- II levels of heart tissue from ischaemic or reperfusion protocols treated with or without 3-MA. Ponceau saved in grey colour image.

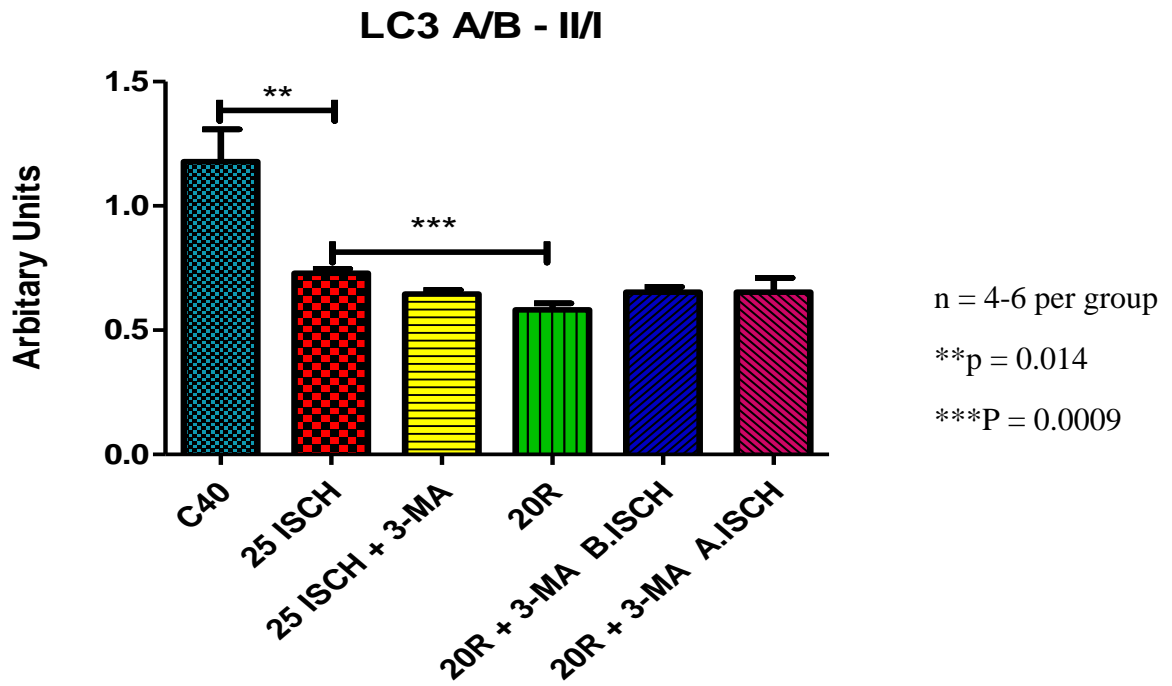


Figure 3:18 LC3A/B- II/I ratio of hearts from ischaemic or reperfusion protocols treated with or without 3-MA

3.4.1. Mitochondrial Function of hearts from ischaemic or reperfusion protocols treated with or without 3-MA with H₂O as a vehicle

In this set of experiments, we aimed to determine the mitochondrial function of heart tissue exposed to different perfusion protocols, including 25 min of global ischaemia or 20 min of reperfusion, each treated with or without 3-MA. For outline of perfusion protocol see Figure 3:13 (mechanical data in Table 3:3). The mitochondrial parameters measured included the ADP/O ratio, states 3 and 4 respiration, the respiratory control index (RCI), oxidative phosphorylation rates for states 3 and 4 and state 3 respiration after re-oxygenation. As in previous studies, glutamate plus malate and palmitoyl-L-carnitine plus malate were used as substrates. The mitochondrial markers of mitophagy, PINK1, Parkin and p62, were measured using Western blotting. The citrate synthase activity of the mitochondria was also determined as an indicator of intact mitochondria (Holloszy et al. 1970).

The QO₂(state 3) (Figure 3:19 B) of mitochondria isolated from hearts subjected to 25 min global ischaemia or reperfusion did not differ from those of hearts subjected to 40 min control perfusion only, regardless of the substrate present. However, administration of the drug at the onset of reperfusion, caused a significant increase in respiration, particularly with glutamate plus malate as substrate ($p=0.0009$) in comparison to the reperfusion control and versus 3-MA administration prior to ischaemia and reperfusion ($p=0.0233$).

The mitochondrial respiratory control index (Figure 3:19 D) was unchanged by exposure of hearts to untreated ischaemia or reperfusion. In the reperfusion protocols there was a significant increase in the mitochondrial RCI levels in palmitoyl-L-carnitine plus malate as substrate of hearts treated with 3-MA either before ischaemia and reperfusion or at the onset of reperfusion in comparison to mitochondria from untreated reperfused hearts ($p = 0.0255$).

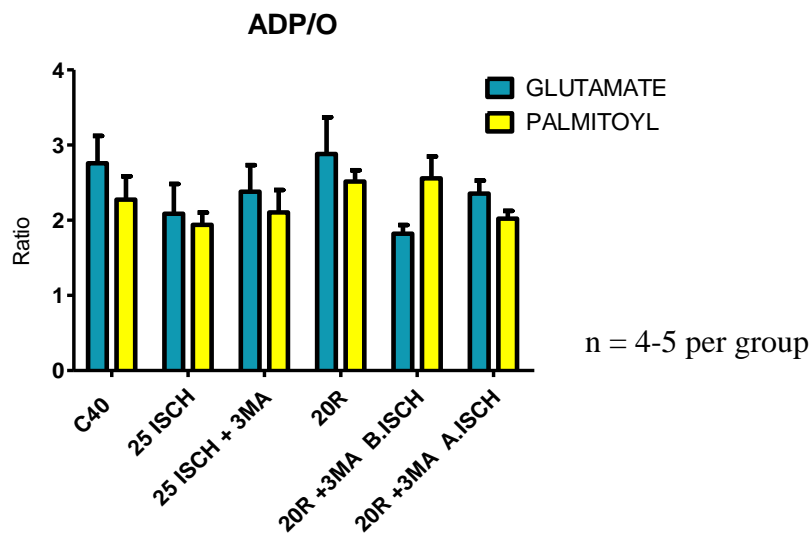
Mitochondria isolated from hearts perfused under baseline conditions had lower oxidative phosphorylation rate (state 4) values (Figure 3:19 F) with palmitoyl-L-carnitine plus malate as substrate than with glutamate plus malate as substrate ($p = 0.0006$). Interestingly, mitochondria from untreated reperfused hearts had higher oxidative phosphorylation rates (State 4) with palmitoyl-L-carnitine plus malate as substrate compared to glutamate plus malate ($p = 0.0095$). Oxidative phosphorylation rates (state 4) were significantly lower in mitochondria of untreated reperfused hearts in comparison to the baseline conditions with glutamate plus malate substrate ($p= 0.0003$). 3-MA did not affect these levels with either substrate.

There were no significant changes observed in the ADP/O ratios (Figure 3:19 A), QO₂ (S₄) (Figure 3:19 C) respiration, oxidative phosphorylation rate for state 3 (QO₂(S₃) *ADP/O) (Figure 3:19 E) and the reoxygenation rate (Figure 3:19 G), of mitochondria isolated after the different perfusion protocols or with 3-MA in either protocol. The mitochondrial substrate present was without effect on the outcome of the data.

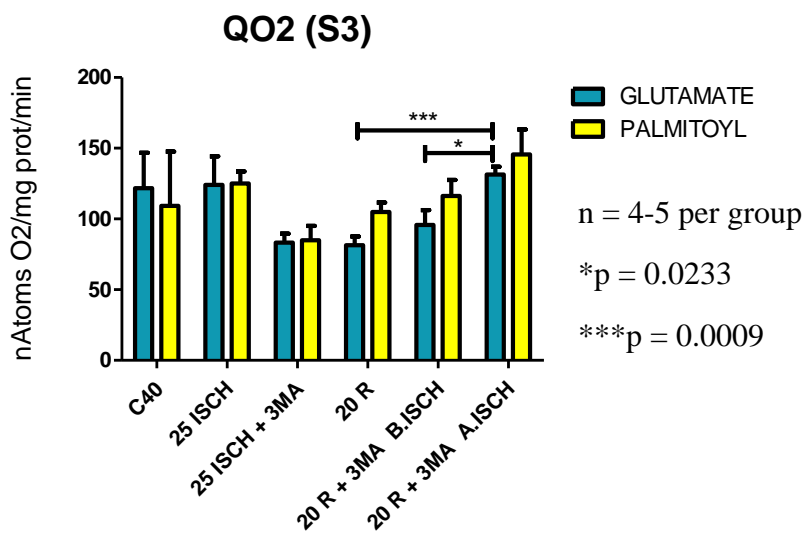
For the mitophagy markers, there were no significant changes between the untreated ischaemic and reperfusion protocols in PINK1 (Figure 3:20) and p62 levels (Figure 3:22) and this was only observed with the Parkin levels. There was a significant decrease in the PINK1 expression levels for mitochondria isolated from hearts exposed to reperfusion when compared to mitochondria from hearts exposed to the stabilisation protocol (C40). There was also a slight down regulation in PINK1 levels for hearts exposed to untreated ischaemia, however, it was not significant ($p = 0.09$). 3-MA administered before ischaemia resulted in a further decline in mitochondrial PINK1 expression, compared to mitochondria isolated from untreated ischaemic hearts (25 ISCH + 3-MA vs 25 ISCH) ($p=0.0475$). The opposite was observed in the reperfusion protocols as there was a significant increase in mitochondrial PINK1 levels when hearts were perfused with 3-MA at the onset of reperfusion, when compared to the untreated reperused hearts (20R+3-MA A. ISCH vs 20R) $p = 0.008$.

Exposure of hearts to ischaemia alone had no effect on mitochondrial Parkin levels, while reperfusion caused a significant lowering in the expression of this parameter (20R vs 25 ISCH $p = 0.0421$). This reduction in Parkin expression upon reperfusion was also observed in mitochondria isolated from ischaemic hearts pre-treated with 3-MA compared with mitochondria isolated from reperused hearts pre-treated with 3-MA ($p= 0.0118$) (Figure 3:21). Overall untreated reperused hearts together with 3-MA pre-treatment before ischaemia and reperfusion had lower Parkin levels in comparison to hearts from the ischaemic protocols $p= 0.0026$. Similarly, for p62 mitochondrial levels, hearts from untreated reperfusion together with 3-MA pre-treatment before ischaemia and reperfusion had lower protein levels in comparison to the ischaemic protocols $p= 0.0076$ (Figure 3:22). There was no significant difference in the levels of mitochondrial citrate synthase activity of mitochondria isolated from hearts subjected to the different protocols in this study (Figure 3:23).

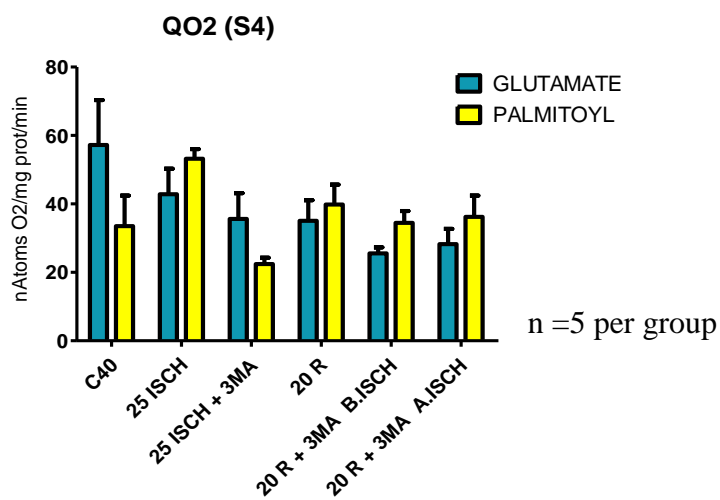
A)



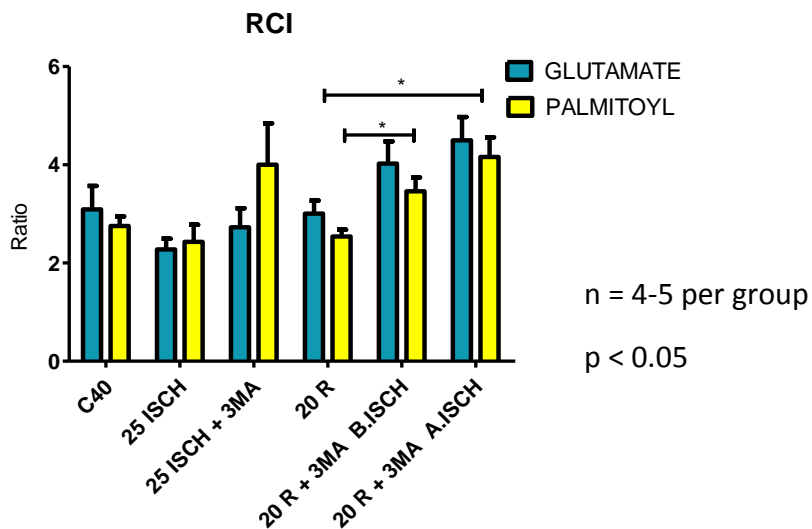
B)



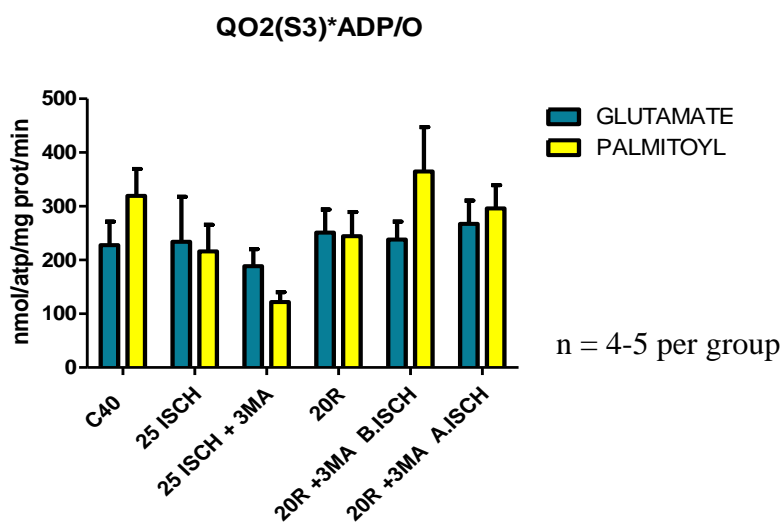
C)



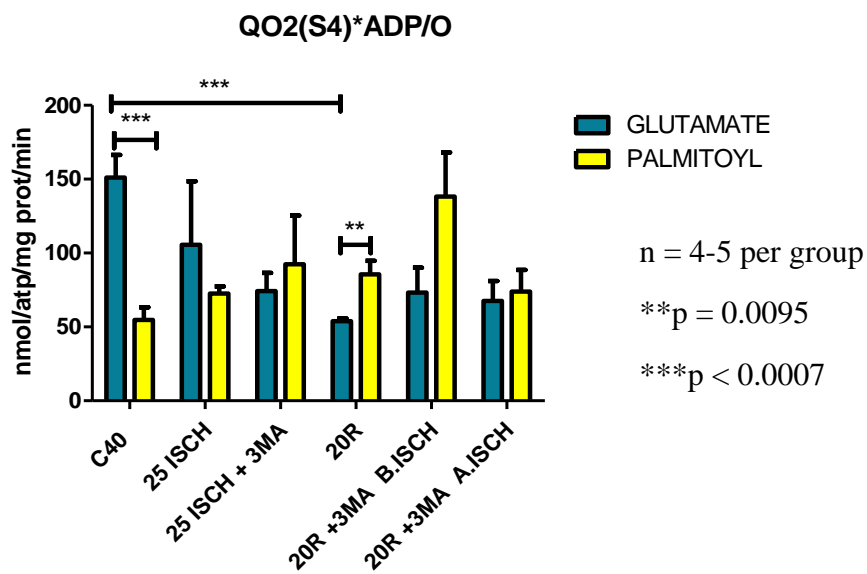
D)



E)



F)



G)

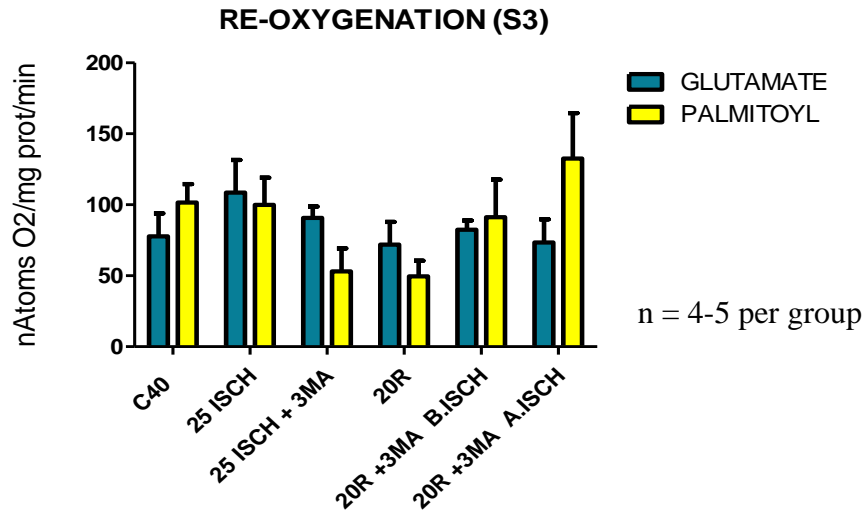


Figure 3:19 Mitochondrial parameters. (A) ADP/O ratio (B) QO₂ state 3 (S3) respiration and (C) QO₂ state 4 (S4) (D) RCI (E) oxidative phosphorylation rate state 3 (S3) (F) oxidative phosphorylation rate state 4 (S4) and (G) re-oxygenation respiration of mitochondria in glutamate plus malate or palmitoyl-L-carnitine plus malate substrate media, isolated from heart tissue exposed to ischaemic and reperfusion protocols perfused with or without 3-MA.

3.4.2. Mitophagic markers of hearts exposed to ischaemic or reperfusion protocols treated with or without 3-MA and H₂O as a vehicle

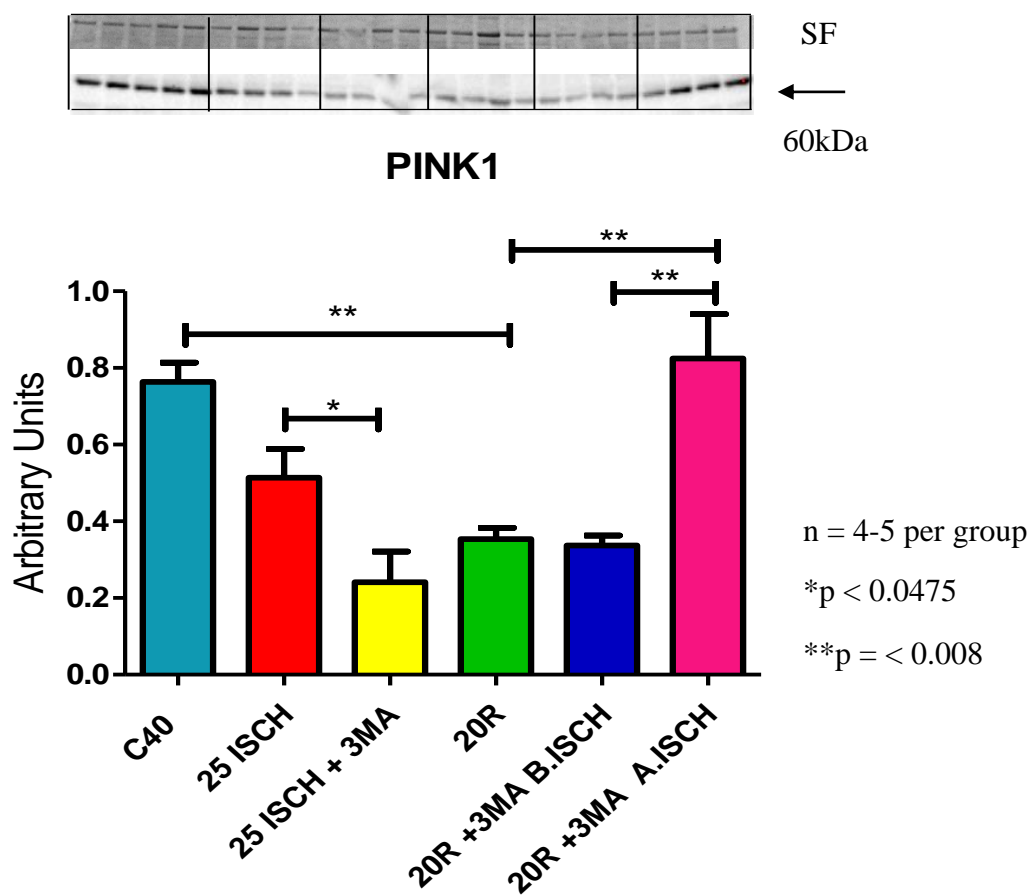


Figure 3:20 PINK1 levels of mitochondria from hearts perfused with or without 3-MA in ischaemic and reperfusion protocols. SF = Stain Free

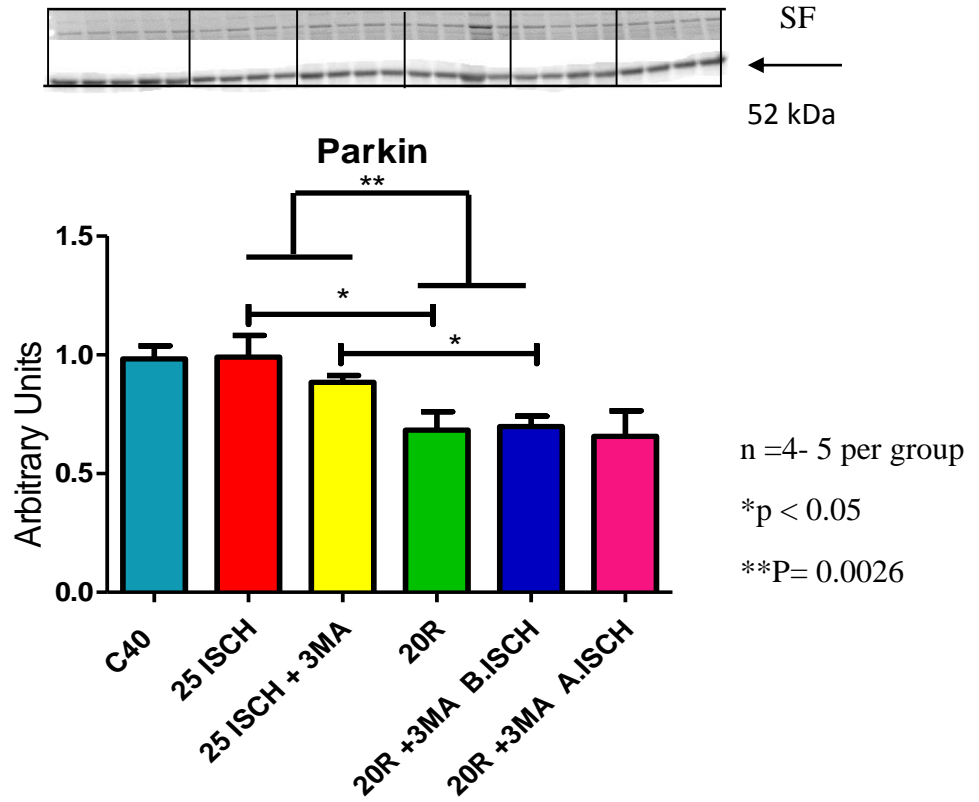


Figure 3:21 Mitochondrial Parkin levels of hearts perfused with or without 3-MA in ischaemic or reperfusion protocols. SF = Stain Free

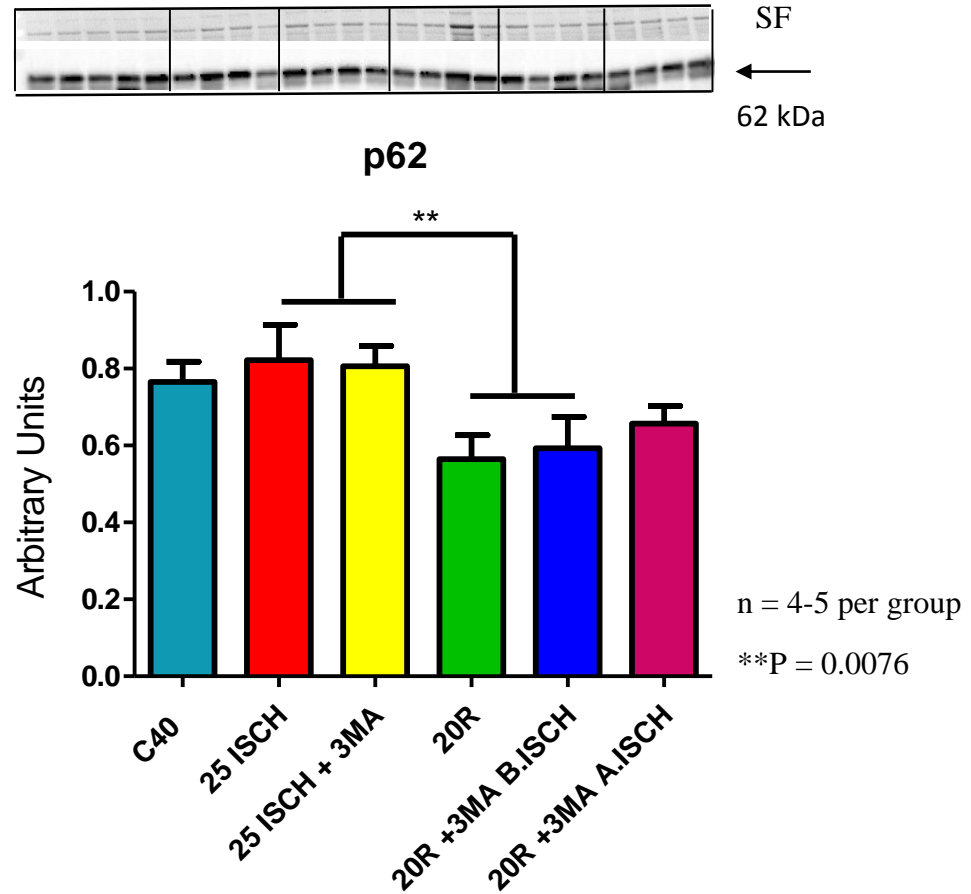


Figure 3:22 Mitochondrial p62 levels of hearts perfused with or without 3-MA in ischaemic and reperfusion protocols. SF = Stain Free

3.4.3. Citrate synthase activity of hearts treated with or without 3-MA in ischaemic or reperfusion protocols

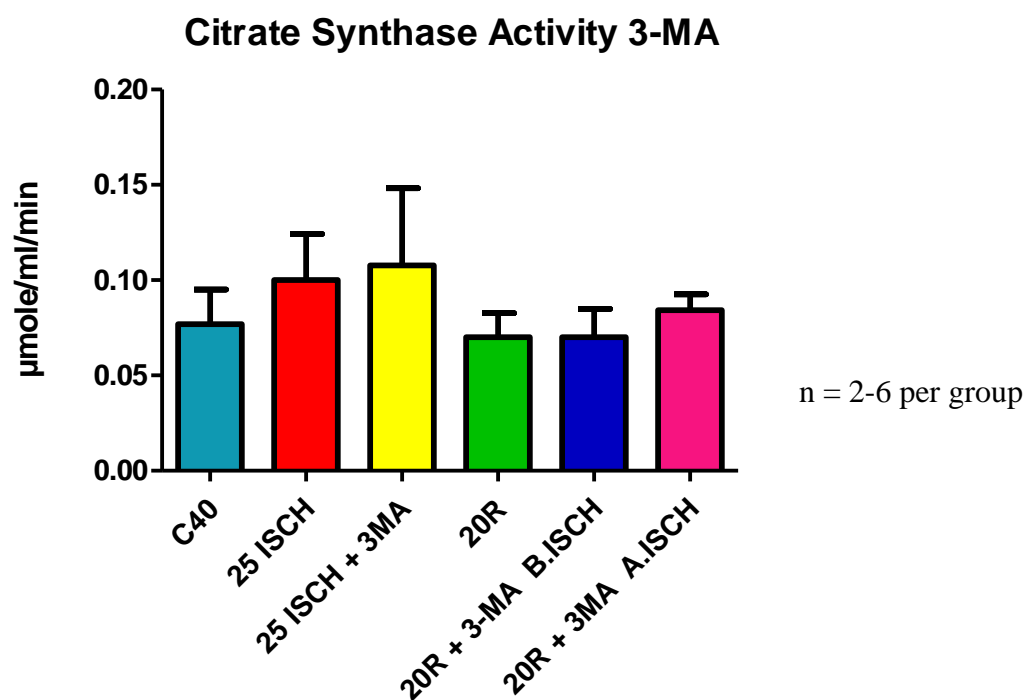


Figure 3:23 Citrate synthase activity from mitochondria isolated from hearts from ischaemic and reperfusion protocols treated with or without 3-MA

3.4.4. Effects of 3-MA pre-treatment on infarct size and area at risk

In this set of experiments, we aimed to determine the effect of 3-MA pre-treatment on infarct size and the area at risk of hearts. For this purpose, 3-MA (1 mM) was administered 10 min before 35 min of regional ischaemia, after ligation of the left anterior descending coronary artery (see Figure 3:24)

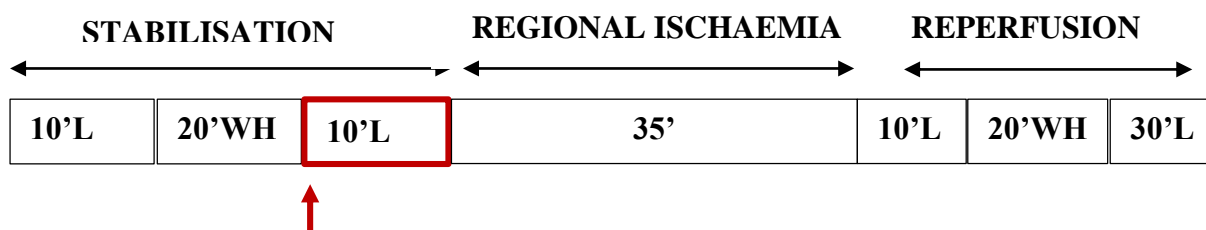


Figure 3:24 Regional ischaemia perfusion protocol for hearts pre-treated with 3-MA. Hearts were initially stabilised for 40 min and in the final 10 min of stabilisation 3-MA was administered to the hearts. This was followed by 35 min of regional ischaemia and finally an hour of reperfusion.

There were no significant differences in mechanical function/recovery (cardiac output and total work) during reperfusion of hearts pre-treated with 3-MA in comparison to the untreated controls (Table 3.4 and Figure 3:26)

3-MA had no effect on the infarct size (Figure 3:25 A) of perfused hearts when administered before induction of regional ischaemia, when compared with those of the untreated controls. However, these hearts had a significant reduction in the percentage of area at risk (compromised cells) compared to the untreated hearts ($p = 0.0001$) (Figure 3:25 B).

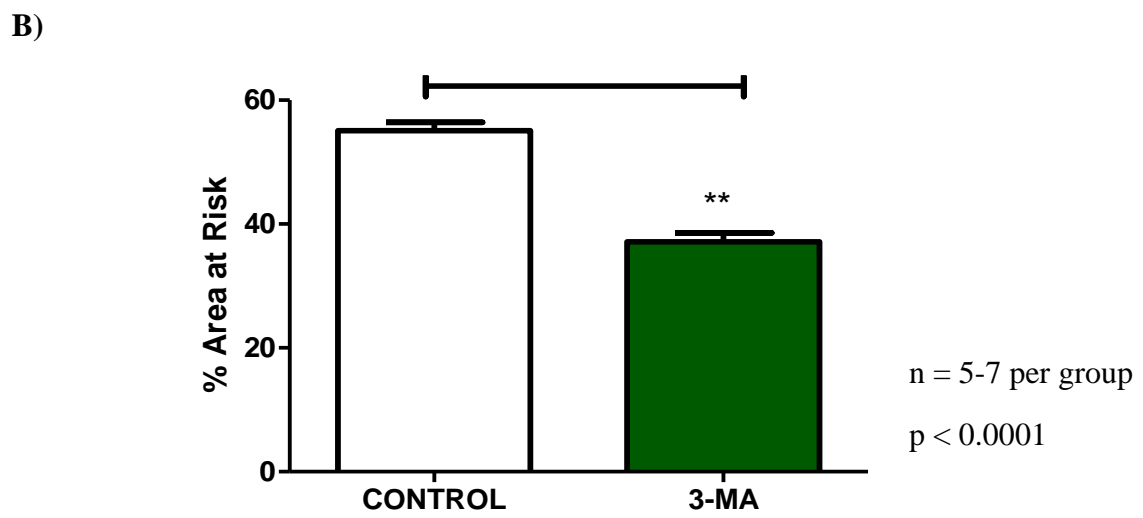
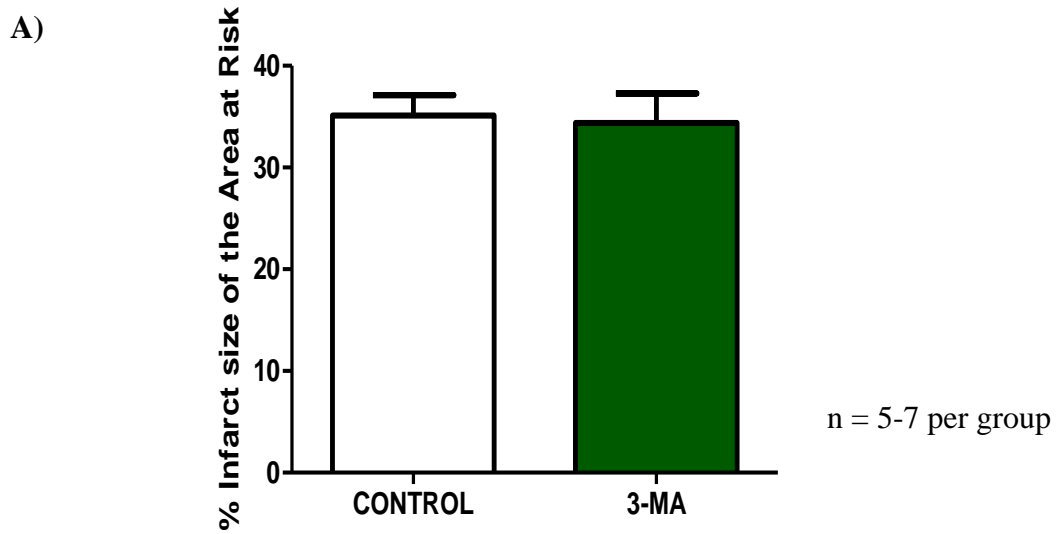


Figure 3:25 Percentage of (A) infarct size and (B) area at risk for hearts pre-treated with 3-MA before regional ischaemia

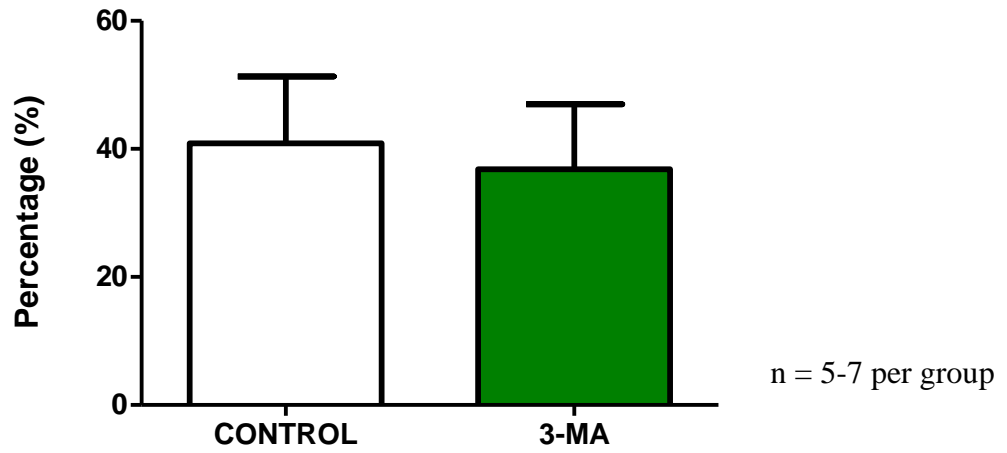
3.4.4.1. Mechanical data of hearts pre-treated with 3-MA

Table 3:4 Mechanical data of hearts (A) before being subjected to 35 min regional ischaemia and (B) after ischaemia: effect of pre-treatment with 3-MA (1 mM) in comparison to untreated controls

A)	TIME	PARAMETERS	CONTROL n=8	3-MA n=9
	BEFORE 35 MIN OF REGIONAL ISCHAEMIA	Coronary Output (mL/min)	12.2 ± 0.9	12.1 ± 0.7
		Aortic Output (mL/min)	41 ± 1.6	36.6 ± 4.1
		Cardiac Output (mL/min)	53.2 ± 2	53.4 ± 2.8
		Peak Systolic Pressure (mm Hg)	87.5 ± 0.9	88.4 ± 2.2
		Diastolic Pressure (mm Hg)	63.3 ± 1.1	63.3 ± 0.8
		Heart Rate (BPM)	309.8 ± 9.7	330.4 ± 16.9
		Total Work (mW)	10.4 ± 0.5	11.3 ± 1.1

B)	TIME	PARAMETERS	CONTROL n=8	3-MA n=9
	AFTER 35 MIN OF REGIONAL ISCHAEMIA	Coronary Output (mL/min)	9.2 ± 1.6	11.5 ± 2.2
		Aortic Output (mL/min)	8.8 ± 2.8	9.1 ± 3.1
		Cardiac Output (mL/min)	17.9 ± 3.6	20.6 ± 4.6
		Peak Systolic Pressure (mm Hg)	70 ± 10	67.3 ± 11.3
		Diastolic Pressure (mm Hg)	54.7 ± 11	53.3 ± 8.9
		Heart Rate (BPM)	254 ± 37.6	274.4 ± 48.8
		Total Work (mW)	3.2 ± 0.7	3.3 ± 0.9

A)

% CARDIAC OUTPUT RECOVERY

B)

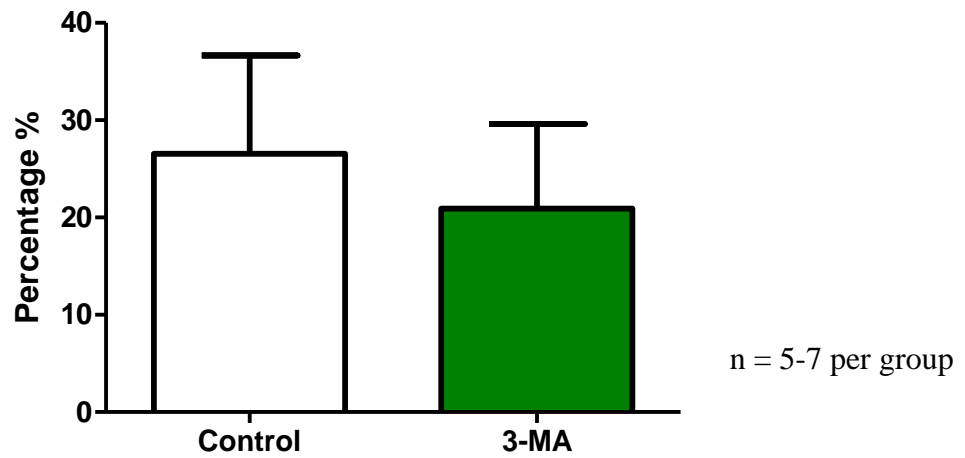
% Total work recovery

Figure 3:26 Percentage of (A) cardiac output recovery and (B) total work recovery of hearts pre-treated with 3-MA during regional ischaemia.

3.5. Effect of FCCP pre-treatment on mitochondrial function, heart mechanical function and infarct size.

The aim of this set of experiments was to evaluate the effect of stimulation of mitophagy on the outcome of ischaemia/reperfusion injury and to correlate these findings with mitochondrial oxidative phosphorylation function. FCCP, a well-established uncoupler of oxidative phosphorylation, was used for this purpose. Pilot experiments were performed to determine the exact dosage to be used in a study of this kind, using the effects of the drug on myocardial functional performance and mitochondrial mitophagy markers as indicators. The perfusion protocol that was used for this aim is illustrated in Figure 3:27

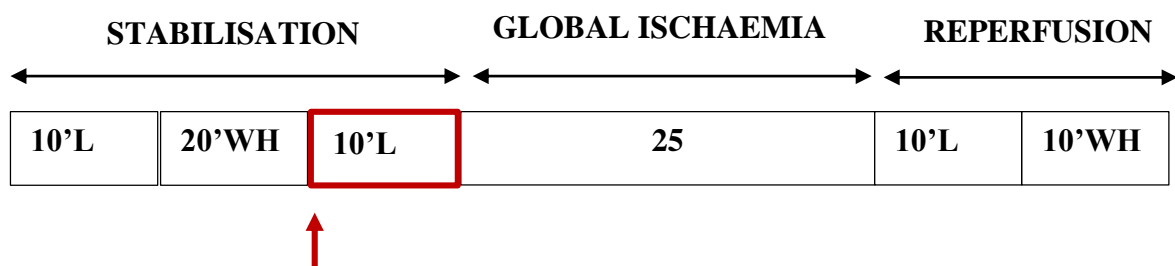


Figure 3:27 Perfusion protocol used for FCCP dose response and subsequent experiments. FCCP was administered 10 min before global ischaemia, represented by the red block and arrow

3.5.1. Dose response of FCCP concentrations 100nM-1µM

A dose response study was done to determine the effects of different FCCP concentrations ranging from 100 nM to 1000 nM (1 µM) on myocardial functional recovery during reperfusion and mitochondrial mitophagy parameters.

FCCP completely inhibited the functional recovery of the hearts during reperfusion (Table 3.5). There was a visible upregulation of PINK1 and Parkin levels (Figure 3:28 A and B respectively) in mitochondria of hearts pre-treated with the different FCCP concentrations in comparison to the untreated control. Mitochondria from hearts pre-treated with 1000 nM FCCP appeared to have the most increased expression of PINK1 and Parkin amongst the different FCCP concentrations. However, p62 seemed to be expressed more by 100 nM and 250 nM FCCP, in comparison to the untreated control and the other FCCP concentrations (Figure 3:29)

Hearts treated with 1000 nM and 500 nM FCCP had higher mitochondrial PINK1 and Parkin expression levels but resulted in mitochondrial damage of the hearts (mitochondrial data not shown).

Table 3:5 Mechanical data of hearts before (A) and after (B) exposure of hearts to 25 min global ischaemia: effects of different concentrations of FCCP (100 nM to 1000 nM). n = 2 per group

A)

TIME	PARAMETERS	1000 nM	500 nM	250 nM	100 nM
Before ischaemia	Coronary Output (mL/min)	13.5 ± 1.5	13.5	12 ± 1.5	12.75 ± 0.8
	Aortic Output (mL/min)	40 ± 8	47 ± 5	43 ± 7	46 ± 10
	Cardiac Output (mL/min)	53.5 ± 6.5	60.3 ± 5.3	55 ± 8.5	58.8 ± 10.8
	Peak Systolic Pressure (mm Hg)	84 ± 1	86.5 ± 0.5	86	82.5 ± 2.5
	Heart Rate (BPM)	269 ± 17	275 ± 44	268	251 ± 40
	Total Work(TW)	10.2 ± 1.2	11.5 ± 1	12.2	10.9 ± 2.3

B)

TIME	PARAMETERS	1000 nM	500 nM	250 nM	100 nM
During reperfusion	Coronary Output (mL/min)	0.3 ± 0.3	0.75 ± 0.75	0	0.25 ± 0.25
	Aortic Output (mL/min)	0	0	0	0
	Cardiac Output (mL/min)	0	0	0	0
	Peak Systolic Pressure (mm Hg)	0	0	0	0
	Heart Rate (BPM)	0	0	0	0
	Total Work (TW)	0	0	0	0

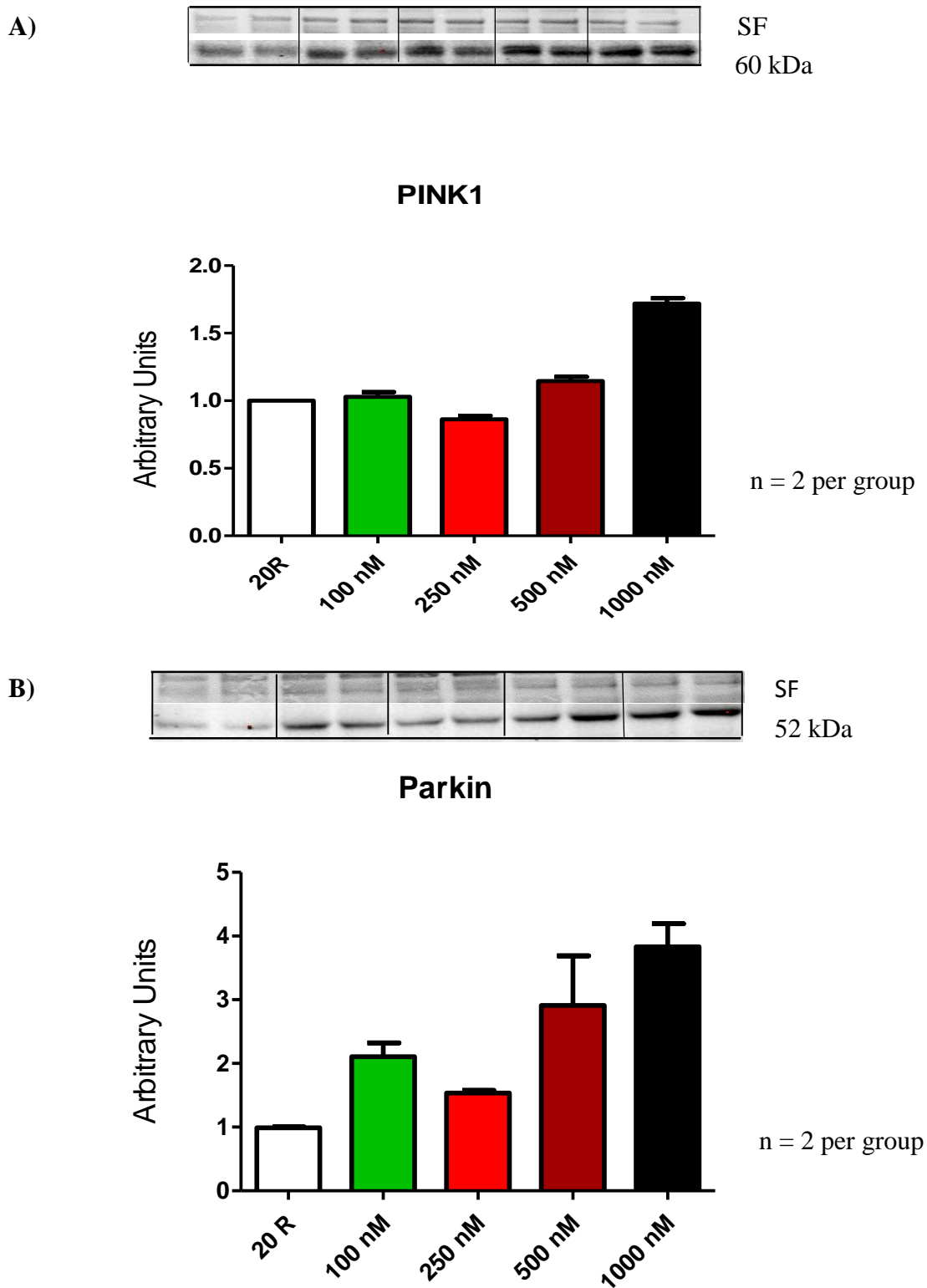


Figure 3:28 Mitochondrial (A) PINK1 and (B) Parkin levels of hearts pre-treated with FCCP concentrations ranging from 100 nM to 1000 nM (1 μ M) in contrast to un-treated hearts (20min R). SF= Stain Free

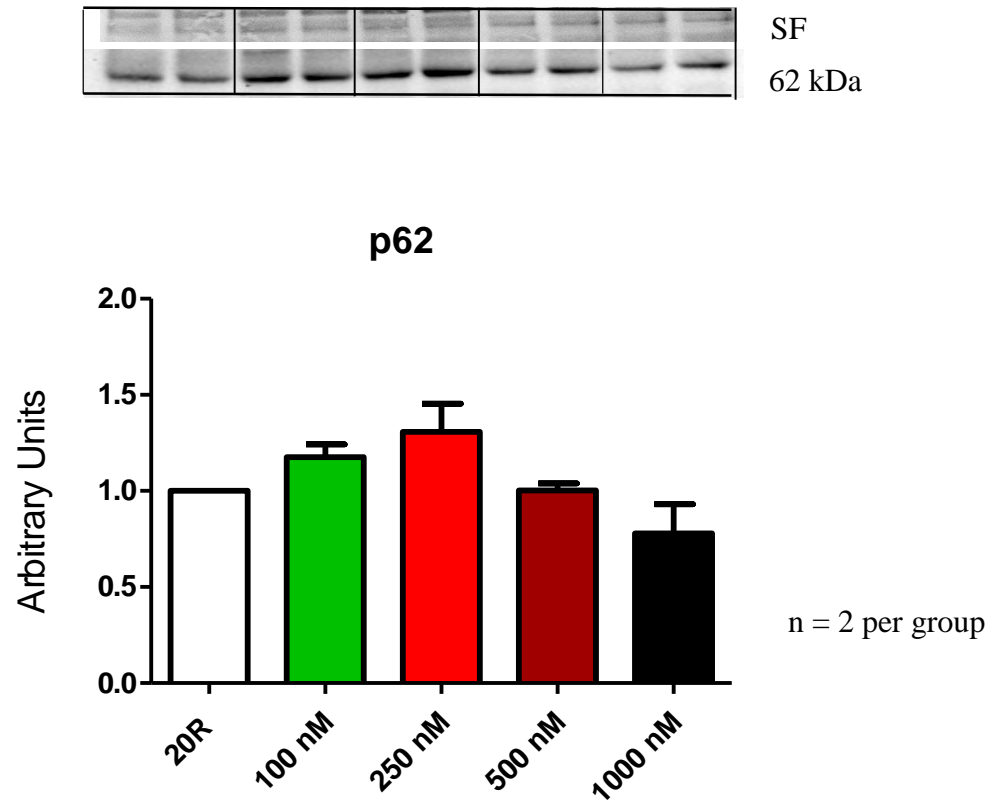


Figure 3:29 Mitochondrial p62 levels of hearts pre-treated with FCCP concentrations ranging from 100nM to 1000nM (1 μ M) in contrast to un-treated hearts. SF = Stain Free

3.5.2. Effects of FCCP pre-treatment after 20 min reperfusion at 100 nM and 250 nM concentrations

Despite the very significant stimulation of mitophagy markers by higher concentrations of FCCP, it became clear that FCCP at high concentrations had severe detrimental effects on the mechanical performance of the heart as well as mitochondrial function. Not only were the hearts unable to function, concentrations higher than 250 nM lead to mitochondrial damage, as indicated by the polarographic studies (data not shown). Since FCCP at 100 and 250 nM did not lead to mitochondrial damage, it was decided to further evaluate the effects of these two concentrations on the mitophagy markers. Hearts were perfused (for perfusion protocol see Figure 3:27) with either 100 or 250 nM FCCP administration before 25 min of global ischaemia. This was followed by mitochondrial analysis and Western blotting for mitophagy markers. The mitophagy markers that were analysed were TOM70, Parkin, p62 and PINK1.

There was a significant up regulation of TOM70 levels in hearts that had been pre-treated with 100 nM of FCCP compared to those pre-treated with 250 nM. This was associated with the opposite effect for Parkin as there was a significant decrease in Parkin levels of hearts pre-treated with 100 nM of FCCP compared to those that were treated with 250 nM. There were no significant changes in the mitochondrial p62 and PINK1 expression levels of hearts treated with either concentration of FCCP (Figure 3:30 and 3:31).

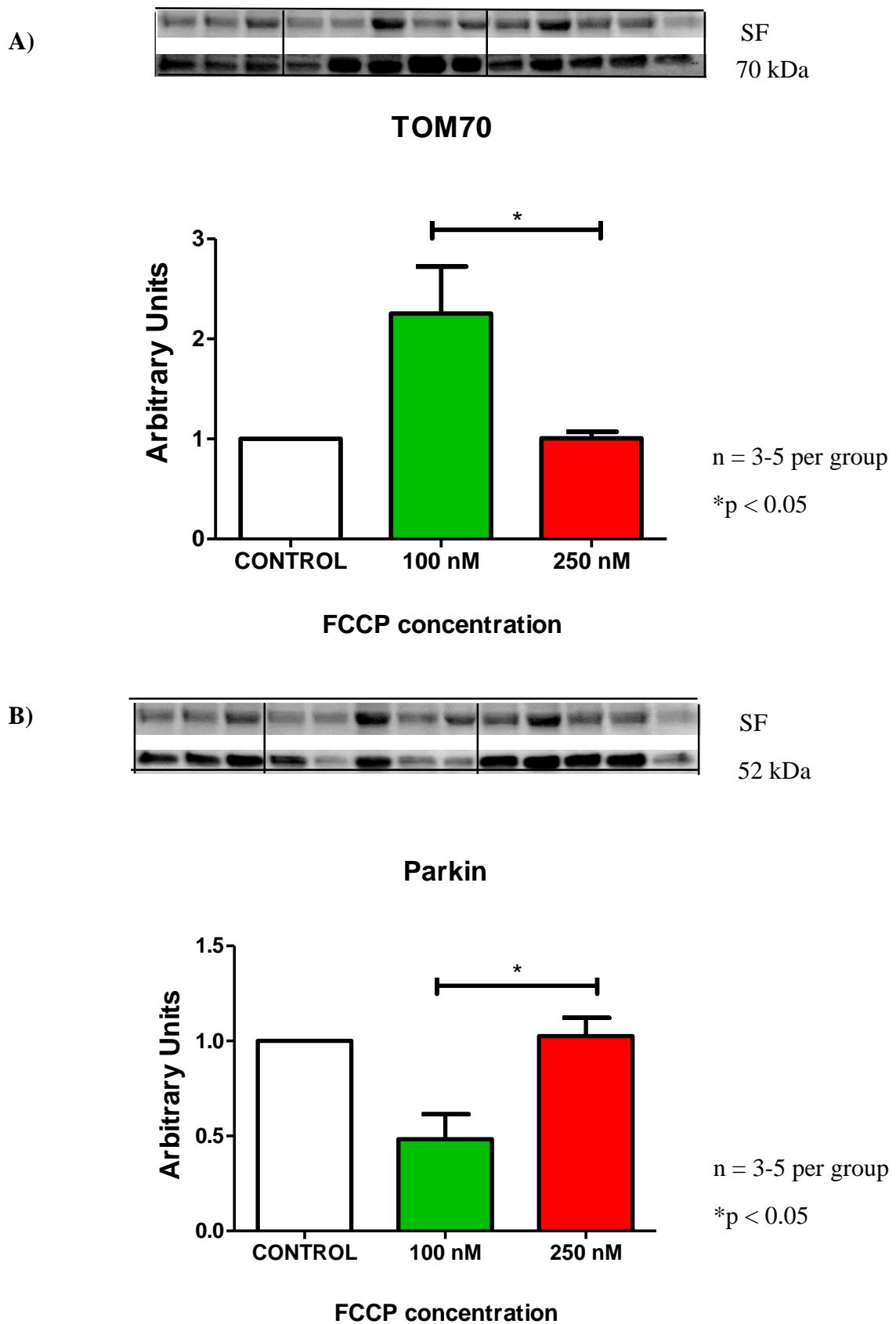


Figure 3:30 Mitochondrial (A) TOM70 and (B) Parkin levels of hearts pre-treated with 100 nM and 250 nM FCCP concentrations in contrast to un-treated hearts. SF= Stain Free

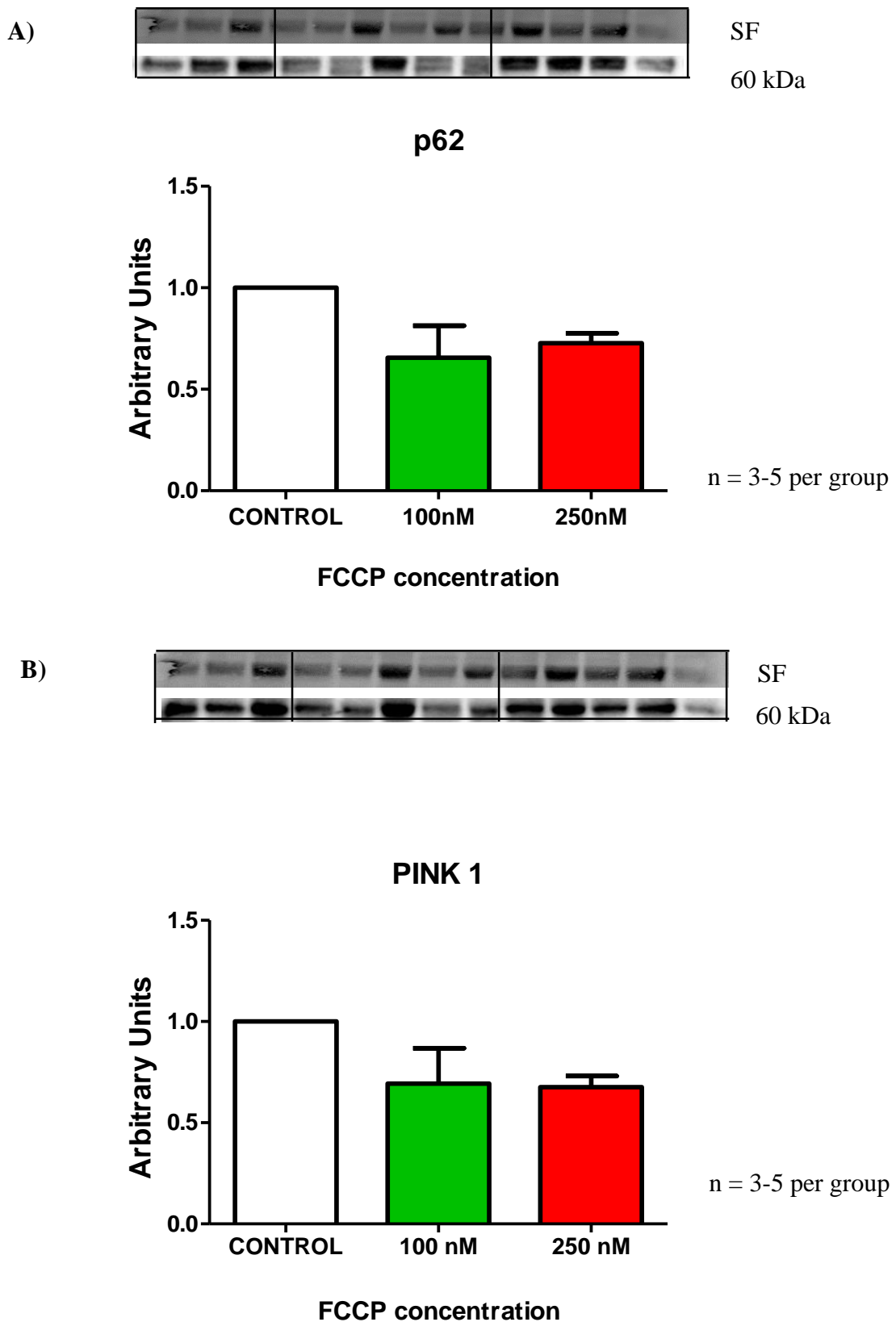


Figure 3:31 Mitochondrial (A) p62 and (B) PINK1 levels of hearts pre-treated with 100 nM and 250 nM FCCP in contrast to the untreated hearts. SF = Stain Free

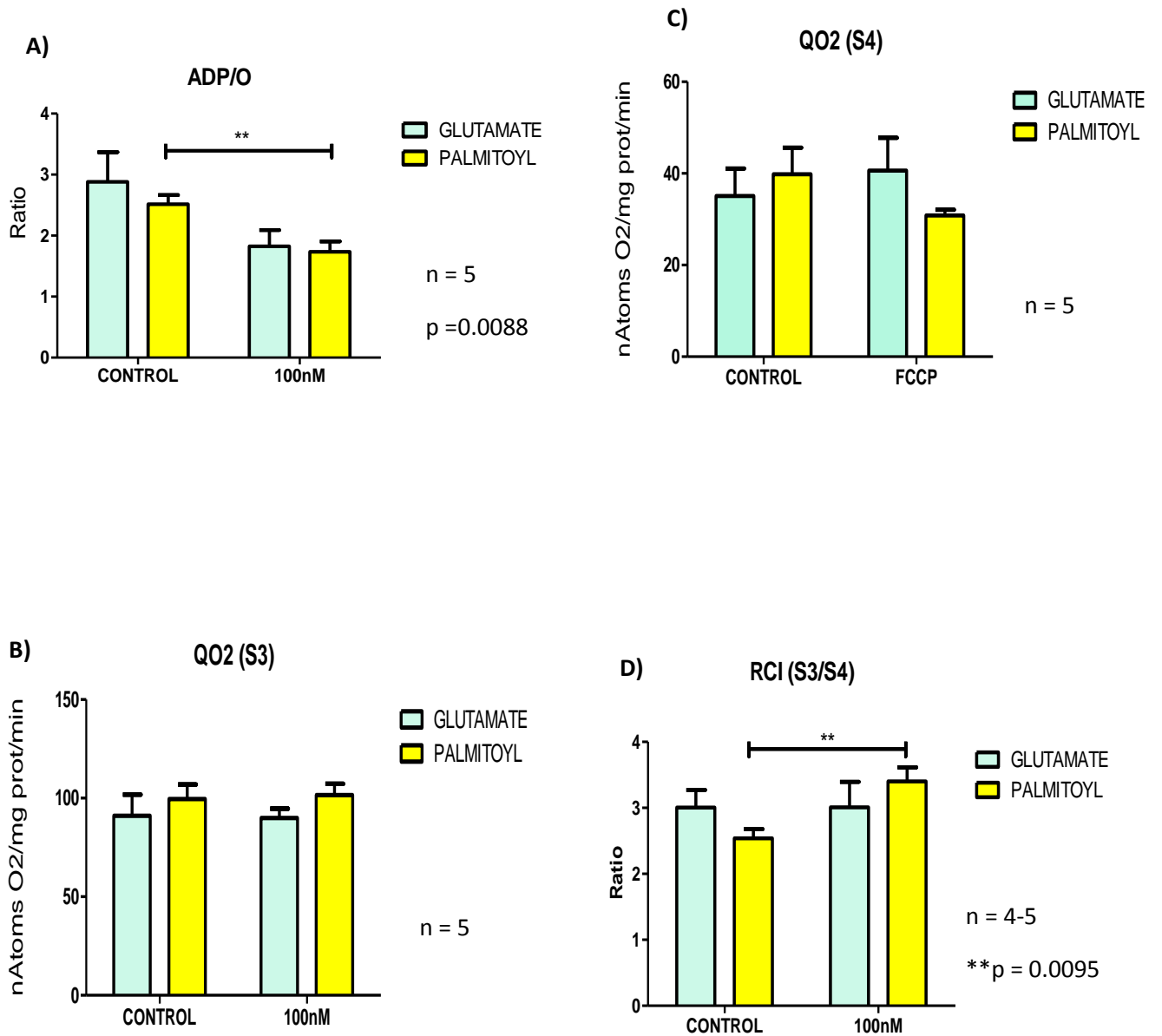
3.5.3. FCCP (100 nM) and Mitochondrial Function

Upon further experimentation, it was observed that pre-treatment with 250 nM FCCP severely affected mitochondrial oxidative phosphorylation function and generated poor polarographic registrations in comparison to the mitochondria from the hearts pre-treated with 100 nM. 100 nM FCCP was then used for the subsequent experiments. Figures 3:32 (A)-(G) illustrate the mitochondrial bioenergetics function of mitochondria isolated from hearts pre-treated with 100 nM FCCP before exposure to global ischaemia/reperfusion.

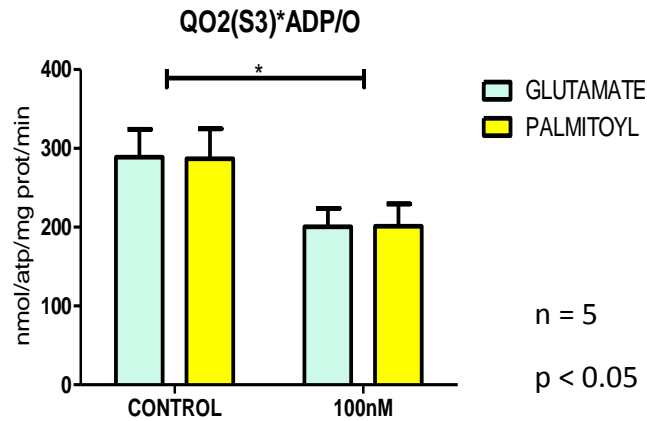
Mitochondria isolated from hearts pre-treated with 100 nM FCCP exhibited the most significant changes in the presence of palmitoyl-L-carnitine plus malate as substrate. For example, a significant reduction in their ADP/O ratio was observed ($p = 0.0088$) (Figure 3:32 A), while showing no changes in QO_2 (States 3 and 4) (Figure 3:32 B and C). However, the RCI (Figure 3.32 D) was significantly increased in the mitochondria of hearts pre-treated with FCCP with palmitoyl-L-carnitine plus malate as a substrate compared to the mitochondria of the untreated hearts $p = 0.0095$. The mitochondrial oxidative phosphorylation rate (State 3) (Figure 3:32 E) of hearts pre-treated with FCCP was significantly reduced with both mitochondrial substrates $p < 0.05$, while these mitochondria had a significantly lower oxidative phosphorylation rates (State 4) (Figure 3:32 F) with palmitoyl-L-carnitine plus malate as substrate only ($p = 0.0196$).

With palmitoyl-L-carnitine plus malate as substrate there was a significant increase in the state 3 respiration during re-oxygenation (Figure 3:32 G) of mitochondria isolated from hearts pre-treated with FCCP in comparison to mitochondria of the untreated hearts ($p = 0.0069$).

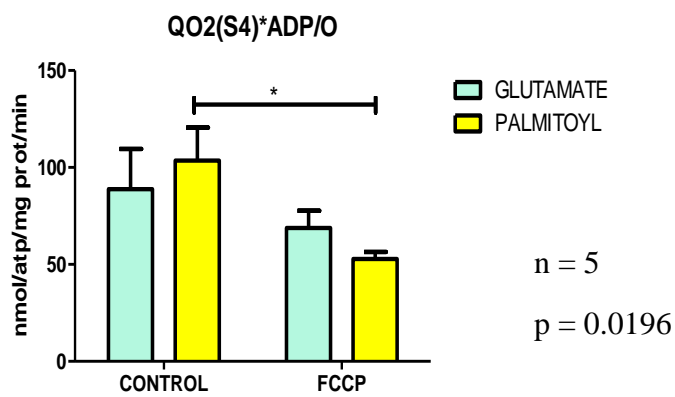
The mitochondrial citrate synthase activity of hearts pre-treated with different concentrations of FCCP did not differ from each other (Figure 3:33).



E)



F)



G)

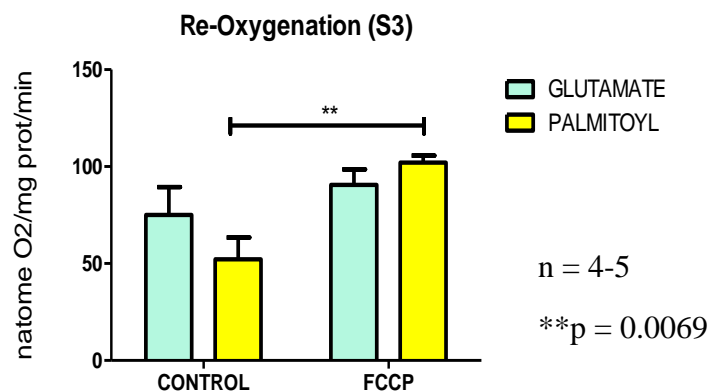


Figure 3:32 (A) ADP/O (B) QO2 state 3 (S3) respiration (C) QO2 state 4 (S4) respiration (D)RCI (E) oxidative phosphorylation rate state3 (S3) (F) oxidative phosphorylation rate state 4 (S4) and (G) re-oxygenation rate in palmitoyl-L-carnitine plus malate and glutamate plus malate substrates of hearts pre-treated with FCCP (100 nM) during global ischaemia/reperfusion. n= 4-5 per group

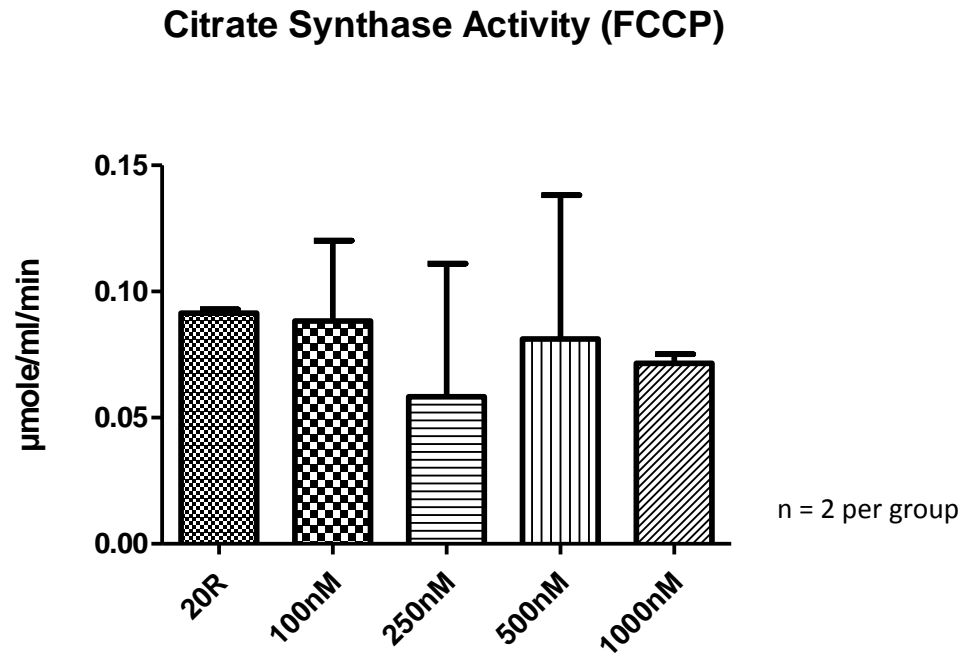


Figure 3:33 Citrate Synthase activity of hearts pre-treated with FCCP at different concentrations

3.5.4. Infarct size and area at risk of hearts pre-treated with FCCP with DMSO as a vehicle

In this set of experiments, we aimed to determine the effect of stimulation of mitophagy by FCCP (100 nM and 250 nM) pre-treatment on infarct size and area at risk of hearts during reperfusion. FCCP was administered for 10 min before the onset of 35 min regional ischaemia, followed by reperfusion for 60 min before measurement of infarct size (See protocol, Figure 3:34).

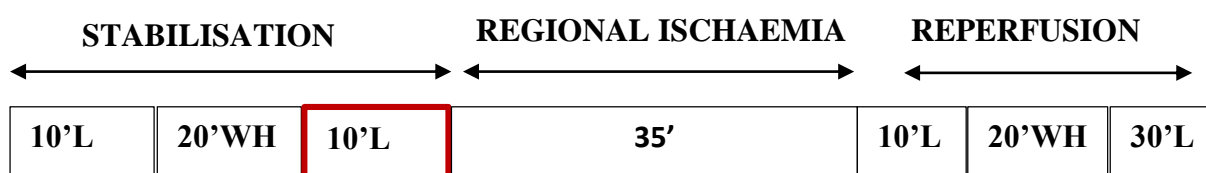
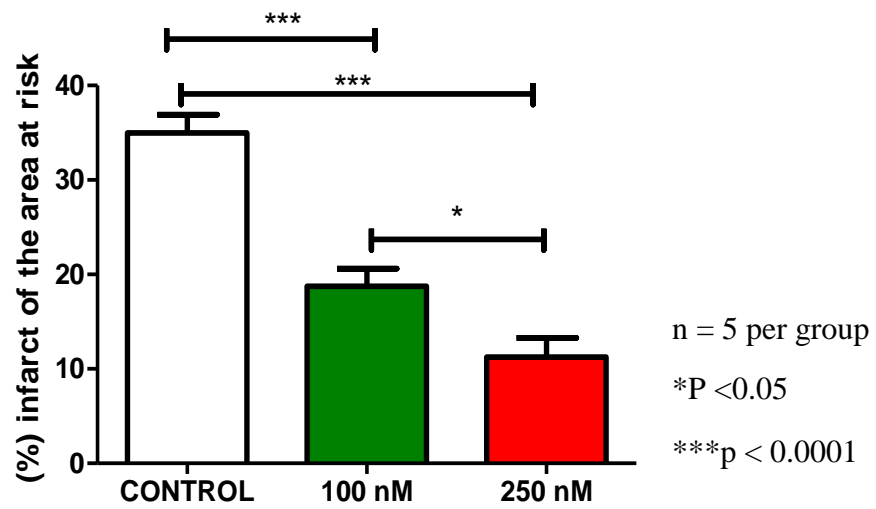


Figure 3:34 Regional ischaemia protocol for infarct size determination. FCCP was administered 10 min before 35 min of regional ischaemia, indicated by the red block and arrow

There was a significant decrease in the percentage of infarct size (Figure 3:35 A) of hearts that were pre-treated with 100 nM and 250 nM of FCCP compared to the untreated control $p=0.0001$. There was also a significant difference between the two concentrations of FCCP, with 250 nM being more effective than 100 nM in reducing the infarct size. However, there was a significant increase in the percentage of area at risk for hearts pre-treated with 100 nM of FCCP compared to the control untreated hearts ($p < 0.05$) while no differences were observed between the two concentrations (Figure 3:35 B)

A)



B)

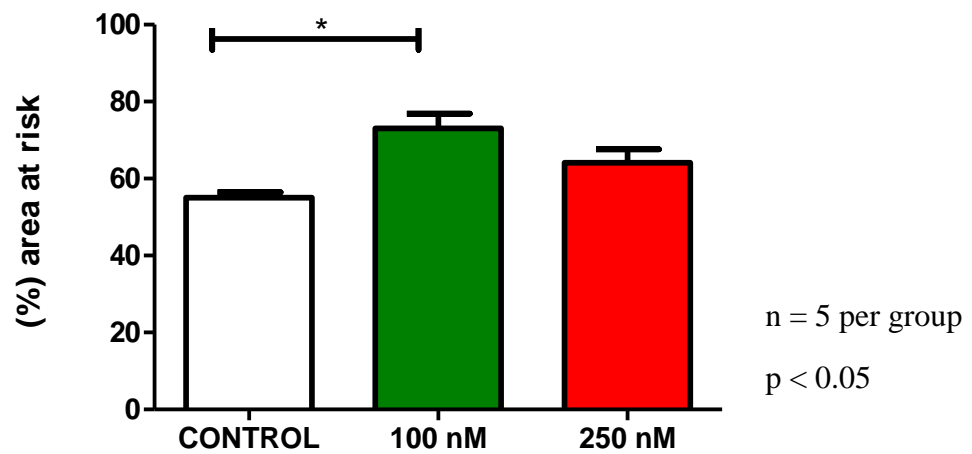


Figure 3:35 (A) Infarct size and (B) (% of area at risk) of hearts pre-treated with FCCP (100 nM and 250 nM), subjected to 35 min regional ischaemia and 60 min reperfusion

3.5.5. Mechanical performance and functional recovery of hearts subjected to 35min regional ischaemia: effect of FCCP

There was a significant reduction in mechanical function for hearts pre-treated with 250 nM FCCP (data not shown) during reperfusion. This was indicated by a complete inability to produce cardiac output and total work during reperfusion when compared to the untreated controls ($p=0.0033$ and $p<0.05$ respectively) (Figure 3:36). However, in contrast to hearts pre-treated with 250 nM FCCP there were no significant differences in cardiac output and total work recovery for hearts pre-treated with 100 nM FCCP in comparison to the controls (Figure 3:37, for mechanical data see Table 3.6). Thus, hearts pre-treated with 100 nM FCCP had improved recovery in both cardiac output and total work in comparison to those pre-treated with 250 nM FCCP ($p < 0.05$).

Table 3:6 Mechanical data of hearts before (A) and after (B) exposure to 35 min regional ischaemia: effects of FCCP (100 nM). n = 8-9

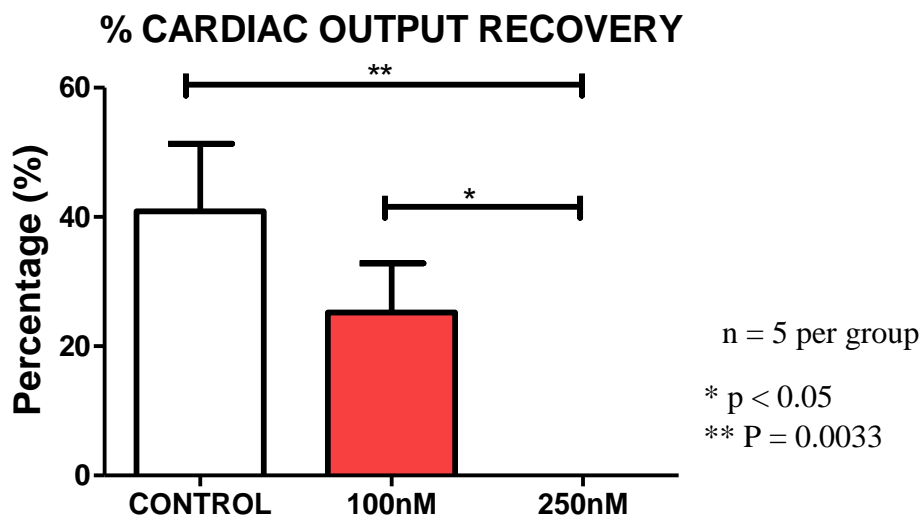
A)

TIME	PARAMETERS	CONTROL	FCCP (100 nM)
BEFORE 35 MIN OF REGIONAL ISCHAEMIA	Coronary Output (mL/min)	12.2 ± 0.9	11.3 ± 0.7
	Aortic Output (mL/min)	41 ± 1.6	39.3 ± 1.9
	Cardiac Output (mL/min)	53.2 ± 2	50.7 ± 2.4
	Peak Systolic Pressure (mm Hg)	87.5 ± 0.9	85.33 ± 0.9
	Heart Rate (BPM)	309.8 ± 9.7	293.6 ± 13.6
	Total Work (mW)	10.4 ± 0.5	9.5 ± 0.6

B)

TIME	PARAMETERS	CONTROL	FCCP (100 nM)
AFTER 35 MIN OF REGIONAL ISCHAEMIA	Coronary Output (mL/min)	9.2 ± 1.6	8 ± 1.3
	Aortic Output (mL/min)	8.8 ± 2.8	3.3 ± 1.4
	Cardiac Output (mL/min)	17.9 ± 3.6	11.3 ± 2.4
	Peak Systolic Pressure (mm Hg)	70 ± 10	69.1 ± 10
	Heart Rate (BPM)	254 ± 37.6	249.4 ± 36.8
	Total Work (mW)	3.2 ± 0.7	1.9 ± 0.4

A)



B)

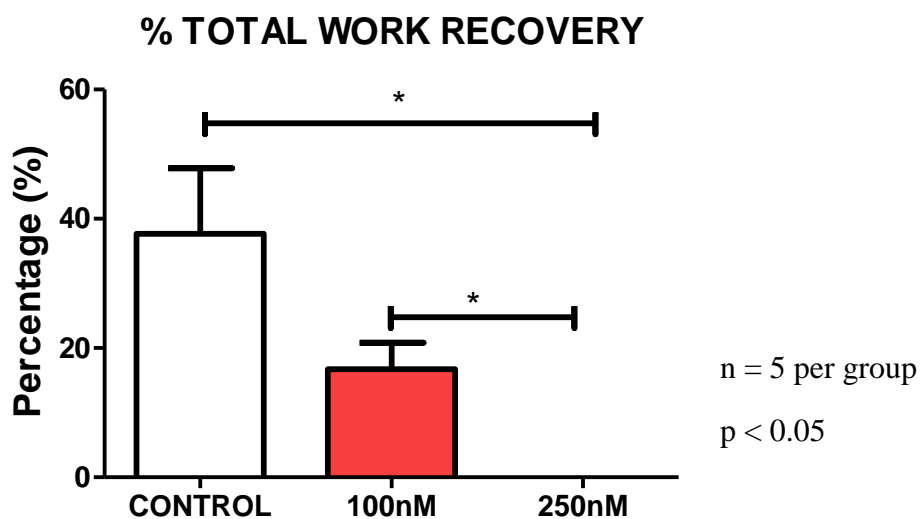


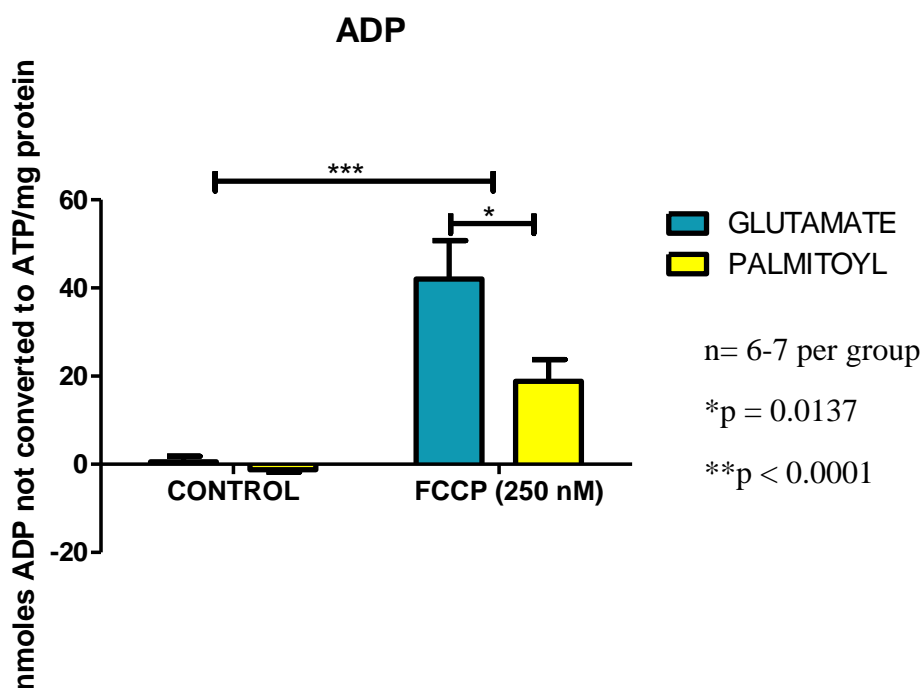
Figure 3:36 Percentage recovery of (A) cardiac output and (B) total work for hearts pre-treated with 100 nM and 250 nM

3.5.6. High energy phosphate levels of hearts pre-treated with 250 nM FCCP

Hearts pre-treated with 250 nM FCCP lead to complete mechanical failure and generated some very poor mitochondrial registrations, with no visible state 3 to state 4 conversion. To further evaluate the phosphorylating potential of FCCP-treated mitochondria, it was decided to analyse the ADP and ATP contents of the mitochondrial incubation media after addition of the conventional amount of ADP. For this purpose, use was made of HPLC analysis.

As expected, the incubation media of the control mitochondria contained no measureable ADP. In contrast the ADP levels were significantly higher in hearts treated with 250 nM FCCP in comparison to the controls in both substrate media, $p < 0.0001$. ADP levels were significantly higher in the glutamate plus malate medium in contrast to the palmitoyl-L-carnitine plus malate media, in the hearts pre-treated with 250 nM FCCP, $p = 0.0137$. These results indicated a significant degree of uncoupling of oxidative phosphorylation induced by FCCP. Interestingly, there were however no significant changes in the amount of ATP produced in both substrate media and in comparison to the controls. These observations suggest that despite the absence of conversion of State 3 to State 4 respiration, the mitochondria were capable of converting substantial amounts of ADP to ATP in the presence of FCCP.

A)



B)

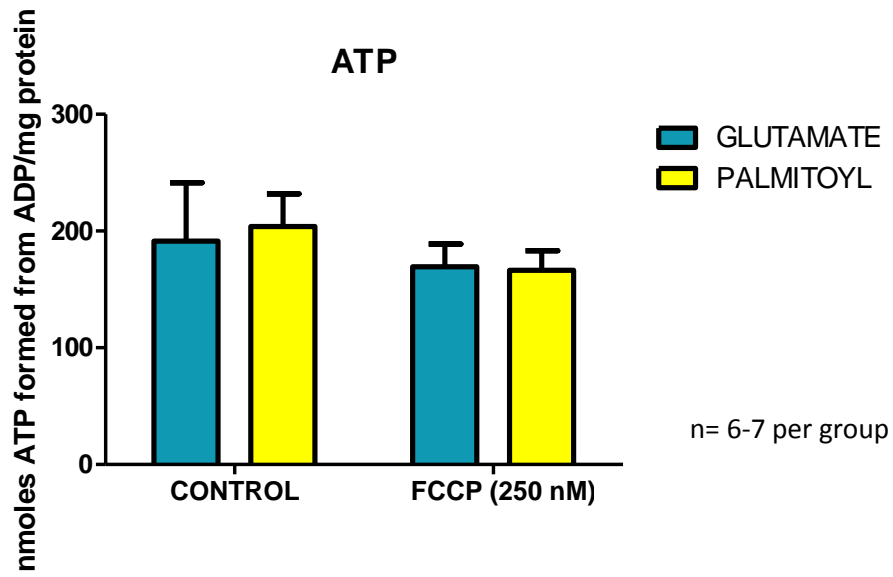


Figure 3:37 (A) ADP and (B) ATP levels of mitochondria from hearts pre-treated with 250 nM FCCP

3.6. Comparison of the effects of 3-MA and FCCP on infarct size, area at risk and mechanical functional recovery.

When comparing the effects of 3-MA and FCCP on the heart, FCCP resulted in a significant decrease in the percentage of infarcted tissue but a significant increase in the percentage of the area at risk, in comparison to the controls ** $p < 0.0002$ and *** $p < 0.0001$ respectively. Hearts pre-treated with 3-MA did not differ in the percentage of infarcted tissue in comparison to the controls but yielded a significant reduction in the area at risk *** $p < 0.0001$. Functional recovery did not differ between both FCCP and 3-MA in comparison to the controls.

3-MA in contrast to FCCP also resulted in a higher percentage of infarcted tissue ## $p < 0.0002$, but a lower percentage in the area at risk ### $p < 0.0001$. Functional recovery did not differ between the two drugs. The summary of the effects of FCCP and 3-MA are shown in Table 3.7

Table 3:7: Comparison of effects of 3-MA vs FCCP. n=6-7 per group. ** $p < 0.0002$ ## $p < 0.0002$ and *** $p < 0.0001$ ### $p < 0.0001$ between the groups.

PARAMETER (%)	CONTROL	FCCP	3-MA
Infarct size of the area at Risk	35.11 ± 2	16.63 ± 2.6 **	34.4 ± 3 ##
Area at Risk	55.07 ± 1.35	73.06 ± 3.8 ***	37.12 ± 1.44 *** ###
Cardiac output recovery	40.88 ± 10.45	25.22 ± 7.63	36.80 ± 10.20
Total work recovery	37.67 ± 10.14	23.88 ± 7.86	26.16 ± 8.93

Chapter 4

Discussion

In this study we aimed to evaluate the significance of mitophagy in the setting of myocardial ischaemia/reperfusion (I/R) damage, its correlation with mitochondrial function and ultimately its effects on heart function. In order to achieve this, mitophagy was inhibited or activated with the aid of 3-methyladenine (3-MA) and carbonilcyanide p-triflouromethoxyphenylhydrazone (FCCP) respectively in hearts using the isolated rat heart perfusion model. 3-MA or FCCP was administered to ex vivo perfused hearts before or after induction of ischaemia followed by reperfusion.

4.1 Standardisation of Mitophagy Markers

We initially carried out preliminary studies to standardise the Western blotting technique for the mitophagy markers to be used throughout the study i.e. PINK1, Parkin and p62, all of which are crucial proteins involved in the process of mitophagy. Mitochondria isolated from hearts perfused for either 40 min (C40) – baseline perfusion protocol or subjected to 20 min of global ischaemia were used for this aim. From the results generated by Dr Karthik Dhanabalan in our laboratory, there was an increase, although not significant, in the levels of PINK1, while p62 levels were significantly higher in mitochondria isolated from hearts subjected to 20 min of ischaemia when compared to the protein levels in mitochondria from baseline perfused hearts (C40). This is consistent with knowledge that the process of mitophagy is initiated by stressful conditions such I/R (Marín-García & Akhmedov 2016). Increased stress leads to dysfunctional mitochondria and the subsequent accumulation of PINK1 proteins on the outer mitochondrial membrane (Narendra et al. 2010). This accumulation of PINK1 proteins also occurs during the initiation of mitophagy. p62 is involved in the binding of the mitochondria, to be degraded, to the autophagosome (Jimenez et al. 2014) and is therefore a key marker of mitophagy. These results would have been perhaps more pronounced if a larger sample size was used. However, there was a successful standardisation of the Western blotting technique for the antibodies of the mitophagy markers to be used in the study (for dilutions see Chapter 2, Table 2.5).

In these initial experiments we also aimed to determine whether the autophagy inhibitor 3-MA was effective at a concentration of 1 mM. For this we administered the drug to the hearts during the baseline perfusions (Results, Figure 3:2 B) with DMF as a solvent, hearts were then freeze-clamped and the tissue used for subsequent Western blotting. The inhibitory mechanism of 3-

MA involves inhibiting the phosphatidylinositol 3-phosphate (PI3P) complex formation, required for the recruitment of the autophagosome (Wu et al. 2010). The autophagy markers that were analysed were Beclin-1, BNIP3L/Nix and LC3 A/B. Our results showed that inhibition of autophagy by 3-MA down regulated Beclin-1 levels in comparison to the un-perfused hearts, but not to the untreated baseline perfused hearts. Beclin-1 is a protein involved in the class III PI3K complex formation which is a positive regulator of autophagy (Hamacher-Brady 2012). The same effect was observed in hearts treated with the solvent DMF and possibly responsible for some of the effects observed with 3-MA.

Inhibition of autophagy by 3-MA was associated with a significant decrease in the LC3 A/B-II levels in comparison to the hearts treated with DMF. This also led to a decrease in the LC3 A/B/-II/I ratio of hearts treated with 3-MA in comparison to hearts treated with DMF alone, suggesting that 3-MA inhibited autophagy despite the presence of DMF (Results, Figure 3:3,4). LC3-II is a model protein to be used as an indicator of autophagy as it is permanently associated with the inner membrane of the autophagosome (Ravikumar et al. 2010; Loos et al. 2014). The increased levels of LC3-II induced by DMF (Figure 3:3) could also possibly indicate an impaired downstream process of the degradation of the autophagosome (Maejima et al. 2015) and hence the accumulation of LC3-II proteins. However, these results could be confirmed through the quantification of the autophagic flux using fluorescence (Loos et al. 2014).

BNIP3L/Nix levels were significantly increased when hearts were perfused with 3-MA in comparison to hearts perfused with DMF. BNIP3L/Nix is a member of the pro-apoptotic Bcl-2 family proteins (Kubli & Gustafsson 2012). It is also proposed to be involved in the mitophagy receptor pathway (Novak et al. 2010). However, these increased levels may also possibly be an indication of BNIP3L/Nix's cross talk between mitochondria autophagy and apoptosis, possibly in response to DMF. Further studies on other apoptotic proteins would be ideal to monitor in these experiments, in order to determine the role of the increased BNIP3L/Nix levels observed.

From the decreased Beclin-1 levels and decreased LC3 A/B-II and ratio levels, we can assume that 3-MA (1 mM) successfully inhibited autophagy but was also associated with increased pro-apoptotic proteins, when added to hearts perfused under control conditions.

Measuring oxidative phosphorylation potential of mitochondria showed that 3-MA had very little effect. Perfusion of hearts reduced the RCI levels in comparison to those of un-perfused hearts when using glutamate plus malate as substrate (Results, Figure 3:6D) while inhibition

of mitophagy using 3-MA did not prevent this decrease. The RCI indicates the capacity for substrate oxidation and ATP formation with low proton leak therefore tight coupling, and is determined by dividing the state 3 respiration (oxidation of substrate in the presence of ADP) by the state 4 respiration (resting respiration) (Brand & Nicholls 2011). In these experiments minor changes in state 3 and state 4 respiration contributed to the reduction seen in RCI. The decrease in the respiratory index was associated with a strong indication of a reduction in mechanical heart function, although not significant (Results, Table 3.1). We also observed a strong decrease in the mitochondrial viability after anoxia from baseline perfused hearts in comparison to the un-perfused hearts, but due to a large variation in our data this outcome was not significant.

The data obtained in these preliminary experiments indicate that the effects observed when perfusing with 3-MA are largely due to the solvent used. We therefore followed up these experiments with a more detailed study where the effects of 3-MA and DMF were evaluated in hearts subjected to ischaemia and reperfusion.

4.1.1. Effects of 3-MA and DMF on hearts subjected to I/R

The follow-up study showed that hearts subjected to 25 min global ischaemia showed a very significant reduction in mechanical function during reperfusion. Pre-treatment as well as post-treatment (at the onset of reperfusion) with 3-MA also completely abolished recovery (Results, Table 3:2).

Tissue isolated from untreated hearts subjected to ischaemia yielded a significant increase in LC3 A/B II/I ratios (Results, Figure 3:12), with 3-MA and DMF causing a reduction. These outcomes are in agreement with literature which states that when energy levels are depleted e.g. during ischaemia, autophagy is activated (Ma et al. 2015). Adenosine monophosphate-activated protein kinase (AMPK), an energy sensor that directly activates autophagy during ischaemia through Unc-51-like kinases 1 (ULK1) (Matsui et al. 2007b; Takagi et al. 2007), would have been another ideal protein to monitor during these experiments to further evaluate autophagy during ischaemia. Interestingly, reperfusion per se, with or without 3-MA, regardless of the timing of administration, was without effect.

BNIP3L/Nix levels were unaffected by ischaemia, but increased by reperfusion, with 3-MA having no significant effect. However, Beclin-1 levels were unchanged by I/R and unaffected by 3-MA (see Figures 3:8, 9). Beclin-1 is known to be the main mediator of autophagy during reperfusion (Ma et al. 2015). However, in the model used in the present study (25 min global

ischaemia/30 min reperfusion) it appears that autophagy was not significantly activated by neither interventions nor 3-MA.

The finding that exposure of the heart to 25 min global ischaemia did not elicit autophagy according to the markers used, is in contrast to previous studies by Hamacher-Brady et al who reported that autophagic flux was suppressed in a cardiac cell line (Hamacher-Brady et al. 2006). However, upregulation of autophagy during reperfusion was also reported by others (Matsui et al. 2007a; Hariharan et al. 2011). Ma and co-workers (2012) reported that increased levels of Beclin-1 leads to impaired rather than increased autophagic flux (Ma et al. 2012). It is unclear why there is such a discrepancy in the outcomes of autophagy using an I/R model.

Autophagy is known to confer harmful effects on the heart during reperfusion with excessive activation leading to cardiomyocyte death (Ma et al 2015), while enhanced autophagy was reported to protect the heart against I/R damage (Matsui et al 2007; Hamacher-Brady et al 2006). However, the marked mechanical failure during reperfusion in our model of I/R is unlikely to be due to activation of autophagy. It is well-established that mitochondria are fragile during the early stages of reperfusion (Jennings 2013). Moreover, levels of reactive oxygen species (ROS) are increased during reperfusion and this inactivates several Krebs cycle and electron transport enzymes. ATP production of mitochondria is also compromised (Nickel et al. 2013) and this subsequently affects the energy levels of the heart for contraction. These factors together would contribute to the extremely poor functional recovery seen with or without 3-MA.

4.1.2. Effects of 3-MA dissolved in water on autophagy in hearts subjected to I/R

Due to the failure of hearts to perform well mechanically whenever DMF had been administered and the fact that the effects of 3-MA appears to be largely due to the solvent, we decided to use water as a vehicle for 3-MA in subsequent experiments to further evaluate the effects of 3-MA. When added during reperfusion, it resulted in a slight but better recovery of hearts in comparison to hearts pre-treated with DMF (Results, Table 3.3b) and these hearts recovered to the same extent as the untreated hearts during reperfusion.

There were significantly higher BNIP3L/Nix expression levels in untreated reperfused hearts compared to ischaemia, while 3-MA was without effect (Results, Figure 3:15). Higher BNIP3L/Nix levels are possibly indicative of increased apoptosis during reperfusion or alternatively that the autophagy of mitochondria was enhanced during reperfusion. In contrast,

the LC3 A/B-II/I ratio was reduced when untreated hearts were exposed to ischaemia in comparison to those from the baseline perfusions. This ratio was then further decreased when untreated hearts were exposed to reperfusion (Results, Figure 3:18). Beclin-1 levels remained unchanged by all interventions. Based on the upregulation observed in BNIP3L/Nix expression, it is possible that activation of autophagy occurs during reperfusion in our model. However, 3-MA was without effect on autophagy in the I/R heart, regardless of the time of administration.

4.2 Effects of 3-MA on mitochondrial mitophagy

The effect of 3-MA treatment on mitophagy was evaluated in mitochondria isolated from hearts exposed to I/R with and without 3-MA treatment. In the untreated perfusion protocols there were no significant changes in the PINK1 levels associated with mitochondria from ischaemic hearts in comparison to mitochondria isolated after reperfusion. However, PINK1 levels were significantly lower in the untreated reperfusion conditions when compared to mitochondria isolated from baseline conditions (C40) (Results, Figure 3:20) but no significant changes were observed between the untreated ischaemic and baseline protocols. Mitochondria from untreated ischaemic hearts had significantly higher PINK1 levels in comparison to when 3-MA was administered before ischaemia. The outcomes of the mitochondrial PINK1 levels in the untreated ischaemic conditions were consistent with literature which states that mitophagy is initiated by stressful conditions such as ischaemia, as these stressful environments lead to the uncoupling and therefore dysfunction and damage of the mitochondria (Marín-García & Akhmedov 2016) which will trigger the initiation of the removal of such mitochondria. It should be kept in mind that the experimental protocol followed in this study measures total mitochondrial PINK1 levels and not redistribution of the protein within the mitochondria.

As mentioned earlier, mitochondria are fragile during the early stages of reperfusion. Dysfunctional mitochondria produce high levels of ROS over and above the other sources of ROS during reperfusion, such as neutrophils and other cells. These high levels of ROS contribute to the oxidative stress within the cell and triggers the opening of the mitochondrial permeability transition pore (mPTP). Opening of this pore commits the cardiomyocytes to cell death and mitophagy is decreased (Hausenloy & Yellon 2013; Marín-García & Akhmedov 2016). Borderline lower PINK1 levels ($p=0.09$, $n=4$) measured in this study indicate the possibility of a lower mitophagy level after 20 min reperfusion than directly after ischaemia (Results, Figure 3:20). A similar reduction in mitophagy is suggested by the decrease in the expression of Parkin levels also from the reperfusion conditions when compared to

mitochondria of hearts exposed to ischaemia. Parkin accumulation on the mitochondrial outer membrane is also a crucial indicator of mitophagy, but as stated above, the distribution of these proteins within the mitochondrion was not studied. A similar trend in the LC3 A/B-II/I ratio was noted in the untreated reperfusion protocol (discussed earlier in section 4.1.2).

In addition to this, parkin is also a stimulator of the ubiquitin-proteasome system (UPS) and uses it to initiate mitophagy. Upon depolarisation of mitochondria, recruitment of Parkin is also associated with the recruitment of the 26S proteasome of the UPS which targets K-48 linked polyubiquitin proteins for degradation. Degradation of several outer mitochondrial membrane proteins, prevents the mitochondria from participating in cellular processes and is thus rendered for removal via mitophagy (Chan & Chan 2011). The UPS is therefore essential for mitophagy to occur. Analysis of proteins participating in the UPS system e.g. absence of certain outer mitochondrial proteins, would also strengthen or confirm the outcomes of whether Parkin levels observed was associated with mitophagy taking place or not.

An attempt was made to correlate mitochondrial oxidative phosphorylation potential with the changes in mitophagy. It should be kept in mind that the mitochondria isolated from hearts subjected to I/R and 3-MA were divided into two aliquots, one to be used for mitochondrial function measurements and the other for evaluation of mitophagy markers. The mitochondria from the untreated reperfused hearts exhibited low state 3 respiration rates and RCI levels confirming that the mitochondria from these hearts had been compromised by the prior exposure to I/R, while 3-MA treatment increased both, particularly with glutamate plus malate as substrates (Results, Figure 3:19B). The state 4 oxidative phosphorylation rate (resting respiration of mitochondria) in the glutamate plus malate medium of mitochondria from untreated reperfusion was significantly lower to those of mitochondria from baseline conditions (Results, Figure 3:19F). This further infers that mitochondria were adversely affected during reperfusion.

However, in the reperfusion protocols there was a significant increase in the PINK1 levels when 3-MA was administered at the onset of reperfusion in comparison to the untreated controls. No changes were observed in PINK1 levels between the untreated controls and when 3-MA was administered before ischaemia/reperfusion. These findings correlated with a similar trend in the mitochondrial state 3 respiration with glutamate plus malate as substrates, with no changes in the palmitoyl -L-carnitine plus malate substrate, as described above. The increase

in PINK1 levels suggests that an increase in mitophagy is associated with higher state 3 respiration and improved RCI levels signifying a possible increase in the ATP levels. This is in agreement with the notion that *autophagy* preserves ATP levels during glucose deprivation (Matsui et al. 2007b). However, these findings of increased state 3 respiration and RCI levels were noted during reperfusion and not during glucose deprivation/ischaemia, therefore one could possibly infer that during increased mitophagy (observed by the increase in PINK1 levels), dysfunctional mitochondria were removed allowing for the remaining functional mitochondria to produce ATP through utilising the energy substrates made available during reperfusion. This possibility remains to be investigated. These outcomes were also positively associated with a slight increase in reperfusion function in comparison to the untreated controls (cardiac output 11.6 ± 4.6 vs 3.5 ± 1.6 ml/min; total work 9 ± 1 vs 0.4 ± 0.3 mW).

This 3-MA –induced stimulation of mitochondrial PINK1 levels upon reperfusion, was not observed with either Parkin or p62: when 3-MA was administered before ischaemia and reperfusion versus administration before ischaemia alone there was a significant reduction in the Parkin levels but not with p62.

Mitophagy is a specialised process of autophagy, it is highly selective and initiated by specific proteins. This would therefore mean that it is not necessarily inhibited or activated by the same pharmacological tools as autophagy. Interestingly, when we inhibited mitophagy with 3-MA our results showed that mitochondria in the presence of 3-MA before exposure to ischaemia had significantly reduced levels of PINK1 in comparison to the mitochondria of the untreated controls (Results, Figure 3:20). Our results were similar to a study that showed starvation induced *autophagy* was inhibited when 3-MA was administered as it led to a decrease in LC3 II/I levels as observed using fluorescence, in that particular study (Matsui et al. 2007b). No changes however were observed in Parkin levels among the ischaemic protocols. These observations were also associated with no changes in the mitochondrial bioenergetics from the same ischaemic protocols.

In summary, the data obtained in this study thus far suggested that 3-MA, well-known for its inhibitory effects on autophagy, had no such outspoken effects in hearts subjected to I/R. In fact, the protocol used showed a significant increase in tissue BNIP3L/Nix levels during reperfusion only, suggesting activation of autophagy after exposure to I/R, however 3-MA was without effect. With regards to mitophagy, 3-MA had opposing effects namely a reduction in PINK1 levels after ischaemia, and a significant upregulation thereof during reperfusion, while

not having marked effects on the other indicators of mitophagy. From these findings we can propose that 3-MA was not effective as an inhibitor of mitophagy in the presence of nutrient rich conditions (i.e. reperfusion) as indicated in a study that showed the inability of 3-MA to inhibit autophagy in cells under nutrient rich conditions (Wu et al. 2010). However, the exposure of 3-MA to the cells was over 9 hours in that particular study, where as ours was for 10 min. Another possibility was that the concentration of 3-MA (1 mM) was not sufficient to induce effective blockade of autophagy. This possibility remains to be investigated.

As indicated in Figure 3.23, the amount of actively respiring mitochondria per mg mitochondrial protein utilized experimentally in all of the above studies, were equal and could therefore not influence any of the results.

Effect of 3-MA on infarct size

As described above, upregulation of autophagy has been associated with cardio protection (Valentim et al. 2006; Ma et al. 2015) and vice versa. To evaluate the effects of inhibition of autophagy/mitophagy on the outcome of I/R, the effect of 3-MA was also evaluated on infarct size after exposure of the heart to 35 min regional ischaemia. Administration of the drug *before* the onset of ischaemia only (pre-treatment) did not have any effect on the infarct size ($35.11 \pm 2\%$ - control vs $34.4 \pm 3\%$ - 3-MA) or functional recovery ($40.88 \pm 10.45\%$ - control vs $36.80 \pm 10.20\%$ -3-MA, for cardiac output) and ($37.67 \pm 10.14\%$ - control vs $26.16 \pm 8.93\%$ -3-MA, for total work), of hearts when compared to the untreated controls (Results, Figure 3:25A). This is not unexpected in view of the fact that 3-MA had mostly insignificant effects on autophagy and mitophagy in our model of I/R. With effective inhibition of mitophagy before ischaemia one would expect to see detrimental effects on the heart as inhibition of the removal of dysfunctional mitochondria would result in an accumulation of harmful substances such as increased ROS and calcium levels which will lead to the opening of the mitochondrial pore and lead to cell death. In addition to this, mitochondrial oxidative phosphorylation capacity would most likely be compromised resulting in a decrease in ATP synthesis and therefore the energy levels available to the cardiomyocytes for heart contraction. From these processes one would expect to see an increase in infarcted heart tissue and ultimately decreased mechanical function of the heart. However, these outcomes were not observed in our studies due to the inability of 3-MA to induce effective inhibition of autophagy/mitophagy. However, the area at risk was significantly reduced ($55.07 \pm 1.35\%$ - control vs $37.12 \pm 1.44\%$ - 3-MA). An explanation for this phenomenon is not readily available. Since infarct size is expressed as a percentage of the

area at risk, one would expect that this would result in a smaller infarct size, which was not the case. Since the technique of ligation is the same in all experiments and the area at risk is routinely the same (Salie et al. 2014), it means that the drug in some or other way affected the size of the damaged tissue, for example affecting coronary flow. However, this phenomenon needs to be further investigated.

4.3 Effects of stimulating Mitophagy with FCCP

Mitophagy is induced by dysfunctional mitochondria - initiated by a loss in membrane potential. Uncouplers are known to depolarise and decrease the membrane potential of mitochondria and thus induce mitophagy (Lou et al. 2007). FCCP is a common pharmacological uncoupler of mitochondria (Lou et al. 2007) and chosen for use in the present study. FCCP acts as an ionophore and dissipates the chemo-osmotic gradient of mitochondria thereby negating the ability to synthesise ATP (Heytler & Prichard 1962).

In these sets of experiments, we began by carrying out a dose response of FCCP in order to determine the concentration to be used throughout the study. It was of importance that the dosage decided upon did not cause complete heart failure as this would hamper evaluation of the effects of stimulation of mitophagy on cardio protection. The concentrations that were tested ranged from 100 nM to 1000 nM (1 μ M). When FCCP was administered before global ischaemia it resulted in complete heart failure during reperfusion with all concentrations, although hearts pre-treated with 100 nM of FCCP showed slight contractions in comparison to the hearts pre-treated with any of the other concentrations. Mitochondria isolated from hearts pre-treated with concentrations of FCCP higher than 250 nM exhibited pronounced increased expression of PINK1 and Parkin which are indicators of mitophagy occurring. In fact, increased p62 levels were already observed at 100 nM FCCP. However, high levels of mitophagy could suggest aggressive mitophagy occurring, caused by the high concentrations of the uncouplers leading to a reduction in the amount of available functional mitochondria, a reduction in ATP synthesis and subsequently the cardiomyocyte capacity to function (Marín-García & Akhmedov 2016) as inferred from the heart failure observed in the present study. These outcomes are consistent with the findings of a study that showed that 300 nM of FCCP completely eradicated the contractility of the heart during the 5 min of drug administration prior to ischaemia, increasing ischaemic injury and conferring no protective effect (Brennan, Southworth, et al. 2006).

Higher concentrations of FCCP i.e. 500 and 1000 nM of FCCP similarly lead to complete failure of hearts during reperfusion associated with such mitochondrial damage that its oxidative function could not be measured polarographically. The citrate synthase activity of mitochondria pre-treated with 1000 nM FCCP was also lower than that of the controls, indicating a reduction in the number of intact mitochondria (Holloszy et al. 1970).

Due to the toxic nature of the higher concentrations of FCCP the study was then continued with the two lower concentration ranges (100 nM and 250 nM), thereby increasing the n values. Mitophagy markers were re-analysed with the addition of TOM70. TOM70 is an outer mitochondrial protein involved in the transportation of PINK1 into the mitochondria where it will be degraded (Kato et al. 2013). As an important receptor of the TOM machinery, TOM70 preferentially binds the internal targeting signals of polytopic membrane proteins (Yamamoto et al. 2009).

TOM70 levels were significantly increased in mitochondria of hearts pre-treated with 100 nM FCCP. This was associated with a significant decrease in the Parkin levels. The opposite effect was observed in the mitochondria of hearts pre-treated with 250 nM FCCP (Results, Figure 3:30). Our outcomes were contrary to the findings of Narendra and colleagues who observed an increase in Parkin levels when 100 nM FCCP was administered for 5 or 15 min to Langendorf perfused hearts from wild type and PINK1 knock-out mice (Narendra et al. 2010). From our studies, no changes were observed in the PINK1 and p62 levels for either concentration.

Pre-treatment with 250 nM FCCP also revealed poor mitochondrial oxidative phosphorylation function as registered polarographically, whereas mitochondria isolated from hearts pre-treated with 100 nM FCCP yielded better mitochondrial registrations for determination of the bioenergetics function. Again our findings are in agreement with a study that showed decreased mitochondrial uncoupling and mitochondrial depolarisation associated with hearts pre-treated with 100 nM FCCP in comparison to higher concentrations (300 nM and above) (Brennan, Berry, et al. 2006). Since polarographic demonstration of state3/state4 conversion could not be seen in mitochondria isolated from hearts exposed to 250 nM FCCP, we decided to measure the amounts of ADP and ATP in the incubation medium using HPLC analyses for evaluation of the phosphorylation processes. Our results showed that when hearts were pre-treated with 250 nM FCCP there were significantly higher levels of unconverted mitochondrial ADP levels with both substrates in comparison to the mitochondrial ADP levels of the untreated controls, confirming partial uncoupling of oxidative phosphorylation, since measureable amounts of ATP were obtained in the presence of the uncoupler.

Our results also showed that mitochondria isolated from hearts pre-treated with 100 nM FCCP were uncoupled in the palmitoyl-L-carnitine plus malate medium, as indicated by the decrease in ADP/O ratio in comparison to the untreated controls. This was not associated with severe proton leak as the RCI levels were increased in the palmitoyl-L-carnitine plus malate substrate medium but was mainly due to reduction in State 4 respiration, since the state 3 respiration rates were not affected by FCCP. However, the decreased ADP/O ratio yielded a reduction in the oxidative phosphorylation rate of mitochondria for both states 3 and 4, in both substrate media for the former and palmitoyl-L-carnitine plus malate for the latter (Results, Figure 3:32 E, F). After exposure to anoxia, mitochondria of pre-treated FCCP hearts yielded an increased state 3 respiration during re-oxygenation in the palmitoyl-L-carnitine plus malate substrate when compared to the mitochondria of the untreated controls, which may be suggestive of protection induced by 100 nM FCCP.

These mitochondrial outcomes were however not associated with increased mechanical function during regional ischaemia in comparison to controls. However, there was a significant improved functional recovery in comparison to hearts pre-treated with 250 nM FCCP which also lead to complete heart failure in regional ischaemia, similarly as in global ischaemia (see Results Table 3:6; Figures 3:37 A, B). Despite this, both concentrations resulted in a very significant decrease in infarct size in comparison to the control hearts, with 250 nM yielding the lowest percentage in comparison to the 100 nM and controls. Interestingly and contrary to expectations, 100 nM FCCP resulted in a higher percentage of the area at risk in comparison to controls, while the increase with 250 nM was insignificant. An explanation for this observation is not readily available, but could account partially for the reduction in infarct size which is expressed as a percentage of the area at risk. However, the amount of necrosis observed was much less in hearts pre-treated with FCCP.

Thus partial uncoupling of the mitochondria with 100 nM FCCP yielded a decrease in the oxidative phosphorylation capacity, an increase in the area at risk but was correlated with no change in the functional recovery compared to the untreated controls (in all mentioned parameters). Uncoupling of mitochondria would result in the release of increased ROS and thus render the mitochondria dysfunctional leading to mitophagy. Removal of dysfunctional mitochondria by upregulation of mitophagy and possibly a reduction in ROS production could account for the reduction in infarct size. Measurement of tissue ATP levels may shed more light on the processes involved.

Interestingly, the very significant reduction in infarct size elicited by FCCP was not associated with improvement in functional recovery during reperfusion. This could be due to concomitant stunning which is characteristic of reperfusion, as well as to prevailing uncoupling effects of the FCCP treatment.

Chapter 5

Conclusion and Future Recommendations

5.1. Comparison of the effects of 3-MA and FCCP on infarct size, area at risk and mechanical functional recovery.

The aims of this study were to determine the effects of manipulation of autophagy/mitophagy on mitochondrial oxidative phosphorylation function and to attempt to correlate this with infarct size and mechanical recovery of the heart during reperfusion. Interestingly, our I/R model showed that exposure to ischaemia per se was without effect on autophagy, while reperfusion caused upregulation of this process. Exposure to I/R however had several effects on mitochondrial mitophagy.

Unfortunately, 3-MA as inhibitor of autophagy/mitophagy had very little effect, probably because of the fact that our model did not show very marked changes in this regard. 3-MA also did not affect the infarct size of the hearts when compared to those of the control hearts. The choice of FCCP to elicit mitophagy yielded much better outcomes: not only did FCCP stimulate mitophagy, but it caused a significant decrease in infarct size compared to both untreated controls and 3-MA (Results, Table 3.7). Interestingly the two drugs had opposite effects on the area at risk: FCCP caused an increase in the percentage of compromised cells when compared to both the untreated and 3-MA pre-treated hearts (Results, Table 3.7). 3-MA on the other hand, caused a reduction in the area at risk. The mechanism whereby these drugs affect the area at risk needs to be further investigated. Mechanical function however, were similar in these hearts, most likely due to the overriding effects of stunning during reperfusion.

Finally, these findings suggest that stimulation of mitophagy prior to ischaemia and reperfusion, as opposed to its inhibition, is cardio protective, as it resulted in the reduction of the necrotic tissue. This therefore confirms our hypothesis that mitophagy is cardio protective in the outcome of ischaemia and reperfusion.

5.2. Limitations and Future studies

The significance of autophagy and mitophagy in myocardial I/R damage has been an important research topic in recent years. Both processes have been shown to occur in I/R, but whether they are protective or detrimental is still under debate. In particular, the role of mitophagy in cardio protection needs to be further investigated. For example, although the effect of ischaemia and reperfusion on mitochondrial function has been known for decades, the

participation of mitophagy in the changes observed is still to be determined and was one of the main aims of our study. However, although our study clarified some of the aspects, there are still many shortcomings which need to be addressed in the future.

Amongst others, effective quantification of autophagy/mitophagy is crucial to determine the significance of this process. Fluorescence microscopy, specifically green fluorescent protein (GFP)-microtubule associated with LC3 is a technique that has been used to successfully quantify autophagy and specifically autophagic flux. The use of this technique in addition to the Western blots generated will confirm and clarify the outcomes of our study. In addition to this, the LC3 proteins could have also been measured in our mitochondrial samples isolated from hearts exposed to the different perfusion protocols and drugs, as these proteins are involved in the process of mitophagy and would further confirm our results. Analyses of the UPS proteins would also have been ideal to monitor in our experiments. Additionally, measurement of the tissue high energy phosphate levels i.e. ADP and ATP, will also be a useful endpoint in the study, however they were only determined in some of the FCCP studies and not in the 3-MA studies.

The specificity of the inhibitor of mitophagy could also have influenced the outcomes of our study. 3-MA has mainly been used to study autophagy which has different initiation processes to mitophagy, a highly selective form of autophagy. Drugs such as chloroquine have been reported to be used in mitophagy studies as it inhibits autophagic flux. However, use of a more specific inhibitor of mitophagy is required in future studies.

Interpretation of the data obtained was hampered in some instances by the rather small sample size, particularly in the case of Western blotting. Increasing the number of samples per experiment could have possibly resulted in significant outcomes.

References

- (WHO), W.H.O., 2016. Cardiovascular Diseases (CVDs). Available at: <http://www.who.int/mediacentre/factsheets/fs317/en/>.
- (WHO), W.H.O., 2014. The top 10 causes of death. *World Health Organisation Fact Sheets*. Available at: <http://www.who.int/mediacentre/factsheets/fs310/en/> [Accessed November 21, 2016].
- Agholme, L., Agnello, M., Agostinis, P., Aguirre-ghiso, J.A., Ahn, H.J., Ait-mohamed, O., et al., 2012. of assays for monitoring autophagy © 2012 Landes Bioscience . Do not distribute . © 2012 Landes Bioscience . Do not distribute . *Autophagy*, (April), pp.445–544.
- Antwerp, I., 2004. Forefronts in Nephrology Evolving Basic Concepts in Ischemic Long-term effects of acute ischemia and reperfusion injury. In *Forefronts in Nephrology*. pp. 523–527.
- Baker, J.E. & Kalyanaraman, B., 1989. Ischemia-induced changes in myocardial paramagnetic metabolites: implications for intracellular oxy-radical generation. *FEBS letters*, 244(2), pp.311–314.
- Behrends, C. & Fulda, S., 2012. Receptor proteins in selective autophagy. *International Journal of Cell Biology*, 2012(673290), pp.1–9.
- Bell, R.M., Mocanu, M.M. & Yellon, D.M., 2011. Retrograde heart perfusion: The Langendorff technique of isolated heart perfusion. *Journal of Molecular and Cellular Cardiology*, 50(6), pp.940–950. Available at: <http://dx.doi.org/10.1016/j.yjmcc.2011.02.018>.
- Berridge, M.J., Lipp, P. & Bootman, M.D., 2000. the Versatility and Universality of Calcium Signalling. *Nature Review*, 1(October), pp.11–21.
- Bhosale, G., Sharpe, J.A., Sundier, S.Y. & Duchon, M.R., 2015. Calcium signaling as a mediator of cell energy demand and a trigger to cell death. *Annals of the New York Academy of Sciences*, 1350(2015), pp.107–116.
- Bialik, S., Simon, H. & Kimchi, A., 2009. Life and death partners : apoptosis , autophagy and the cross-talk between them. *Nature Publishing Group*, 16(7), pp.966–975. Available at:

<http://dx.doi.org/10.1038/cdd.2009.33>.

- Billia, F., Hauck, L., Konecny, F., Rao, V., Shen, J. & Wah, T., 2011. PTEN-inducible kinase 1 (PINK1)/Park6 is indispensable for normal heart function. *Proceedings of the National Academy of Sciences of the United States of America*, 108(23), pp.9572–7.
- Bradford, M.M., 1976. A rapid and sensitive method for the quantitation of microgram quantities of protein utilizing the principle of protein-dye binding. *Analytical Biochemistry*, 72(1-2), pp.248–254.
- Brand, M.D. & Nicholls, D.G., 2011. Assessing mitochondrial dysfunction in cells. *Biochemical Journal*, 312, pp.297–312.
- Brennan, J.P., Berry, R.G., Baghai, M., Duchen, M.R. & Shattock, M.J., 2006. FCCP is cardioprotective at concentrations that cause mitochondrial oxidation without detectable depolarisation. *Cardiovascular Research*, 72(2), pp.322–330.
- Brennan, J.P., Southworth, R., Medina, R.A., Davidson, S.M., Duchen, M.R. & Shattock, M.J., 2006. Mitochondrial uncoupling, with low concentration FCCP, induces ROS-dependent cardioprotection independent of KATP channel activation. *Cardiovascular Research*, 72(2), pp.313–321.
- Buja, L.M., 2005. Myocardial ischemia and reperfusion injury. *Cardiovascular Pathology*, 14(4), pp.170–175.
- Busiello, R.A., Savarese, S. & Lombardi, A., 2015. Mitochondrial uncoupling proteins and energy metabolism. *Frontiers in Physiology*, 6(FEB), p.36.
- Canini, F. & Batandier, C., 2016. Cinnamon intake alleviates the combined effects of dietary-induced insulin resistance and acute stress on brain mitochondria. *The Journal of Nutritional Biochemistry*, 28(2016), pp.183–190. Available at: <http://dx.doi.org/10.1016/j.jnutbio.2015.10.016>.
- Caprette, D.R., 2007. Overview of Mitochondria Structure and Function. *Rice University*. Available at: <http://www.ruf.rice.edu/~bioslabs/studies/mitochondria/mitoverview.html>.
- Castilho, R.F., 1996. Effect of Inorganic Phosphate Concentration on the Nature of Inner Mitochondrial Membrane Alterations Mediated by Ca²⁺ Ions. *Journal of Biological Chemistry*, 271(6), pp.2929–2934.

- Chain, T.E.T., Electron transport and oxidative phosphorylation • *Transport*.
- Chan, D.C., 2006. Mitochondria: Dynamic Organelles in Disease, Aging, and Development. *Cell*, 125(7), pp.1241–1252.
- Chan, N.C. & Chan, D.C., 2011. Parkin uses UPS to ship off dysfunctional mitochondria. *Landes Bioscience*, 7(7), pp.771–772.
- Chance, B. and Williams, G.R., 1955. Respiratory enzymes in oxidative phosphorylation. I. Kinetics of oxygen utilization. *J. Biol. Chem*, (217), pp.383–393.
- Chen, G., Han, Z., Feng, D., Chen, Y., Chen, L., Wu, H., et al., 2014. A regulatory signaling loop comprising the PGAM5 phosphatase and CK2 controls receptor-mediated mitophagy. *Molecular Cell*, 54(3), pp.362–377. Available at: <http://dx.doi.org/10.1016/j.molcel.2014.02.034>.
- Crompton, M., 1999. The mitochondrial permeability transition pore and its role in cell death. *The Biochemical journal*, 341 (Pt 2, pp.233–249. Available at: <http://www.ncbi.nlm.nih.gov/pubmed/21081127>.
- Csordás, G. & Hajnóczky, G., 2009. SR/ER-mitochondrial local communication: Calcium and ROS. *Biochimica et Biophysica Acta - Bioenergetics*, 1787(11), pp.1352–1362. Available at: <http://dx.doi.org/10.1016/j.bbabi.2009.06.004>.
- Denton R.M, M.J.G., 1985. Calcium transport by mammalian mitochondria and its role in hormone action. *American Journal of Physiology*, (249), pp.E543–E554.
- Duncker, D.J., Schulz, R., Ferrari, R., Garcia-Dorado, D., Guarnieri, C., Heusch, G., et al., 1998. “Myocardial stunning” remaining questions. *Cardiovascular Research*, 38(3), pp.549–558.
- Edoute, Y., van der Merwe, E., Sanan, D., Kotze, J.C., Steinmann, C. & Lochner, A., 1983. Normothermic ischemic cardiac arrest of the isolated working rat heart. Effects of time and reperfusion on myocardial ultrastructure, mitochondrial oxidative function, and mechanical recovery. *Circulation research*, 53(5), pp.663–678. Available at: <http://ovidsp.ovid.com/ovidweb.cgi?T=JS&PAGE=reference&D=med2&NEWS=N&AN=6627616>.
- Fox, S.I., 2009. Human Physiology. In *Human Physiology*. McGraw Hill, pp. 360–369.

- Geisler, S., Holmström, K.M., Skujat, D., Fiesel, F.C., Rothfuss, O.C., Kahle, P.J., et al., 2010. PINK1/Parkin-mediated mitophagy is dependent on VDAC1 and p62/SQSTM1. *Nature cell biology*, 12(2), pp.119–131. Available at: <http://dx.doi.org/10.1038/ncb2012>.
- Gonnern, C.P. & Halestrap, A.P., 1996. Chaotropic agents and increased matrix volume enhance binding of mitochondrial cyclophilin to the inner mitochondrial membrane and sensitize the mitochondrial permeability transition to [Ca²⁺]. *Biochemistry*, 35(25), pp.8172–8180.
- Gottlieb, R.A. & Mentzer, R.M., 2013. Autophagy : an affair of the heart. *Heart Failure Reviews*, (November 2012), pp.575–584.
- Halestrap, A.P., 2009. What is the mitochondrial permeability transition pore? *Journal of Molecular and Cellular Cardiology*, 46(6), pp.821–831. Available at: <http://dx.doi.org/10.1016/j.yjmcc.2009.02.021>.
- Halestrap, A.P. & Richardson, A.P., 2015. The mitochondrial permeability transition: A current perspective on its identity and role in ischaemia/reperfusion injury. *Journal of Molecular and Cellular Cardiology*, 78, pp.129–141. Available at: <http://dx.doi.org/10.1016/j.yjmcc.2014.08.018>.
- Hamacher-Brady, A., 2012. Autophagy Regulation and Integration with Cell Signaling. *Antioxidants & Redox Signaling*, 17(5), pp.756–765.
- Hamacher-Brady, A., Brady, N.R. & Gottlieb, R.A., 2006. Enhancing macroautophagy protects against ischemia/reperfusion injury in cardiac myocytes. *Journal of Biological Chemistry*, 281(40), pp.29776–29787.
- Hanna, R.A., Quinsay, M.N., Orogo, A.M., Giang, K., Rikka, S. & Gustafsson, Å.B., 2012. Microtubule-associated protein 1 light chain 3 (LC3) interacts with Bnip3 protein to selectively remove endoplasmic reticulum and mitochondria via autophagy. *Journal of Biological Chemistry*, 287(23), pp.19094–19104.
- Hariharan, N., Zhai, P. & Sadoshima, J., 2011. Oxidative stress stimulates autophagic flux during ischemia/reperfusion. *Antioxidants & redox signaling*, 14(11), pp.2179–90. Available at: <http://www.pubmedcentral.nih.gov/articlerender.fcgi?artid=3085947&tool=pmcentrez&rendertype=abstract>.

- Hausenloy, D. & Yellon, D., 2013. Myocardial ischemia-reperfusion injury: a neglected therapeutic target. *J Clin Invest*, 123(1), pp.92–100. Available at: <http://www.ncbi.nlm.nih.gov/pubmed/23281415>.
- Heytler, P.G. & Prichard, W.W., 1962. A new class of uncoupling agents — Carbonyl cyanide phenylhydrazones. *Biochemical and Biophysical Research Communications*, 7(4), pp.272–275. Available at: <http://www.sciencedirect.com/science/article/pii/0006291X62901894>.
- Holloszy, J.O., Oscai, L.B. & Mole, P.A., 1970. Mitochondrial citric acid cycle and related enzymes: adaptive response to exercise. *Biomedical and Biophysical Research Communications*, 40(6), pp.1368–1373.
- Imazu, T., Shimizu, S., Tagami, S., Matsushima, M., Nakamura, Y., Miki, T., et al., 1999. Bcl-2/E1B 19 kDa-interacting protein 3-like protein (Bnip3L) interacts with bcl-2/Bcl-xL and induces apoptosis by altering mitochondrial membrane permeability. *Oncogene*, 18(January), pp.4523–4529. Available at: <http://www.nature.com/doi/10.1038/sj.onc.1202722>.
- Jennings, R.B., 2013. Historical perspective on the pathology of myocardial ischemia/reperfusion injury. *Circulation Research*, 113(4), pp.428–438.
- Jennings, R.B., Sommers, H.M., Smyth, G.A., Flack, H.A. & Linn, H., 1960. Myocardial necrosis induced by temporary occlusion of a coronary artery in the dog. *Archives of pathology*, 70, pp.68–78. Available at: <https://www.ncbi.nlm.nih.gov/pubmed/14407094>.
- Jimenez, R.E., Kubli, D.A. & Gustafsson, Å.B., 2014. Autophagy and mitophagy in the myocardium: Therapeutic potential and concerns. *British Journal of Pharmacology*, 171(8), pp.1907–1916.
- Kalogeris, T., Baines, C.P., Krenz, M. & Korthuis, R.J., 2012. Cell Biology of Ischemia/Reperfusion Injury. *Int Rev Cell Mol Biol*, 298, pp.229–317.
- Kaplan, 2014. *Kaplan MCAT Biochemistry Review* B. G. Macnow, Alexander Stone; Hall-Pogar, Tyra; Starkman, ed., New York: Kaplan.
- Kato, H., Lu, Q., Rapaport, D. & Kozjak-Pavlovic, V., 2013. Tom70 Is Essential for PINK1 Import into Mitochondria. *PLoS ONE*, 8(3), pp.1–6.
- Khalil, P.N., Neuhof, C., Huss, R., Pollhammer, M., Khalil, M.N., Neuhof, H., et al., 2005.

- Calpain inhibition reduces infarct size and improves global hemodynamics and left ventricular contractility in a porcine myocardial ischemia / reperfusion model. *European Journal of Pharmacology*, 528, pp.124–131.
- Kubli, D.A., Cortez, M.Q., Moyzis, A.G., Najor, R.H., Lee, Y. & Gustafsson, Å.B., 2015. PINK1 is dispensable for mitochondrial recruitment of parkin and activation of mitophagy in cardiac myocytes. *PLoS ONE*, 10(6), pp.1–16.
- Kubli, D.A. & Gustafsson, A.B., 2012. Mitochondria and mitophagy: The yin and yang of cell death control. *Circulation Research*, 111(9), pp.1208–1221.
- Kubli, D.A., Zhang, X., Lee, Y., Hanna, R.A., Quinsay, M.N., Nguyen, C.K., et al., 2013. Parkin protein deficiency exacerbates cardiac injury and reduces survival following myocardial infarction. *Journal of Biological Chemistry*, 288(2), pp.915–926.
- Lee, Y., Lee, H.-Y., Hanna, R. a. & Gustafsson, a. B., 2011. Mitochondrial autophagy by Bnip3 involves Drp1-mediated mitochondrial fission and recruitment of Parkin in cardiac myocytes. *AJP: Heart and Circulatory Physiology*, 301(5), pp.H1924–H1931.
- Lesnefsky, E.J., Moghaddas, S., Tandler, B., Kerner, J. & Hoppel, C.L., 2001. Mitochondrial dysfunction in cardiac disease: ischemia--reperfusion, aging, and heart failure. *Journal of molecular and cellular cardiology*, 33(6), pp.1065–1089.
- Lin, G.G. & Scott, J.G., 2012. NIH Public Access. , 100(2), pp.130–134.
- Liu, L., Feng, D., Chen, G., Chen, M., Zheng, Q., Song, P., et al., 2012. Mitochondrial outer-membrane protein FUNDC1 mediates hypoxia-induced mitophagy in mammalian cells. *Nature cell biology*, 14(2), pp.177–85. Available at: <https://www.ncbi.nlm.nih.gov/pubmed/22267086>.
- Loos, B., du Toit, A. & Hofmeyr, J.-H.S., 2014. Defining and measuring autophagosome flux—concept and reality. *Autophagy*, 10(11), pp.2087–96. Available at: <http://www.pubmedcentral.nih.gov/articlerender.fcgi?artid=4502790&tool=pmcentrez&rendertype=abstract>.
- Lou, P.-H., Hansen, B.S., Olsen, P.H., Tullin, S., Murphy, M.P. & Brand, M.D., 2007. Mitochondrial uncouplers with an extraordinary dynamic range. *The Biochemical journal*, 407(1), pp.129–140.
- Ma, S., Wang, Y., Chen, Y. & Cao, F., 2015. *Biochimica et Biophysica Acta* The role of the

- autophagy in myocardial ischemia / reperfusion injury ☆. *BBA - Molecular Basis of Disease*, 1852(2), pp.271–276. Available at: <http://dx.doi.org/10.1016/j.bbadis.2014.05.010>.
- Ma, X., Liu, H., Foyil, S.R., Godar, R.J., Weinheimer, C.J., Hill, J.A., et al., 2012. Impaired autophagosome clearance contributes to cardiomyocyte death in ischemia/reperfusion injury. *Circulation*, 125(25), pp.3170–3181.
- Maejima, Y., Chen, Y., Isobe, M., Gustafsson, Å.B., Kitsis, R.N. & Sadoshima, J., 2015. Recent progress in research on molecular mechanisms of autophagy in the heart. *American journal of physiology. Heart and circulatory physiology*, 308(4), pp.H259–68. Available at: <http://www.ncbi.nlm.nih.gov/pubmed/25398984>.
- Mammucari, C., Patron, M., Granatiero, V. & Rizzuto, R., 2011. Molecules and roles of mitochondrial calcium signaling. *BioFactors*, 37(3), pp.219–227.
- Manuscript, A. & Protection, M., 2013. NIH Public Access. , 60(2), pp.125–132.
- Manuscript, A. & Syndromes, G.P., 2010. NIH Public Access. , 48(Suppl 2), pp.1–6.
- Marín-García, J. & Akhmedov, A.T., 2016. Mitochondrial dynamics and cell death in heart failure. *Heart Failure Reviews*, 21(2), pp.123–136.
- Masumoto, H. & Yamashita, J.K., 2016. Human iPS Cell-Derived Cardiac Tissue Sheets: a Platform for Cardiac Regeneration. *Current Treatment Options in Cardiovascular Medicine*, 18(11), p.65. Available at: <http://link.springer.com/10.1007/s11936-016-0489-z>.
- Matsui, Y., Takagi, H., Qu, X., Abdellatif, M., Sakoda, H., Asano, T., et al., 2007a. Distinct Roles of Autophagy in the Heart During Ischemia and Reperfusion Roles of AMP-Activated Protein Kinase and Beclin 1 in Mediating Autophagy. *American Heart Association Journals*, (100), pp.914–922.
- Matsui, Y., Takagi, H., Qu, X., Abdellatif, M., Sakoda, H., Asano, T., et al., 2007b. Distinct Roles of Autophagy in the Heart During Ischemia and Reperfusion: Roles of AMP-Activated Protein Kinase and Beclin 1 in Mediating Autophagy. *American Heart Association Journals*, pp.914–922. Available at: <http://circres.ahajournals.org/content/100/6/914>.
- Matti, S., 1999. Oxidative phosphorylation at the fin de siècle. *Science*, 283(5407), pp.1488–

1493.

- McBride, H.M., Neuspiel, M. & Wasiak, S., 2006. Mitochondria: More Than Just a Powerhouse. *Current Biology*, 16(14), pp.551–560.
- Morgunov, I. & Srere, P., 1998. Interaction between citrate synthase and malate dehydrogenase. *Journal of Biological Chemistry*, 273(45), pp.29540–29544. Available at: <http://www.jbc.org/content/273/45/29540.short>.
- Nagendran, J., Waller, T.J. & Dyck, J.R.B., 2013. AMPK signalling and the control of substrate use in the heart. *Molecular and Cellular Endocrinology*, 366(2), pp.180–193. Available at: <http://dx.doi.org/10.1016/j.mce.2012.06.015>.
- Nakagawa, T., Shimizu, S., Watanabe, T., Yamaguchi, O., Otsu, K., Yamagata, H., et al., 2005. Cyclophilin D-dependent mitochondrial permeability transition regulates some necrotic but not apoptotic cell death. *Nature*, 434(7033), pp.652–658.
- Narendra, D., Tanaka, A., Suen, D.F. & Youle, R.J., 2008. Parkin is recruited selectively to impaired mitochondria and promotes their autophagy. *Journal of Cell Biology*, 183(5), pp.795–803.
- Narendra, D.P., Jin, S.M., Tanaka, A., Suen, D.F., Gautier, C.A., Shen, J., et al., 2010. PINK1 is selectively stabilized on impaired mitochondria to activate Parkin. *PLoS Biology*, 8(1).
- Narendra, D.P., Jin, S.M., Tanaka, A., Suen, D.-F., Gautier, C.A., Shen, J., et al., 2010. PINK1 Is Selectively Stabilized on Impaired Mitochondria to Activate Parkin. *PLoS Biol*, 8(1), p.e1000298. Available at: <http://dx.doi.org/10.1371%2Fjournal.pbio.1000298>.
- Nickel, A., Löffler, J. & Maack, C., 2013. Myocardial energetics in heart failure. *Basic Research in Cardiology*, 108(4).
- Novak, I., Kirkin, V., McEwan, D.G., Zhang, J., Wild, P., Rozenknop, A., et al., 2010. Nix is a selective autophagy receptor for mitochondrial clearance. *EMBO reports*, 11(1), pp.45–51.
- Opie, L.H., 2004. *Heart Physiology From Cell to Circulation* 4th ed. F. Wernberg, Ruth W ; Bersin, Joanne; Aversa, ed., Lippincott Williams and Wilkins.
- Philipson, K.D. & Nicoll, D. a, 2000. Sodium-calcium exchange: a molecular perspective. *Annual review of physiology*, 62, pp.111–33. Available at:

<http://www.ncbi.nlm.nih.gov/pubmed/10845086>.

- Qian, T., Nieminen, A.-L., Herman, B. & Lemasters, J.J., 1997. Mitochondrial permeability transition in pH-dependent reperfusion injury to rat hepatocytes. *American Journal of Physiology - Cell Physiology*, 273(6), pp.C1783–C1792. Available at: <http://ajpcell.physiology.org/content/273/6/C1783.abstract>.
- Quan, X., Nguyen, T.T., Choi, S.K., Xu, S., Das, R., Cha, S.K., et al., 2015. Essential role of mitochondrial Ca²⁺ uniporter in the generation of mitochondrial pH gradient and metabolism-secretion coupling in insulin-releasing cells. *Journal of Biological Chemistry*, 290(7), pp.4086–4096.
- Ravikumar, B., Sarkar, S., Davies, J.E., Futter, M., Garcia-Arencibia, M., Green-Thompson, Z.W., et al., 2010. Regulation of mammalian autophagy in physiology and pathophysiology. *Physiological reviews*, 90(4), pp.1383–435. Available at: <http://www.ncbi.nlm.nih.gov/pubmed/20959619>.
- Rikka, S., Quinsay, M.N., Thomas, R.L., Kubli, D.A., Zhang, X., Murphy, A.N., et al., 2011. Bnip3 impairs mitochondrial bioenergetics and stimulates mitochondrial turnover. *Cell death and differentiation*, 18(4), pp.721–31. Available at: <http://www.pubmedcentral.nih.gov/articlerender.fcgi?artid=3058880&tool=pmcentrez&rendertype=abstract>.
- Rizzuto, R., De Stefani, D., Raffaello, A. & Mammucari, C., 2012. Mitochondria as sensors and regulators of calcium signalling. *Nature Reviews Molecular Cell Biology*, 13(9), pp.566–578. Available at: <http://dx.doi.org/10.1038/nrm3412>.
- Salie, R., Huisamen, B. & Lochner, A., 2014. High carbohydrate and high fat diets protect the heart against ischaemia / reperfusion injury. *Cardiovascular Diabetology*, 13(109), pp.1–12.
- Sargsyan, A., Cai, J., Fandino, L.B., Labasky, M.E., Forostyan, T., Colosimo, L.K., et al., 2015. Rapid parallel measurements of macroautophagy and mitophagy in mammalian cells using a single fluorescent biosensor. *Scientific reports*, 5(July), p.12397. Available at: <http://www.pubmedcentral.nih.gov/articlerender.fcgi?artid=4517063&tool=pmcentrez&rendertype=abstract>.
- Schagger, H., Cramer, W.A. & Vonjagow, G., 1994. The folin by oliver. *Analytical*

Biochemistry, 217(2), pp.220–230. Available at:
<http://linkinghub.elsevier.com/retrieve/pii/S0003269784711122>.

Schoultz, I., Söderholm, J.D. & McKay, D.M., 2011. Is metabolic stress a common denominator in inflammatory bowel disease? *Inflammatory Bowel Diseases*, 17(9), pp.2008–2018.

Shires, S.E. & Gustafsson, B., 2015. Mitophagy and heart failure. *Journal of Molecular Medicine*, 93(3), pp.253–262.

Siemen, D. & Ziemer, M., 2013. What is the nature of the mitochondrial permeability transition pore and What is it Not? *IUBMB Life*, 65(3), pp.255–262.

Smith, M.A. & Schnellmann, R.G., 2012. Calpains , mitochondria , and apoptosis. *European Society of Cardiology*, 4(96), pp.32–37.

Stanley, W.W.C., Recchia, F. a & Lopaschuk, G.D., 2005. Myocardial Substrate Metabolism in the Normal and Failing Heart. *Physiological reviews*, 85(3), pp.1093–1129. Available at:
<http://physrev.physiology.org/highwire/citation/10663/mendeley>
<http://physrev.physiology.org/content/85/3/1093.short>.

Stefan, J., 2015. The heart: our first organ. *Euro Stem cell*. Available at:
<http://www.eurostemcell.org/factsheet/heart-our-first-organ>.

De Stefani, D., Rizzuto, R. & Pozzan, T., 2016. Enjoy the Trip: Calcium in Mitochondria Back and Forth. *Annual review of biochemistry*, 85(1), pp.annurev–biochem–060614–034216. Available at: <http://www.annualreviews.org/doi/10.1146/annurev-biochem-060614-034216>
<http://www.ncbi.nlm.nih.gov/pubmed/27145841>.

Stephen C; Kolwicz, Jr, Suneet, Purohit, R.T., 2013. Growth , and Survival of Cardiomyocytes. *American Heart Association Journals*, 113, pp.603–617.

Tait, S.W.G. & Green, D.R., 2012. Mitochondria and cell signalling. *Journal of Cell Science*, 125, pp.807–815.

Takagi, H., Matsui, Y., Hirotsani, S., Sakoda, H., Asano, T. & Sadoshima, J., 2007. AMPK mediates autophagy during myocardial ischemia in vivo. *Autophagy*, 3(4), pp.405–407.

Tsai, M.-F., Phillips, C.B., Ranaghan, M., Tsai, C.-W., Wu, Y., Williams, C., et al., 2016. Dual

- functions of a small regulatory subunit in the mitochondrial calcium uniporter complex. *eLife*, 5, p.e15545. Available at: <http://elifesciences.org/lookup/doi/10.7554/eLife.15545>.
- Valentim, L., Laurence, K.M., Townsend, P.A., Carroll, C.J., Soond, S., Scarabelli, T.M., et al., 2006. Urocortin inhibits Beclin1-mediated autophagic cell death in cardiac myocytes exposed to ischaemia/reperfusion injury. *Journal of Molecular and Cellular Cardiology*, 40(6), pp.846–852.
- Varanyuwatana, P. & Halestrap, A.P., 2012. The roles of phosphate and the phosphate carrier in the mitochondrial permeability transition pore. *Mitochondrion*, 12(1), pp.120–125. Available at: <http://dx.doi.org/10.1016/j.mito.2011.04.006>.
- Wang, W. & Lopaschuk, G.D., 2007. Metabolic therapy for the treatment of ischemic heart disease: reality and expectations. *Expert Rev Cardiovasc Ther*, 5(6), pp.1123–1134. Available at: http://www.ncbi.nlm.nih.gov/entrez/query.fcgi?cmd=Retrieve&db=PubMed&dopt=Citation&list_uids=18035928.
- Watson, S., 2009. Amazing facts about the heart and heart disease. *WEBMD*. Available at: http://www.webmd.com/heart/features/amazing-facts-about-heart-health-and-heart-disease_#1 [Accessed February 7, 2017].
- Wu, Y.T., Tan, H.L., Shui, G., Bauvy, C., Huang, Q., Wenk, M.R., et al., 2010. Dual role of 3-methyladenine in modulation of autophagy via different temporal patterns of inhibition on class I and III phosphoinositide 3-kinase. *Journal of Biological Chemistry*, 285(14), pp.10850–10861.
- Xie, Z. & Klionsky, D.J., 2007. Autophagosome formation: core machinery and adaptations. *Nature cell biology*, 9(10), pp.1102–1109.
- Yamamoto, H., Fukui, K., Takahashi, H., Kitamura, S., Shiota, T., Terao, K., et al., 2009. Roles of Tom70 in import of presequence-containing mitochondrial proteins. *Journal of Biological Chemistry*, 284(46), pp.31635–31646.
- Yellon, D.M. & Hausenloy, D., 2007. Myocardial reperfusion injury. *The New England Journal of Medicine*, 357, pp.1121–35.
- Youle, R.J. & Narendra, D.P., 2011. Mechanisms of mitophagy. *Nature Publishing Group*, 12(1), pp.9–14. Available at: <http://dx.doi.org/10.1038/nrm3028>.

Yusuf, S., Hawken, S., Ôunpuu, S., Dans, T., Avezum, A., Lanas, F., et al., 2004. Effect of potentially modifiable risk factors associated with myocardial infarction in 52 countries in a case-control study based on the INTERHEART study. *Lancet*, 364, pp.937–952.

Zhang, J., 2013. Autophagy and mitophagy in cellular damage control. *Redox Biology*, 1(1), pp.19–23. Available at: <http://dx.doi.org/10.1016/j.redox.2012.11.008>.